

PH.D. THESIS

Routing and Scheduling Algorithms in Resource-Limited Wireless Multi-Hop Networks

by Anastassios Michail

Advisor: Anthony Ephremides

CSHCN PhD 2001-1
(ISR PhD 2001-1)



The Center for Satellite and Hybrid Communication Networks is a NASA-sponsored Commercial Space Center also supported by the Department of Defense (DOD), industry, the State of Maryland, the University of Maryland and the Institute for Systems Research. This document is a technical report in the CSHCN series originating at the University of Maryland.

Web site <http://www.isr.umd.edu/CSHCN/>

| Report Documentation Page | | | | Form Approved OMB No. 0704-0188 | |
|--|------------------------------------|-------------------------------------|----------------------------|--|---------------------------------|
| Public reporting burden for the collection of information is estimated to average 1 hour per response, including the time for reviewing instructions, searching existing data sources, gathering and maintaining the data needed, and completing and reviewing the collection of information. Send comments regarding this burden estimate or any other aspect of this collection of information, including suggestions for reducing this burden, to Washington Headquarters Services, Directorate for Information Operations and Reports, 1215 Jefferson Davis Highway, Suite 1204, Arlington VA 22202-4302. Respondents should be aware that notwithstanding any other provision of law, no person shall be subject to a penalty for failing to comply with a collection of information if it does not display a currently valid OMB control number. | | | | | |
| 1. REPORT DATE 2001 | | 2. REPORT TYPE | | 3. DATES COVERED - | |
| 4. TITLE AND SUBTITLE Routing and Scheduling Algorithms in Resource-Limited Wireless Multi-Hop Networks | | | | 5a. CONTRACT NUMBER | |
| | | | | 5b. GRANT NUMBER | |
| | | | | 5c. PROGRAM ELEMENT NUMBER | |
| 6. AUTHOR(S) | | | | 5d. PROJECT NUMBER | |
| | | | | 5e. TASK NUMBER | |
| | | | | 5f. WORK UNIT NUMBER | |
| 7. PERFORMING ORGANIZATION NAME(S) AND ADDRESS(ES) Army Research Laboratory, 2800 Powder Mill Road, Adelphi, MD, 20783 | | | | 8. PERFORMING ORGANIZATION REPORT NUMBER | |
| 9. SPONSORING/MONITORING AGENCY NAME(S) AND ADDRESS(ES) | | | | 10. SPONSOR/MONITOR'S ACRONYM(S) | |
| | | | | 11. SPONSOR/MONITOR'S REPORT NUMBER(S) | |
| 12. DISTRIBUTION/AVAILABILITY STATEMENT Approved for public release; distribution unlimited | | | | | |
| 13. SUPPLEMENTARY NOTES The original document contains color images. | | | | | |
| 14. ABSTRACT see report | | | | | |
| 15. SUBJECT TERMS | | | | | |
| 16. SECURITY CLASSIFICATION OF: | | | 17. LIMITATION OF ABSTRACT | 18. NUMBER OF PAGES 153 | 19a. NAME OF RESPONSIBLE PERSON |
| a. REPORT unclassified | b. ABSTRACT unclassified | c. THIS PAGE unclassified | | | |

ABSTRACT

Title of Dissertation: Routing and Scheduling Algorithms in Resource-limited
Wireless Multi-hop Networks

Anastassios Michail, Doctor of Philosophy, 2001

Dissertation directed by: Professor Anthony Ephremides
Department of Electrical and Computer Engineering

The recent advances in the area of wireless networking present novel opportunities for network operators to expand their services to infrastructure-less wireless systems. Such networks, often referred to as ad-hoc or multi-hop or peer-to-peer networks, require architectures which do not necessarily follow the cellular paradigm. They consist of entirely wireless nodes, fixed and/or mobile, that require multiple hops (and hence relaying by intermediate nodes) to transmit their messages to the desired destinations. The distinguishing features of such all-wireless network architectures give rise to new trade-offs between traditional concerns in wireless communications (such as spectral efficiency, and energy conservation) and the notions of routing, scheduling and resource allocation. The purpose of this work is to identify and study some of these novel issues, propose solutions in the

context of network control and evaluate the usual network performance measures as functions of the new trade-offs.

To these ends, we address first the problem of routing connection-oriented traffic with energy efficiency in all-wireless multi-hop networks. We take advantage of the flexibility of wireless nodes to transmit at different power levels and define a framework for formulating the problem of session routing from the perspective of energy expenditure. A set of heuristics are developed for determining end-to-end unicast paths with sufficient bandwidth and transceiver resources, in which nodes use local information in order to select their transmission power and bandwidth allocation. We propose a set of metrics that associate each link transmission with a cost and consider both the cases of plentiful and limited bandwidth resources, the latter jointly with a set of channel allocation algorithms. Performance is measured by call blocking probability and average consumed energy and a detailed simulation model that incorporates all the components of our algorithms has been developed and used for performance evaluation of a variety of networks.

In the sequel, we propose a "blueprint" for approaching the problem of link bandwidth management in conjunction with routing, for ad-hoc wireless networks carrying packet-switched traffic. We discuss the dependencies between routing, access control and scheduling functions and propose an adaptive mechanism for solving the capacity allocation (at both the node-level and the flow-level) and the route assignment problems, that manages delays due to congestion at nodes and packet loss due to error prone wireless links, to provide improved end-to-end delay/throughput. The capacity allocations to the nodes and flows and the route assignments are iterated periodically and the adaptability of the proposed approach allows the network to respond to random channel error bursts and congestion

arising from bursty and new flows.

Routing and Scheduling Algorithms in Resource-limited Wireless Multi-hop Networks

by

Anastassios Michail

Dissertation submitted to the Faculty of the Graduate School of the
University of Maryland, College Park in partial fulfillment
of the requirements for the degree of
Doctor of Philosophy
2001

Advisory Committee:

Professor Anthony Ephremides, Chairman/Advisor
Dr. M. Scott Corson
Professor Evaggelos Geraniotis
Professor Steven Marcus
Professor A. Udaya Shankar

©Copyright by
Anastassios Michail
2001

ACKNOWLEDGEMENTS

I would like to express my gratitude to my advisor, Professor Anthony Ephremides. His valuable support and exceptional guidance throughout my graduate school years have helped me achieve much more than I had expected when I came to Maryland. He made me believe in myself and without his persistence and encouragement I would have never felt confident to pursue the Doctoral program. I gained a lot of knowledge and valuable experience while working with him. His unique personality turned every single moment of interaction into a learning experience.

I am thankful to the members of the dissertation committee, Dr. Scott Corson and Professors Evaggelos Geraniotis, Steve Marcus and Udaya Shankar for kindly reviewing my dissertation and consenting to serve on the defense committee. I also wish to specially thank Professors Steve Marcus and Leandros Tassiulas for their valuable comments and advice on my research proposal. They provided me with constructive criticism that helped improve my work. Unfortunately Professor Tassiulas was on leave at the time of the defense and could not participate in the committee.

I had the opportunity to work closely on one of the research problems with Dr. Deepak Ayyagari. Deepak has been a very good friend and having known each other very well made it easier to collaborate. I wish to thank him for several discussions we had and for his valuable help.

It is extremely hard to find words that express my gratitude to my parents Tolis and Dora and my sister Nadia for their invaluable help over all these years. They gave me courage and strength whenever I needed it and supported me in every possible way throughout the course of my studies. I am also grateful to Marianna who has been very supportive and patient all this time and with her love and dedication she gave me the extra courage and confidence I needed to accomplish this work.

Throughout the six years I spent in Maryland I had the chance to meet a lot of new friends. They made life easier and I wish them all luck in their future plans. It would be a very long list if I had to mention names but I ought to express my special thanks to all my roommates for sharing a house with me most of these years and for bearing with me during both the good and the bad times.

Least, but not last, I wish to thank my fellow graduate students, all my officemates and the members of the Systems Engineering and Integration Lab for creating a pleasant working environment.

This work wouldn't have been possible without the financial support of the Institute for Systems Research. Funding was provided by the Advanced Telecommunications/Information Distribution Research Program (ATIRP) Consortium sponsored by the U.S. Army Research Lab-

oratory under Cooperative Agreement DAAL01-96-2-0002.

TABLE OF CONTENTS

| | |
|---|-----------|
| List of Tables | ix |
| List of Figures | x |
| 1 Introduction | 1 |
| 1.1 Summary and organization of dissertation | 5 |
| 2 Energy-Efficient Routing of Connection-Oriented Traffic, Part I: | |
| Limited Transceiver Resources | 7 |
| 2.1 Motivation and objectives | 7 |
| 2.1.1 Related work | 9 |
| 2.1.2 Research contributions | 10 |
| 2.1.3 Outline of the chapter | 12 |
| 2.2 Wireless network model | 13 |
| 2.3 Proposed algorithms | 16 |
| 2.3.1 Overview | 16 |
| 2.3.2 Link metrics | 18 |
| 2.4 Simulation model | 24 |
| 2.5 Performance results | 26 |
| 2.5.1 Blocking probability (P_b) | 26 |

| | | |
|----------|--|-----------|
| 2.5.2 | Average energy per session (E_s) | 31 |
| 2.5.3 | Effect of node density on performance | 33 |
| 2.5.4 | Effect of average node degree on performance | 39 |
| 2.5.5 | Energy versus blocking trade-off and yardstick (Y) perfor- mance | 42 |
| 2.5.6 | Effect of receive and processing power on energy consumption | 43 |
| 2.5.7 | Network “lifetime” | 46 |
| 2.6 | Conclusions | 50 |
| 3 | Energy-Efficient Routing of Connection-Oriented Traffic, Part II: | |
| | Limited Bandwidth Resources | 53 |
| 3.1 | Introduction | 53 |
| 3.2 | Interference model | 58 |
| 3.3 | Algorithmic considerations | 61 |
| 3.4 | Heuristic algorithms | 65 |
| 3.4.1 | Link metrics for determining minimum cost path | 65 |
| 3.4.2 | Frequency allocation algorithms | 67 |
| 3.5 | Exhaustive search mechanisms | 71 |
| 3.5.1 | Complete exhaustive search implementation (ExSrch) | 71 |
| 3.5.2 | Exhaustive search of minimum-cost path (ESMP) | 73 |
| 3.6 | Performance analysis | 74 |
| 3.6.1 | Comparison of frequency allocation heuristics versus exhaus- tive search mechanisms | 75 |
| 3.6.2 | Performance comparison of LLG versus MCLF for random topologies | 80 |

| | | |
|----------|--|-----------|
| 3.6.3 | Performance characteristics of link metrics for use with link- by-link greedy frequency allocation scheme | 83 |
| 3.7 | Conclusions | 87 |
| 4 | A “Blueprint” towards an Integrated Scheduling, Access Control and Routing Scheme in Wireless Ad-Hoc Networks | 91 |
| 4.1 | Motivation | 91 |
| 4.2 | Background | 94 |
| 4.2.1 | Scheduling disciplines for wire-line networks | 94 |
| 4.2.2 | Scheduling disciplines for cellular wireless networks | 98 |
| 4.2.3 | Scheduling in wireless LANs | 101 |
| 4.2.4 | Scheduling in wireless multi-hop networks | 102 |
| 4.3 | A unified approach to scheduling, access-control and routing in ad- hoc networks | 103 |
| 4.3.1 | Overview | 103 |
| 4.3.2 | Proposed model | 104 |
| 4.3.3 | Link error adjusted rate (LEAR) measure | 107 |
| 4.3.4 | Routing updates | 109 |
| 4.4 | Description of algorithms | 110 |
| 4.4.1 | Notation | 110 |
| 4.4.2 | Node-level scheduling | 111 |
| 4.4.3 | Flow-level scheduling | 112 |
| 4.4.4 | Routing | 113 |
| 4.5 | Performance results | 114 |
| 4.5.1 | Network and traffic patterns | 114 |
| 4.5.2 | Performance measures | 115 |

| | | |
|----------|---|------------|
| 4.5.3 | Simulation results | 115 |
| 4.6 | Future directions | 116 |
| 5 | Conclusions | 119 |
| | Appendix | 122 |
| A | Simulation model for energy-efficient routing algorithms | 122 |
| | Bibliography | 132 |

LIST OF TABLES

| | | |
|-----|---|-----|
| 2.1 | Average number of hops and standard deviation per admitted session for $N = 20$ | 31 |
| 2.2 | Consumed energy per node for low traffic | 51 |
| 2.3 | Consumed energy per node for high traffic | 51 |
| 3.1 | Frequency blocking status for example of figure 3.2 | 62 |
| 3.2 | Blocking probabilities for topology of Example 1 | 76 |
| 3.3 | Energy per session for topology of Example 1 | 77 |
| 3.4 | Blocking probabilities for topology of Example 2 | 81 |
| 3.5 | Energy per session for topology of Example 2 | 82 |
| 3.6 | Simulation parameters for comparing LLG with MCLF | 83 |
| 3.7 | Simulation parameters for comparing MPM with PIM | 86 |
| 4.1 | Performance results for average slot error rate $P_e = 0.1$ | 116 |
| 4.2 | Performance results for average slot error rate $P_e = 0.2$ | 117 |
| A.1 | Input parameters for simulation iteration | 130 |

LIST OF FIGURES

| | | |
|------|--|----|
| 2.1 | Connectivity properties and maximum transmission range | 14 |
| 2.2 | Path cost computation | 17 |
| 2.3 | Example illustrating properties of M3 | 21 |
| 2.4 | Blocking probability vs per node arrival rate, $N = 20, d_{max} = 30$. . | 28 |
| 2.5 | Blocking probability vs per node arrival rate, $N = 20, d_{max} = 50$. . | 28 |
| 2.6 | Blocking probability vs per node arrival rate for $N = 10, d_{max} = 30$. | 29 |
| 2.7 | Blocking probability vs per node arrival rate for $N = 10, d_{max} = 50$. | 29 |
| 2.8 | Blocking probability vs per node arrival rate for $N = 50, d_{max} = 30$. | 30 |
| 2.9 | Blocking probability vs per node arrival rate for $N = 50, d_{max} = 50$. | 30 |
| 2.10 | Energy per session vs per node arrival rate for $N = 10, d_{max} = 30$. . | 32 |
| 2.11 | Energy per session vs per node arrival rate for $N = 10, d_{max} = 50$. . | 33 |
| 2.12 | Energy per session vs per node arrival rate for $N = 20, d_{max} = 30$. . | 34 |
| 2.13 | Energy per session vs per node arrival rate for $N = 20, d_{max} = 50$. . | 34 |
| 2.14 | Energy per session vs per node arrival rate for $N = 50, d_{max} = 30$. . | 35 |
| 2.15 | Energy per session vs per node arrival rate for $N = 50, d_{max} = 50$. . | 35 |
| 2.16 | Blocking probability vs arrival rate for variable network sizes and M1 | 37 |
| 2.17 | Blocking probability vs arrival rate for variable network sizes and M3 | 37 |
| 2.18 | Energy per session vs arrival rate for variable network sizes and M1 | 38 |
| 2.19 | Energy per session vs arrival rate for variable network sizes and M3 | 38 |

| | | |
|------|--|----|
| 2.20 | Blocking prob. vs average node degree, $N = 20, d_{max} = 50, \lambda = 0.5$ | 40 |
| 2.21 | Energy per session vs average node degree, $N = 20, d_{max} = 50, \lambda = 0.5$ | 40 |
| 2.22 | Blocking probability for all samples, $N = 20, d_{max} = 50, \lambda = 0.5$ | 41 |
| 2.23 | Energy per session for all samples, $N = 20, d_{max} = 50, \lambda = 0.5$ | 41 |
| 2.24 | Energy-Blocking trade-off | 42 |
| 2.25 | Yardstick Y vs. per node arrival rate for $N = 20, d_{max} = 30$. | 43 |
| 2.26 | Yardstick Y vs. per node arrival rate for $N = 50, d_{max} = 30$. | 44 |
| 2.27 | Effect of processing power on E_s | 45 |
| 2.28 | Sample network connectivities with $N=10$ for studying effects of energy exhaustion | 46 |
| 2.29 | Number of accepted calls vs time; $N = 10, d_{max} = 40$ and $\lambda = 0.3$ | 48 |
| 2.30 | Number of accepted calls vs time; $N = 10, d_{max} = 40$ and $\lambda = 0.9$ | 48 |
| 2.31 | Number of accepted calls vs time; $N = 10, d_{max} = 50$ and $\lambda = 0.3$ | 49 |
| 2.32 | Number of accepted calls vs time; $N = 10, d_{max} = 50$ and $\lambda = 0.9$ | 49 |
| 3.1 | Example: Route selection involves power and frequency selection | 57 |
| 3.2 | Example network to illustrate interference model | 61 |
| 3.3 | Two instances of the same path showing the available frequencies | 64 |
| 3.4 | Example of purely greedy scheme operation | 68 |
| 3.5 | Network topologies of example 1 | 73 |
| 3.6 | Network topology of Example 2 | 80 |
| 3.7 | Comparison of LLG, MCLF through blocking probability, $d_{max} = 30$ | 84 |
| 3.8 | Comparison of LLG, MCLF through blocking probability, $d_{max} = 50$ | 84 |
| 3.9 | Comparison of LLG, MCLF through blocking probability and num- ber of frequency channels, $N = 20, d_{max} = 50$ | 85 |
| 3.10 | Comparison of MPM and PIM in terms of P_b ($d_{max} = 30$). | 87 |

| | | |
|------|---|-----|
| 3.11 | Comparison of MPM and PIM in terms of P_b ($d_{max} = 50$). | 88 |
| 3.12 | Comparison of MPM and PIM in terms of E_s ($d_{max} = 30$). | 88 |
| 3.13 | Comparison of MPM and PIM in terms of E_s ($d_{max} = 50$). | 89 |
| 3.14 | Comparison of MPM and PIM in terms of Y ($d_{max} = 30$). | 89 |
| 3.15 | Comparison of MPM and PIM in terms of Y ($d_{max} = 50$). | 90 |
| 4.1 | A node with several flows sharing a common channel | 95 |
| 4.2 | Example network topology organized into “clusters” | 105 |
| 4.3 | Sample network topology for simulation | 114 |

Chapter 1

Introduction

The abundance and variety of information services provided by the Internet along with the possibility to access such services via light, hand-held, cord-less devices such as portable computers, mobile phones and personal digital assistants (PDAs), have transformed wireless communication systems into a prominent part of any state of the art network. The studies and the developments in wireless networking have primarily been driven by the success of the dominant cellular architecture model. Thus, although significant progress has been achieved in the thorough understanding of wireless networking characteristics through the study of cellular systems, many of the developments are still not directly applicable to satisfy the needs of wireless systems that require network architectures which may not follow the cellular paradigm. Such networks, sometimes referred to as wireless *ad-hoc*, or *peer-to-peer*, or *multi-hop* networks, consist entirely of wireless and often mobile nodes that may communicate either directly or via multiple hop paths that require the support of intermediate nodes to achieve connectivity.

Wireless ad-hoc networks are autonomous systems of fixed or mobile wireless nodes with routing capabilities, that may operate in a stand-alone fashion or as

part of a larger heterogeneous network (e.g. in hybrid configurations). Although their development was initially driven by the needs of military networks (prior term used to describe them was *packet radio networks*), they are expected to embrace commercial systems as well, especially with the evolving use of personal communication services systems. It is envisioned that future applications will not be limited to the needs of the military (wireless digital battlefield, war-fighter's wireless internet etc.) but will include several civilian applications as well. For instance they can be deployed in collaborative network scenarios (e.g. conferences or company meetings) where individual users need to share or exchange information without depending on a local network of access points. They are a viable solution in situations of emergency and rescue operations where the infrastructure-based network may not be available. Ad-hoc networks can also serve as platforms for micro-sensor networks that can be deployed in remote or inaccessible areas to collect, process and transmit various signals (e.g. acoustic, seismic etc.) for multiple purposes. And there are many more potential applications such as home networks of heterogeneous devices, industrial robotics and others.

The all-wireless architectures studied here exhibit several noticeable characteristics that make them quite different from existing cellular systems and wireless LANs ([1]). In wireless ad-hoc networks the existence of a link between any two nodes depends on a multitude of parameters, such as transmission power level, distance from the receiver, interference from other transmitters, propagation effects (e.g. multipath, shadowing etc.), type of antennas being used (e.g. omnidirectional or highly-directional) etc. Nodes may move frequently and in an arbitrary fashion and/or may select to turn their power "OFF" at any time in order to conserve their battery reserves. Thus, the ad-hoc network topology is not stable,

may change randomly and unpredictably and consists of varying capacity links. Moreover, even if the physical locations of the nodes are fixed, the availability of a link is not only a function of the signal transmission parameters and the propagation effects, but also depends on the status of node resources, such as radio transceivers (ie. transmitter-receiver pairs), available bandwidth and energy reserves. In fact, in most of the situations, wireless ad-hoc networks have to operate under the stringent constraint of limited network resources. For example, wireless nodes cannot be equipped with large numbers of transceivers since this would increase dramatically their cost and restrict their portability. At the same time, nodes operating on battery power will possibly have as their primary objective the conservation of their energy reserves rather than routing performance. In addition to these constraints, bandwidth is typically scarce and must be used efficiently so that effects such as co-channel interference or link congestion, which have direct impact on network performance, are avoided.

Another crucial issue in wireless ad-hoc networks is the lack of a central coordinator node. Although in some situations there may or may not be certain nodes in role of local coordinators (similar to that of a base station), protocols designed to perform network control and signaling functions must operate in a distributed fashion. The overhead associated with collecting and maintaining global network state information prohibits the use of schemes that control operation through a central controller node. Moreover, distributed algorithms that do not depend on the status of a single node are not directly affected by individual node/link failures that occur quite often in such environments.

The distinguishing features of multi-hop wireless network architectures give rise to new trade-offs between traditional concerns in wireless communications (such as

spectral efficiency, and energy conservation) and the notions of routing, scheduling and resource allocation. It is the purpose of this work to identify and study some of these novel trade-offs and propose solutions in the context of network control. To these ends our work focuses on the following issues:

- **Energy-constrained operation:** Wireless ad-hoc networks must fulfill their communication requirements under the constraint of finite battery life. The fact that most nodes are likely to play the role of a relay node, having to draw on their energy resources even when they do not need to engage in communication activity themselves, illustrates the importance of energy efficiency. Although energy conservations are really important, improvements in battery technology are not always sufficient to support the demand for wireless devices with enhanced capabilities (support of multimedia traffic for example). Therefore the possibility to design network control functions (such as routing, scheduling and resource reservation) in a way that takes into consideration energy expenditures presents a novel opportunity.
- **Shared medium and limited bandwidth:** Due to the broadcast nature of the wireless channel, communication is “node-based”; when omnidirectional antennas are being used every transmission by a node can be received by all nodes that lie within its transmission range. Nodes need to use efficient channel access mechanisms to schedule their transmissions effectively so that the parallel objectives of minimizing interference and utilizing the bandwidth efficiently are satisfied. Moreover, the consequences of signal power levels on bandwidth allocation schemes must be thoroughly investigated.
- **Fairness and link bandwidth management:** Ad-hoc networks will be ex-

pected to provide integrated services and support heterogeneous users with different Quality-of-Service (QoS) requirements. Therefore, packet scheduling and access control mechanisms must be developed that provide fair access to the available bandwidth and at the same time are capable of adapting to channel and topology characteristics, such as location-dependent and bursty channel errors and local congestion. The possibility to develop such schemes that interact with the routing algorithms and adjust their schedules based on the current route assignments as well as the flexibility to adjust the routes upon changes in traffic requirements and/or network conditions must be investigated.

Throughout this work, we explore these new networking trade-offs and propose solutions, in the context of network control, that have a direct impact on the performance and functionality of wireless multi-hop networks. In certain cases, our approach departs from the traditional layered structure in that we jointly address connectivity properties and transmission power selection (a physical layer function), bandwidth reservation, (a MAC layer functions) and route discovery (network layer). Our ultimate objective is to quantify and analyze the new networking trade-offs that arise in this type of wireless systems and evaluate network performance measures as functions of these trade-offs.

1.1 Summary and organization of dissertation

With this background, the dissertation is organized in three chapters. In the first chapter we present a detailed study of the problem of routing connection-oriented traffic with energy efficiency. We assume that bandwidth resources are plentiful

and propose a framework for developing algorithms that determine appropriate connection paths relying only on local information. A simulation tool, developed for the purposes of this work, is used to model the proposed algorithms for a variety of network examples. Performance is captured by the average blocking probability and the average energy expenditures and our performance analysis illustrates the trade-offs between these two measures and leads to important conclusions on the design of energy-efficient wireless systems.

In the second chapter, we study the effects of limited bandwidth resources on energy-efficient routing algorithms, again for the case of session-oriented traffic. We assume that nodes must schedule their transmissions in a “conflict-free” fashion, by selecting frequency channels among a limited set and develop algorithms that address the problem of efficient channel allocation over selected routes. The algorithms are compared via simulations and are also evaluated against mechanisms that exhaustively search the state space for the optimum solutions.

Finally, the third chapter describes a “blueprint” towards a unified approach to the problem of fair scheduling, access control and routing in ad-hoc networks carrying packet-switched traffic. We review related research work on fair scheduling and capacity allocation for various networking environments and discuss the difficulties in adapting existing algorithms to wireless ad-hoc networks. A methodology of addressing the dependencies between the scheduling and the routing mechanisms is proposed and a preliminary performance analysis of an algorithm based on this methodology is provided.

Chapter 2

Energy-Efficient Routing of Connection-Oriented Traffic, Part I: Limited Transceiver Resources

2.1 Motivation and objectives

Energy efficiency is important in the design of battery-operated wireless devices that are used in wireless networks. While users' demand for improved and more sophisticated functionalities of wireless devices increases rapidly, improvements in battery technology come at a slower pace. Therefore the possibility to design and evaluate network control functions (such as routing, scheduling and resource allocation mechanisms) in a way that takes into consideration energy expenditures presents a novel opportunity.

This chapter addresses the problem of energy-efficient routing of connection-oriented traffic in wireless ad-hoc networks, a typical paradigm of networks whose performance and functionality depends crucially on battery power. The fact that most nodes are likely to play the role of a relay node, having to draw on their energy resources even when they do not need to engage in communication themselves, illustrates the importance of energy efficiency.

A crucial choice in wireless transmission is that of RF power level. Due to the nonlinear attenuation of the received signal power with distance, a transmission over multiple short hops may require less total power than a single transmission over one long hop. On the other hand, multiple short transmissions could result in significant overhead and routing complexity along with utilization of a larger amount of network resources, thereby potentially increasing the overall energy consumption. Note also that nodes consume energy not only during transmission, but also when they receive, store and process information. The use of sophisticated algorithms that deal with congestion, or of more efficient coding schemes that perform better in bandwidth constrained links, results in needs for additional processing by the wireless routers and hence in demand for more energy. Nodes that have to relay information have to dedicate part of their transceivers for this purpose. Therefore, it is quite possible that some nodes will be over-used for routing functionalities, while other will remain idle for longer intervals, due to the topology characteristics. Such an “unfair” utilization could cause certain users to exhaust their energy reserves and be forced to turn their radios “OFF” which could invoke severe performance degradation or even network partitioning.

Another crucial issue associated with the choice of the transmission power level is the interference caused to non-intended recipient nodes located in the vicinity of the transmitter, unlike wire-line networks where a link connecting two nodes is exclusively used by them. Hence, transmitting at higher power reduces the efficiency of bandwidth re-use and causes increased interference for a fixed allocation of bandwidth resources. On the other hand, if a path consisting of multiple short hops is used, the total power required for transmission may be lower, but there is need for efficient scheduling mechanisms to avoid conflicts among consecutive links

of a path.

The focus of this work is on source initiated unicast (single source and single destination) connection-oriented traffic. Our objective is to develop routing algorithms that are capable of identifying paths connecting the source to the destination that provide the required resources from end to end, and subsequently keep them reserved until the completion of the session. Such resources in a wireless environment are represented by node transceivers, energy reserves and bandwidth availability (frequency channels, time slots or orthogonal CDMA codes, depending on the multiple access scheme assumed).

In order to assess the already complex trade-offs one at a time, we start this study by assuming plentiful bandwidth resources and we focus our attention to the case of limited number of transceivers. Once a good framework has been defined for our algorithms, we incorporate the effects of limited bandwidth (in chapter 3). The rest of the introductory discussion continues with a brief overview of related work in the area of energy-efficient routing, followed by a summary of our approach and our assumptions.

2.1.1 Related work

Related work on multi-hop networks that support connection-oriented traffic is for multicast routing. In [2], Wieselthier *et. al.* study the effects of wireless network characteristics and of energy constraints on multicast protocol operation and propose an algorithm that exploits the node-based nature of wireless communications for multicasting. In [3], a set of algorithms is proposed for the construction of minimum energy broadcast and multicast trees, which is extended in [4] to capture the

effects of limited bandwidth resources. In [5], multicast routing algorithms that use capacity results for multiuser detectors are developed. A variety of approaches for energy efficiency in packet-switched networks have been presented in [6], [7], [8] and [9]. In [6], an algorithm is proposed that given a randomly deployed ad-hoc topology finds a graph that contains the minimum power paths from each node to a master site. In [7] and [8], the authors propose a suite of algorithms that based on network flow theory try to balance the minimum lifetime of each flow path, by redirecting or augmenting the flow of certain paths and by identifying traffic splits that optimize energy consumption. However, these principles cannot be applied in the case of sessions where a path must be reserved end-to-end for the whole duration of a session. A different approach is taken in [9] where a model is presented that overcomes the complication that arises with the interference caused by increasing the traffic on a link. This model allows extension of optimal routing methodology for wire-based networks to do minimum-energy-and-delay routing for packet radio networks.

2.1.2 Research contributions

The ultimate objective in traditional circuit-switched networks (e.g. telephony networks) is to route the traffic in a way that the overall blocking probability is minimized. In our study, in addition to minimizing blocking probability, we want to achieve it with the minimal energy expenditures and our equivalent objectives are (i) to maximize communication performance subject to limited energy and (ii) to minimize required energy to meet prescribed communication performance.

The algorithms we propose jointly address the issues of transmission power levels (a physical layer function), route discovery (a network layer function) and re-

source reservation (a MAC layer function). In particular, each node determines its transmission power and next-hop neighbor, based on local information of network parameters (ie., transmission power, energy reserves, availability of transceivers and frequency channels), with the objective of identifying unicast routes that optimize performance as captured by the overall blocking probability and the average energy expenditures. Our approach is characterized by three innovative features. First, we address the unicast problem which is not characterized by the combinatorial complexity of multicasting; in fact under simplifying assumptions regarding interference and node resources minimum-energy solutions can be found. However, the reduced amount of complexity allows us to extend our approach to study also the effects of local interference and limited node resources (e.g. transceivers) without the additional requirements that multicasting would impose. Moreover, even though some objectives may be parallel to those encountered in the multicasting problems, the actual algorithms, metrics and trade-offs are quite different as we will see in the sequel. Secondly, we convert session routing to link metric based, even though algorithms based on minimum-distance paths are normally intended for packet-switched networks (where the cost of using a link is typically the estimated packet delay). In particular, in telephony networks it is hard to define such metrics since energy is not a concern and delay is not an appropriate metric. Unlike telephone networks, we are able to map the overall objectives (blocking probability and energy consumption) to individual link metrics. Finally we evaluate the effects of receive and processing power in addition to transmission power. Even though processing power typically depends on a set of network parameters, we consider constant energy depletion rate per node (for receiving and signal processing) and observe its effects on the performance of our algorithms.

We concentrate our effort on developing algorithms for wireless static topologies, without considering the effects of mobility. As we have seen in our prior work ([10],[11]), mobility effects can be addressed through the use of soft-failure mechanisms. In a sense, the efficiency of an algorithm is determined by how effectively it reacts in the event of topological changes by rerouting ongoing sessions to new paths. The possibility to use the transmission power (or the residual energy) as a factor to decide on selecting a path adds a new degree of flexibility. In fact, in the case of a link failure we may either adjust the power to maintain connectivity or choose to reroute along an alternative path, depending on the current circumstances. A similar approach has been presented in [10],[11] and has been shown to yield satisfactory results in the case of relatively low mobility. Nonetheless, there are wireless ad-hoc networks (such as sensor networks) that are inherently static and involve no mobility.

2.1.3 Outline of the chapter

Following the introductory discussion, the rest of the chapter is organized as follows. In the next section we define our wireless network model and discuss some basic assumptions on link existence and resource modeling. In the sequel, we give an initial high level description of our algorithm and discuss the difficulties in obtaining exact optimal solutions. We continue with a detailed discussion of our heuristic approach and analyze the properties of the proposed link metrics that are used towards route selection. Following the algorithm description, we describe our simulation model (a more detailed section on the simulation model has been placed in the appendix) and then proceed to a detailed analysis and discussion of performance results. We conclude the chapter with a summary of the most

significant results along with ideas for future research.

2.2 Wireless network model

We consider a network consisting of N nodes randomly deployed over a given area. Connectivity of the network depends on the Euclidean distance between nodes, the maximum transmission power level and the minimum required received power at a node. Throughout our study, we assume that all nodes may transmit at any power level P which may not exceed a maximum value P_{max} , equal for all nodes. Received signal power varies as $d^{-\alpha}$, where d is the Euclidean distance between transmitting and receiving node and α is the path-loss exponent. Assume here that the path loss depends only on the distance between transmitter and receiver ignoring for simplicity any possible antenna height difference which would make the dependence three-dimensional. Note also that our algorithms will be independent of the value of α , so that they are applicable in various propagation environments. Additionally, α is considered constant throughout the region of interest, there are no obstacles and the antennas are omnidirectional so that all nodes within communication range of the transmitting node can successfully receive the transmission.

Given the value of P_{max} , the distances between nodes and the minimum required received power for error-free communication, we can determine the communication range of all nodes and the connectivity of the network. For notation purposes we define the set $\mathcal{R}^{(i)}$ of node i to be the set of nodes within transmission range of i . We assume that the existence of a link depends solely on the distance the transmission power and the path-loss exponent, therefore all links can be considered bi-directional and the set $\mathcal{R}^{(i)}$ of node i can be thought of as the set of

nodes to which i can transmit or from which it can receive. For example in the topology depicted in figure 2.1, $\mathcal{R}^{(3)} = \{1, 2, 4, 5\}$ and $\mathcal{R}^{(6)} = \{4, 5, 7, 8\}$. Note that different values of P_{max} result in different connectivity maps and for node i all nodes in $\mathcal{R}^{(i)}$ are considered one-hop neighbors of i . Node i may successfully transmit to node $j \in \mathcal{R}^{(i)}$ provided $P_{ij} < P_{max}$.

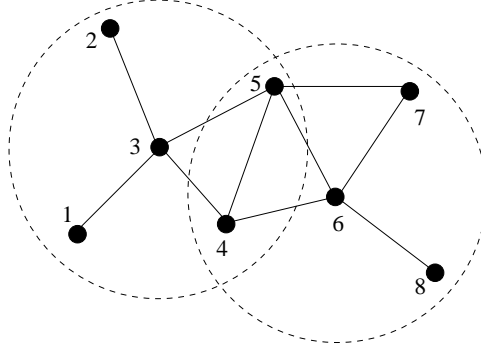


Figure 2.1: Connectivity properties and maximum transmission range

Complete knowledge of the set of neighbors located within transmission range indicates the potential recipients of a transmission but is not sufficient for determining whether a connection can be established, since the required resources must also be available. Recall that in this chapter we have assumed no interference conditions (ie unlimited bandwidth resources) and therefore nodal resources are modeled by:

- (a) **Transceivers:** node i has C_i communication transceivers and can therefore support up to C_i sessions simultaneously. The number of “reserved” or “occupied” transceivers (B_i) varies with time according to the network state. We denote by R_i the residual capacity of each node, ie the number of free transceivers; thus $R_i = C_i - B_i$.

- (b) **Energy:** at time t , node i has a residual amount of energy $E_i^R(t)$, which may be used for transmission or processing of information. The initial amount of energy available to node i is denoted by $E_i^o = E_i^R(0)$. We assume that all nodes keep track of their residual energy at all times and only nodes with nonzero residual energy can participate in the network.¹

Sessions are source-initiated and all nodes generate connection requests according to independent Poisson distributions with average rate λ . The durations of the sessions are exponentially distributed with average value μ and the destination of every session is chosen uniformly among the remaining nodes. In order to admit a session request, a path p must exist from the source to the destination that meets the following requirements:

- all nodes $i \in p$ must have one transceiver available for use at the time of the request, which will be reserved throughout the duration of the session, ie $\forall i \in p, R_i \neq 0$,
- all nodes $i \in p$ must have nonzero residual energy, ie $\forall i \in p, E_i^R(t) \neq 0$.

Each node maintains up-to-date information about the identities of its one-hop neighbors, its required transmission power levels, its residual capacity and residual energy. All nodes periodically broadcast updates of the above information to the nodes that are located within transmission range, so that they are used by the routing protocol. This can be implemented via an underlying link-level mechanism that is not the purpose of this study.

¹modern battery-monitoring technology permits accurate knowledge of battery energy reserves

2.3 Proposed algorithms

2.3.1 Overview

Our objective is to develop algorithms that achieve good communication performance subject to constraints in energy consumption. Therefore our performance measures must reflect the characteristics of the routing problem as well as the energy consumption limitations. Such measures would be the call blocking probability P_b and the average energy per session E_s . Alternatively, we can define a global reward function (a performance “yardstick”) that couples P_b and E_s , as follows:

$$Y = \frac{1 - P_b}{E_s} \quad (2.1)$$

In fact, Y can be viewed as the average acceptance ratio per energy unit consumed and the algorithm objective is translated to selecting routes in a way that the reward function Y is maximized.

A first alternative towards maximizing Y , is to develop a greedy algorithm that attempts to maximize the reward associated with each newly arriving call. Such an algorithm though would be infeasible (except for the case of trivially small networks) due to the following reasons:

- It would require “global information” on the system state which will not typically be available. Such global information would include the network topology, the required transmission power levels, the amounts of residual energy at each node, the number of available transceivers and the traffic patterns. Moreover, this information should be updated at the arrival and termination of each session.

- Even if we assumed that we had a centralized mechanism that could collect “global information”, the greedy maximization approach would have to perform an exhaustive search of all possible paths (given the current network state) if the true optimal solution was to be found. Such an exhaustive search is infeasible unless we consider trivially small topologies.

The second alternative is to concentrate our efforts on developing distributed heuristics that rely only on local information to select a route. Each link (i, j) is associated with a distance metric that indicates the cost of using that link and may incorporate local information of the transmission power, the residual energy and/or the availability of transceivers. If the cost of using link (i, j) is denoted by $D_{i,j}$, the cost of using a path p consisting of M nodes i_1, i_2, \dots, i_M (see figure 2.2) will be given by

$$\mathcal{C}_p = \sum_{(i,j) \in p} D_{ij}. \quad (2.2)$$

Given the selection of the link metric, distributed Bellman-Ford [12] algorithm can be applied for shortest-path computation.

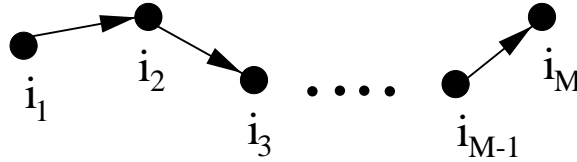


Figure 2.2: Path cost computation

Note here, that although algorithms based on minimum-distance paths are normally intended for packet-switched networks (where the cost of using a link is typically the estimated packet delay), we are using this approach for connection-

oriented traffic, by defining a cost for each link that involves various local parameters. In telephony networks such a metric is hard to define since energy is not a concern and delay is not an appropriate metric. Therefore, in the telephone network the overall objective (blocking probability) cannot be directly mapped to individual link metrics.

It is very difficult to predict a priori which link metric will result in better performance. This can only be done by extensive simulation comparison. In the subsequent sections we define a set of candidate link metrics and compare them via simulation.

2.3.2 Link metrics

A call request is rejected only if no path exists between source and destination with available transceivers at each node. Note that if the number of transceivers per node was large enough, so that availability was always guaranteed (ie no blocking at all), the problem of minimum energy routing would reduce to determining the minimum total power path and all calls would be admitted and completed with minimum energy expenditures ². When the nodal capacity is finite (as it is in our case) some nodes have temporarily no transceivers available and they cannot route or place any new calls. Since the minimum power path will not always be available, we can search for the lowest total power path in the subgraph defined by the nodes with nonzero residual capacity and energy and their corresponding links. In all the proposed metrics, a link that consists of at least one node with zero residual capacity or residual energy will have an infinite cost.

²provided that all nodes had still some energy reserves

(a) Metric M1

Based on the above remarks, we first define link metric **M1** which is a direct measure of the power needed to transmit over a link, provided both nodes have nonzero residual capacity and energy. Hence the cost of using link (i, j) is defined by:

$$D_{ij}^{(1)} = \begin{cases} P_{ij} & \text{if } R_i, R_j \neq 0 \text{ and } E_i^R, E_j^R \neq 0 \\ \infty & \text{otherwise} \end{cases} \quad (2.3)$$

where P_{ij} is the power that i needs to transmit to j .

M1 will always provide the minimum power path available, which might not always be advantageous in terms of overall network performance. A minimum power path will usually be a multi-hop path as we previously observed and therefore will occupy more network resources, which could result in blocking of more new calls. It is also possible, depending on the traffic patterns, that some paths get heavily utilized and act as bottlenecks (in a static topology the minimum power path will be the same until any node is blocked), while others consist of lightly used nodes. Finally, if processing power is not negligible compared to transmitter power, multi-hop paths could sometimes result in larger energy expenditures.

(b) Metric M2

To address the problem of congested nodes, we define link metric **M2** which attempts to discourage use of heavily used paths. Metric **M2** is defined by:

$$D_{ij}^{(2)} = \begin{cases} \frac{P_{ij}}{\min\{R_i, R_j\}} & \text{if } R_i, R_j \neq 0 \text{ and } E_i^R, E_j^R \neq 0 \\ \infty & \text{otherwise} \end{cases} \quad (2.4)$$

M2 favors links that are not heavily utilized by increasing the cost of links that connect nodes with smaller residual capacity, trying this way to spread the offered traffic evenly over all paths.

(c) Metric M3

Both M1 and M2 rely on the power level required to successfully transmit to a one-hop neighbor but ignore an important parameter of the receiving node: its residual energy. Under certain circumstances, it may be preferable to route a call over a path that consists of nodes with larger amounts of residual energy, even though this may result in additional energy consumption by the session. Such a feature could be used to avoid loading nodes that are low on energy reserves and we wish to make conservative usage of the remaining energy in order to prolong their lifetime.

To these ends we propose the use of link metric M3 which is defined by:

$$D_{ij}^{(3)} = \begin{cases} W_p \frac{P_{ij}}{P_{max}} + W_e \frac{E_j^o}{E_j^R} & \text{if } R_i, R_j \neq 0 \text{ and } E_i^R, E_j^R \neq 0 \\ \infty & \text{otherwise} \end{cases} \quad (2.5)$$

W_p and W_e are weights that may be adjusted to favor either of the two terms. Note that in the beginning of network operation the second term is equal for all nodes (with value 1) and therefore our metric is similar to M1. As the residual energy of every node begins to drop, the second term will increase and when the amount of residual energy is low the cost of using the link will become very high. M3 attempts to introduce some fairness considerations in node usage, so that the contribution of each node to the aggregate energy consumed by the network is as even as possible, provided the traffic requirements are uniform.

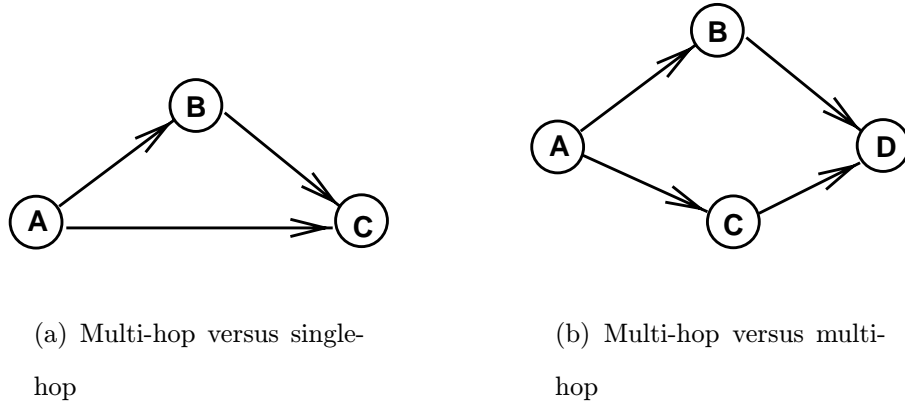


Figure 2.3: Example illustrating properties of M3

Properties of M3

Metric M3 exhibits some important features that have a direct impact on performance, depending on the connectivity map of the topology under consideration. Even though the intuition for this metric was to “favor” paths that consist of nodes with higher levels of residual energy, we can prove that if the algorithm has to choose between a direct-hop path and a multi-hop path, then M3(1,1) will always select the former. To see why this is true, let us consider the example shown in figure 2.3.

Consider nodes A,B,C as shown in the figure and let P_{AB} , P_{BC} and P_{AC} be the powers needed for the respective transmissions. Consider also two possible paths from A to C: $p_1(A \rightarrow B \rightarrow C)$ and $p_2 : (A \rightarrow C)$. Let’s assume that $P_{AC} > P_{AB} + P_{BC}$. Then if we use metric 3 the costs of paths 1 and 2 are given by:

$$C_{p_1} = \frac{P_{AB}}{P_{max}} + \frac{E^o}{E_B^R} + \frac{P_{BC}}{P_{max}} + \frac{E^o}{E_C^R}$$

$$C_{p_2} = \frac{P_{AC}}{P_{max}} + \frac{E^o}{E_C^R}$$

To compare the path costs:

$$D_C = C_{p_2} - C_{p_1} = \frac{P_{AC} - (P_{AB} + P_{BC})}{P_{max}} - \frac{E^o}{E_B^R}$$

But

$$0 \leq \frac{P_{AC} - (P_{AB} + P_{BC})}{P_{max}} \leq 1$$

and

$$1 \leq \frac{E^o}{E_B^R} < \infty$$

Therefore

$$D_C = C_{p_2} - C_{p_1} < 0 \rightarrow C_{p_2} < C_{p_1}$$

The above example can be easily generalized in the case when the comparison is between a path with a direct link versus a path with M links where $M \in [2, N-1]$.

Proposition: Let p_1 denote a multiple hop path from A to B ($p_1 : (A \rightarrow X_1 \rightarrow X_2 \rightarrow \dots \rightarrow X_{N-1} \rightarrow B)$) and p_2 a direct path (single link) from A to B ($p_2 : (A \rightarrow B)$) and let $P_{AB} > P_{AX_1} + \sum_{i=1}^{N-2} P_{X_i X_{i+1}} + P_{X_{N-1} B}$. If the link cost is given by metric M3(1,1) (equation 2.5) then $C_{p_1} > C_{p_2}$ will always hold.

Proof: Applying the definitions we have:

$$C_{p_1} = \frac{P_{AX_1} + \sum_{i=1}^{N-2} P_{X_i X_{i+1}} + P_{X_{N-1} B}}{P_{max}} + E^o \left(\sum_{i=1}^{N-1} \frac{1}{E_i^R} + \frac{1}{E_B^R} \right)$$

$$C_{p_2} = \frac{P_{AB}}{P_{max}} + \frac{E^o}{E_B^R}$$

To compare the path costs:

$$D_C = C_{p_2} - C_{p_1} = \frac{P_{AB} - (P_{AX_1} + \sum_{i=1}^{N-2} P_{X_i X_{i+1}} + P_{X_{N-1} B})}{P_{max}} - \sum_{i=1}^{N-1} \frac{E^o}{E_i^R}$$

But

$$0 \leq \frac{P_{AB} - (P_{AX_1} + \sum_{i=1}^{N-2} P_{X_i X_{i+1}} + P_{X_{N-1} B})}{P_{max}} \leq 1$$

and

$$N \leq \sum_{i=1}^{N-1} \frac{E^o}{E_i^R} < \infty$$

Therefore

$$D_C = C_{p_2} - C_{p_1} < 0 \rightarrow C_{p_2} < C_{p_1}$$

Q.E.D.

Despite this limitation, M3 is very appropriate in situations when the comparison is between multiple multi-hop paths. In that case the above proposition does not apply and the factor which has a large impact on the decision is the residual energy of the relay nodes. To illustrate this better, consider for example the case of two multi-hop paths p_1 and p_2 as shown in figure 2.3, where both paths have the same number of hops (2-hops). Hence let $p_1 : (A \rightarrow B \rightarrow D)$ and $p_2 : (A \rightarrow C \rightarrow D)$. Here the critical parameter is the residual energy of

the intermediate node of each path and of course the difference in the sum of the transmission powers of each path.

$$D_C = C_{p_2} - C_{p_1} = \frac{(P_{AC} + P_{CD}) - (P_{AB} + P_{BD})}{P_{max}} + \left(\frac{E^o}{E_C^R} - \frac{E^o}{E_B^R} \right)$$

Even though the first term of the above equation will be $\in [-2, 2]$ we cannot determine for sure whether D_C will be positive or negative unless we know the values of E_B^R and E_C^R .

2.4 Simulation model

We have evaluated the performance of the proposed algorithms for a variety of network parameters such as network size, node density, traffic load, transmission power level and initial energy resources. We consider random network topologies, by generating each node's location randomly within a square region of size 100×100 units. We assume that the existence of a link between any two nodes depends solely on their Euclidean distance and the propagation loss exponent is taken $\alpha = 2$. All links are full-duplex and error-free and without loss of generality, let a node transmitting at a power level of $P_o = 0.1$ be received by all nodes located within distance $d \leq d_o = 10$ units. Using this value as a reference, we may compute the transmission range d_{max} corresponding to a given P_{max} by,

$$\frac{P_{max}}{P_o} = \left(\frac{d_{max}}{d_o} \right)^2 \quad (2.6)$$

For example if we want a node's transmission range not to exceed 30 units, its maximum transmission power level must not exceed $P_{max} = 0.9$.

In order to model both sparse and dense topologies, we present results for networks of $N = 10, 20$ and 50 nodes and for transmission range values (d_{max}) between 30 and 70 units, which as we will show have a direct effect on the resulting average node degree and the connectivity of the network.

For every network size, we generate 100 random topologies. Note that we are only interested in connected topologies (performance of a partitioned network in which not all nodes may communicate with each other was not considered). Each simulation runs until 20000 call requests have been scheduled, which was determined to be a sufficient amount of offered load in all the experiments, so that transient effects can be neglected.

All nodes have equal amounts of initial energy E^o and unless otherwise specified this energy level is sufficient for the duration of the simulation. We assume initially that energy is only consumed during transmission and for the whole duration of a session. For example, a session from node i to node k via node j that lasts for t time units would consume $E = (P_{ij} + P_{jk}) \times t$ units of energy. The effects of receive and processing power are incorporated in a separate section. Finally each node is assumed to have a total of five transceivers ($C = 5$).

We have assumed in all the simulations that calls arrive independently at each node following a Poisson distribution with average rate λ such that $0 \leq \lambda \leq 1$. Average session durations are exponentially distributed with $\mu = 1$. For every new call arrival, the destination is uniformly selected among the remaining nodes.

Performance is measured by the blocking probability P_b , the average energy per session E_s and the performance yardstick Y that we defined in equation 2.1. In some of the experiments we were also interested in additional performance metrics,

such as the the average lifetime of the nodes and the network or the average number of links per path.

A discrete-event simulation tool has been developed in ANSI C for the purpose of performance measurements. An overview of the model structure and a description of the main routines and components is provided in the appendix.

2.5 Performance results

2.5.1 Blocking probability (P_b)

In this section we examine the algorithm performance in terms of blocking probability versus network parameters, such as the average call arrival rate, the maximum transmission power, the network size and the node density. We compare M1, M2 and two different cases of M3; one which accounts only for the residual energy of the receiver ($W_p = 0, W_e = 1$) and one that equally considers transmission power and residual energy ($W_p = 1, W_e = 1$).

Figures 2.4 and 2.5 illustrate graphically the blocking probability P_b as a function of the offered load per node, for $N = 20$ and the cases of $d_{max} = 30$ and 50 respectively. The curves plotted in these graphs lead to the following observations:

- In all cases P_b increases as the offered load increases.
- In both graphs M1 exhibits the worst performance among all metrics. The reason is that M1 always searches for the lowest total power path available, which is usually a path with a larger number of hops, and therefore it results in utilization/reservation of larger number of transceivers.

- Use of M1 results also in heavier utilization of some paths while at the same time others may consist of idle nodes. M2 partially solves this problem and the improvement in P_b is larger especially for the case of larger $d_{max} = 50$ (figure 2.5) since increased connectivity provides additional paths and incoming traffic can be spread over the network more effectively.
- M3 achieves much lower P_b , especially when the transmission range increases, mainly because of the inherent property of M3 to favor a direct link from source to destination (if such a link exists which is often the case for high d_{max}), but also because of the property to spread the traffic more evenly among paths in order to balance energy expenditures among all nodes. However, this comes at the cost of higher amounts of energy expenditures as we will see in subsequent results.

Similar conclusions, as far as the relative performance comparison of our metrics is concerned, can be drawn from figures 2.6, 2.7, 2.8 and 2.9, which depict blocking probability versus offered traffic for networks with $N = 10$ and $N = 50$ nodes.

To verify our intuition that M1 and M2 provide on average paths with larger number of hops, we computed the average number of hops per accepted session for the above simulations. Our results are summarized in table 2.1 for the cases of $\lambda = 0.1$ and 0.5 . Each cell in the table consists of the average number of hops per session and the corresponding standard deviation. These results clearly indicate that M1 and M2 tend to utilize paths with larger number of hops.

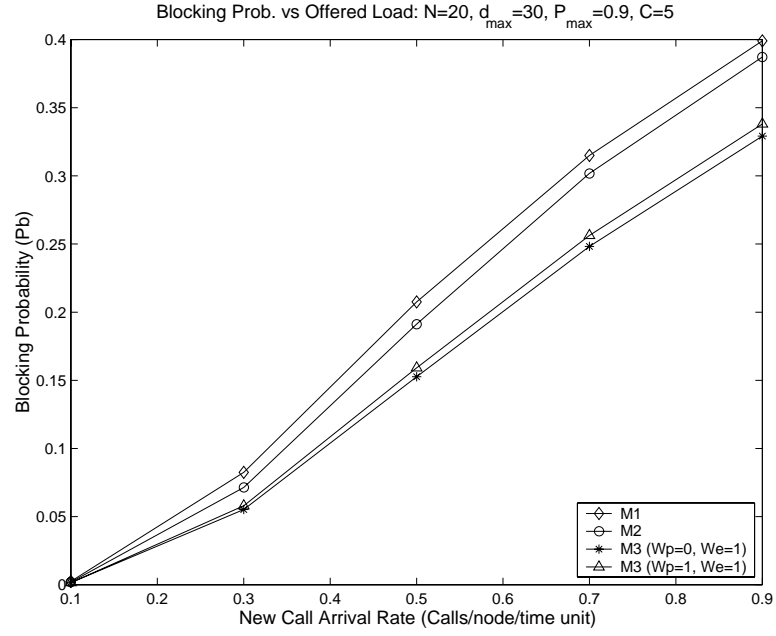


Figure 2.4: Blocking probability vs per node arrival rate, $N = 20$, $d_{\max} = 30$

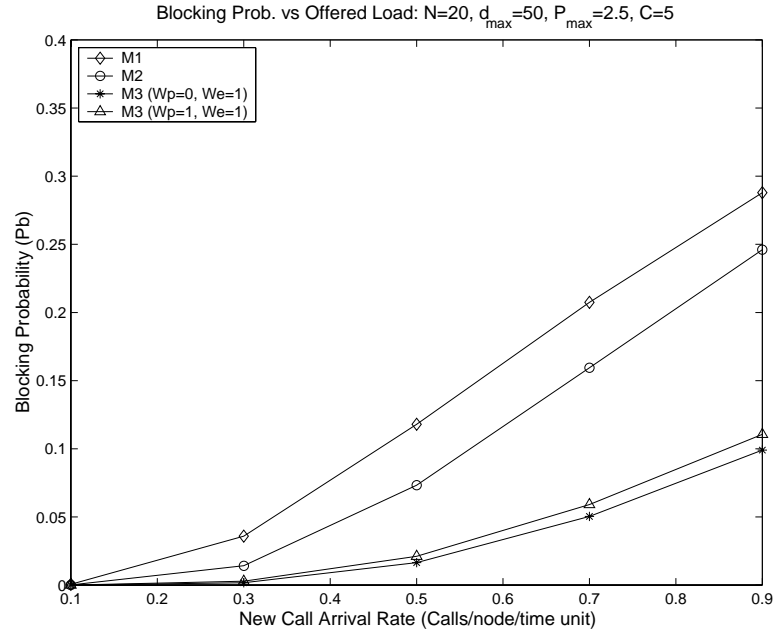


Figure 2.5: Blocking probability vs per node arrival rate, $N = 20$, $d_{\max} = 50$

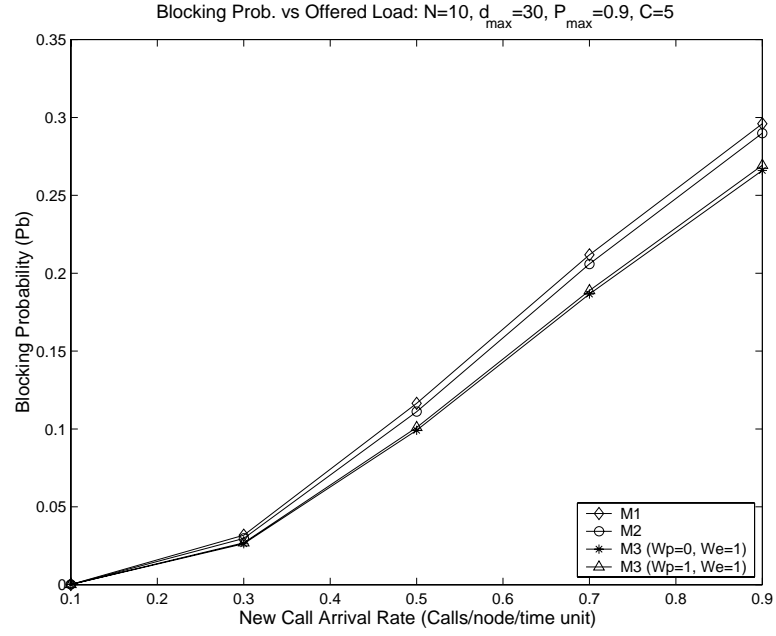


Figure 2.6: Blocking probability vs per node arrival rate for $N = 10$, $d_{\max} = 30$.

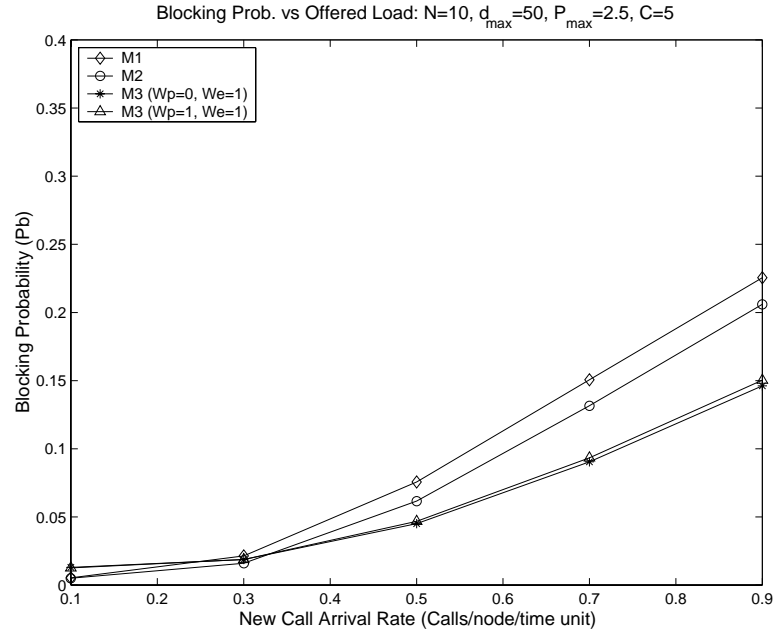


Figure 2.7: Blocking probability vs per node arrival rate for $N = 10$, $d_{\max} = 50$.

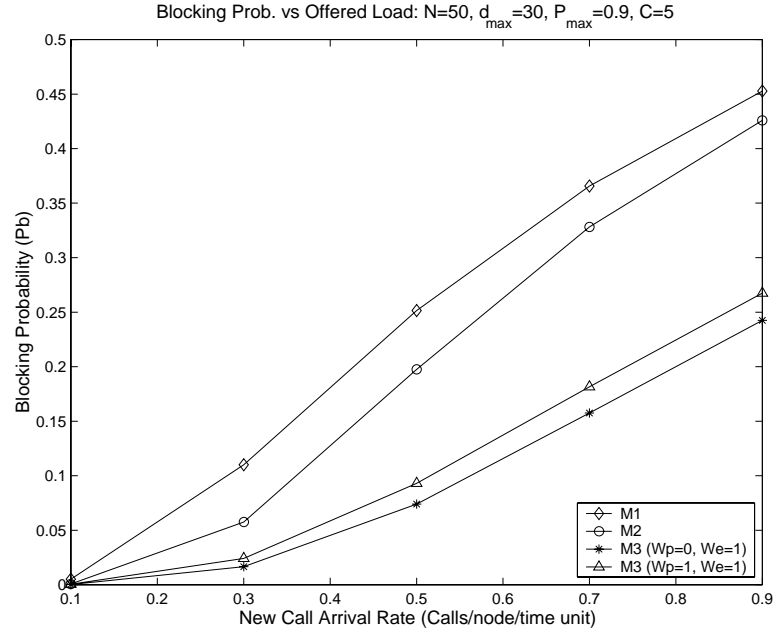


Figure 2.8: Blocking probability vs per node arrival rate for $N = 50$, $d_{\max} = 30$.

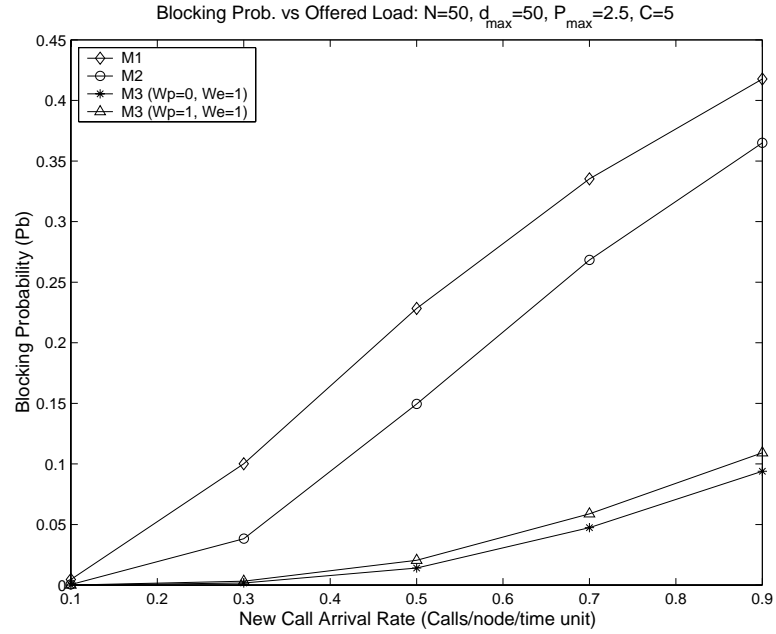


Figure 2.9: Blocking probability vs per node arrival rate for $N = 50$, $d_{\max} = 50$.

| | $\lambda = 0.1$ | | $\lambda = 0.5$ | |
|---------|-----------------|----------------|-----------------|----------------|
| Metric | $d_{max} = 30$ | $d_{max} = 50$ | $d_{max} = 30$ | $d_{max} = 50$ |
| M1 | 4.06 ; 0.59 | 3.89 ; 0.44 | 3.62 ; 0.44 | 3.51 ; 0.36 |
| M2 | 4.10 ; 0.58 | 3.98 ; 0.41 | 3.62 ; 0.42 | 3.46 ; 0.31 |
| M3(0,1) | 2.87 ; 0.38 | 2.79 ; 0.30 | 1.59 ; 0.14 | 1.59 ; 0.14 |
| M3(1,1) | 2.87 ; 0.38 | 2.80 ; 0.30 | 1.60 ; 0.14 | 1.60 ; 0.14 |

Table 2.1: Average number of hops and standard deviation per admitted session for $N = 20$

2.5.2 Average energy per session (E_s)

Figures 2.10 and 2.11 depict the average energy per accepted session (E_s) versus the arrival rate λ , again for $N = 20$ and the cases of $d_{max} = 30$ and $d_{max} = 50$.

We can draw the following remarks from these plots:

- M1 and M2 result in lower energy consumption, since by definition they admit sessions in the lowest transmission power path available. Nonetheless, this comes at the cost of higher P_b as we pointed out in the previous section. The inherent trade-off between P_b and E_s is rather clear from these results and is evaluated separately by examining the behavior of the yardstick Y .
- For the case of lower d_{max} (figure 2.10) we observe that E_s starts exhibiting some decrease with higher values of λ . The reason for such a behavior is that when traffic load (and therefore blocking) is high, calls that require fewer hops from source to destination (ie fewer node resources) have a higher chance of being admitted. For $N = 10$ (sparse topologies) and for low transmission range we do not have significant route redundancy (in fact, the average node

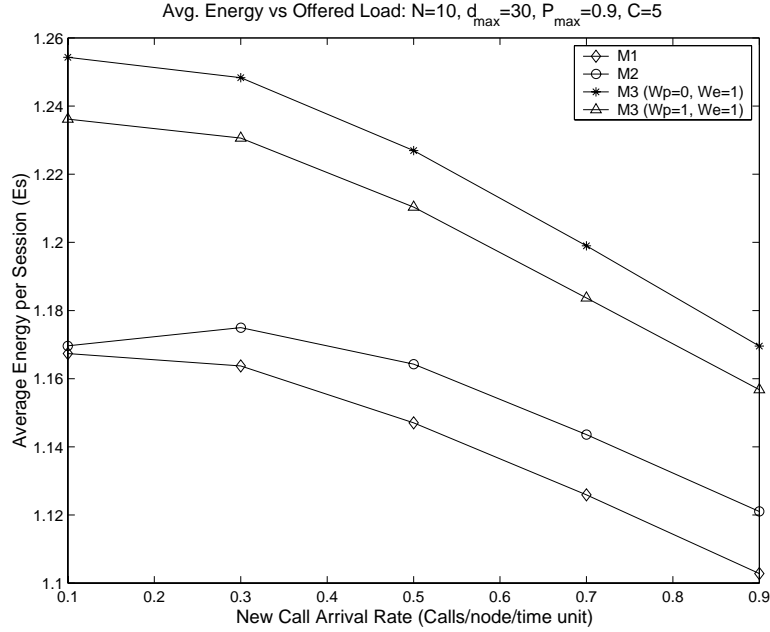


Figure 2.10: Energy per session vs per node arrival rate for $N = 10$, $d_{max} = 30$.

degree over 100 sample networks was measured to be in the range of 2 to 4) By increasing the transmission range (figure 2.11, $d_{max} = 50$), we increase the network connectivity and hence the possibility to select between a multi-hop path and a direct link from source to destination. M1 and M2 primarily search for the multi-hop path (which would lead to lower E_s) and if not available the typical alternative is a direct link (with higher E_s). When P_b is higher the direct link is more likely to exist and this is why E_s exhibits this increase. On the other hand M3 always looks for the direct link first and hence for increased range its behavior is not significantly affected by blocking.

In figures 2.12, 2.13 we present similar results for a topology of 20 nodes and in figures 2.14 and 2.15 for topology of 50 nodes. As far as the relative performance

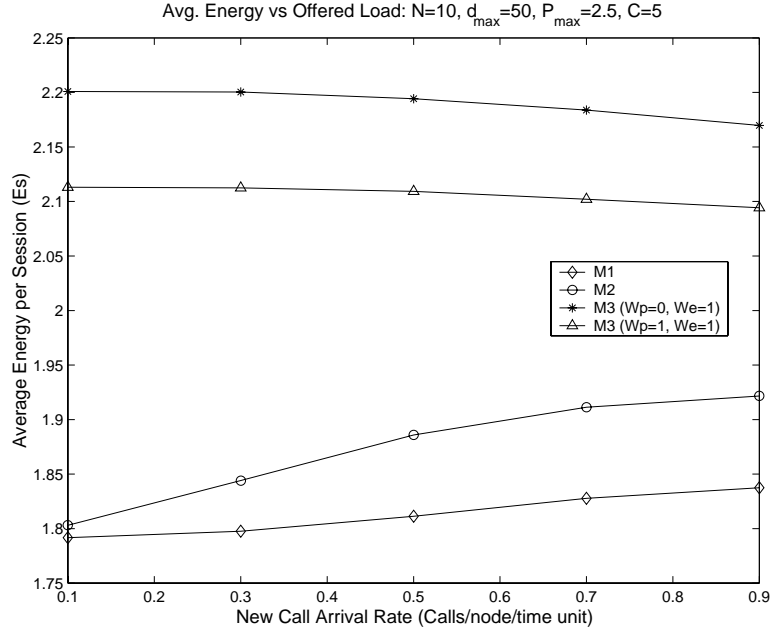


Figure 2.11: Energy per session vs per node arrival rate for $N = 10$, $d_{max} = 50$.

of the metrics is concerned M1 and M2 always outperform M3. It is interesting to notice however that in the case of $N = 50$ even for low d_{max} M1 and M2 increase with blocking, because the node density is very high that if the multi-hop path is blocked it is very likely that a direct link exists.

Finally, note also that M3 performs better in terms of E_s when $W_p = 1$ rather than when $W_p = 0$. Since performance in terms of P_b is almost equivalent (see figures 2.4 and 2.5), we conclude that the first term of M3 should not be completely ignored.

2.5.3 Effect of node density on performance

The variety of results that we obtained, especially when we were evaluating E_s for different network sizes and transmission ranges, have motivated us to look into the

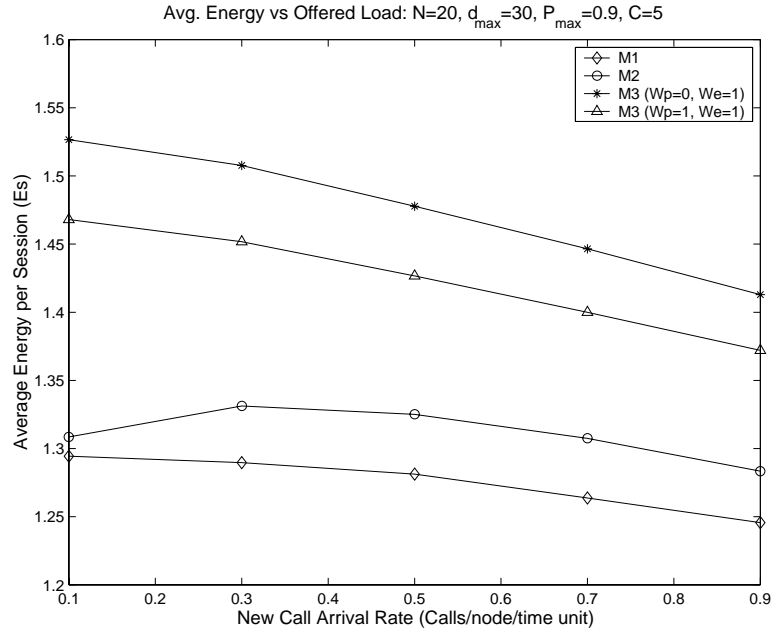


Figure 2.12: Energy per session vs per node arrival rate for $N = 20$, $d_{\max} = 30$.

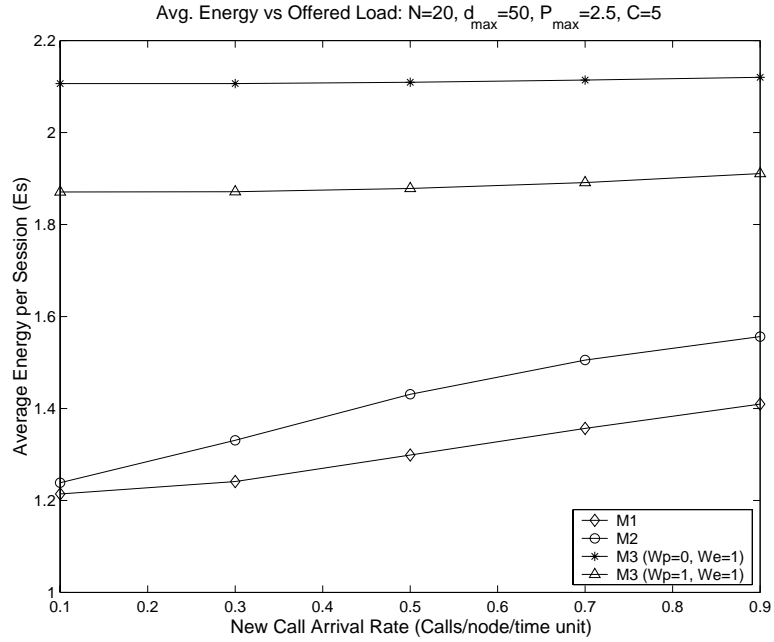


Figure 2.13: Energy per session vs per node arrival rate for $N = 20$, $d_{\max} = 50$.

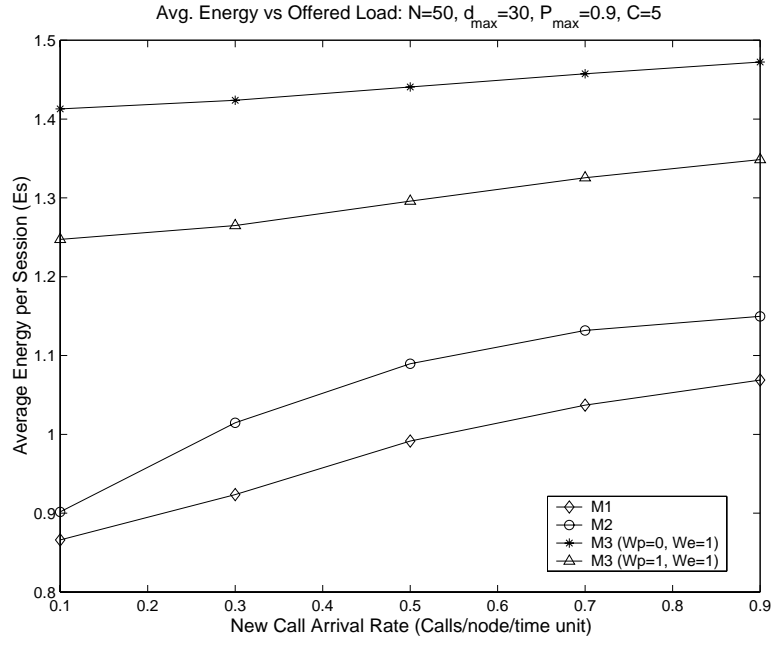


Figure 2.14: Energy per session vs per node arrival rate for $N = 50$, $d_{\max} = 30$.

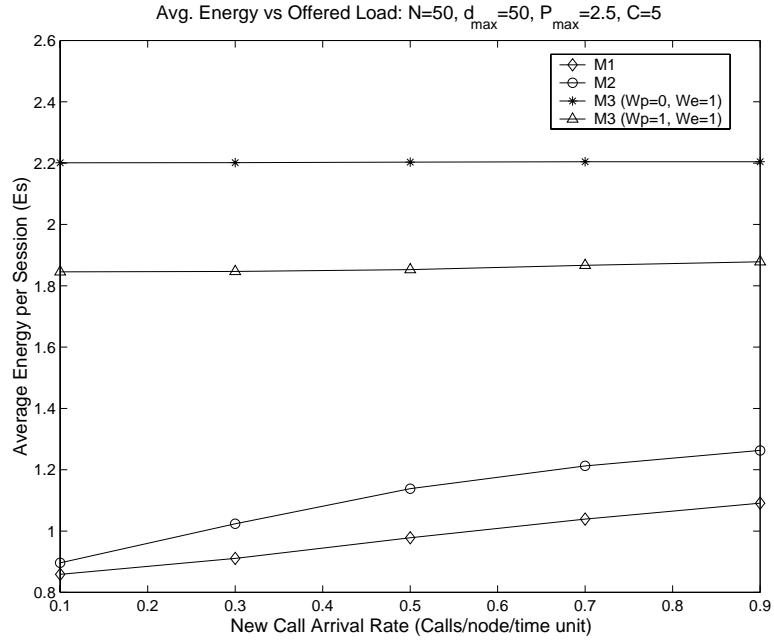


Figure 2.15: Energy per session vs per node arrival rate for $N = 50$, $d_{\max} = 50$.

effects of network size and node density on performance. We focus our attention to M1 and M3 with ($W_p = W_e = 1$) and to the case of $d_{max} = 50$. In figures 2.16 and 2.17 we can show the blocking probability as a function of the offered load, for network sizes of 10,20 and 50 nodes. Similarly, in figures 2.18 and 2.19, the average energy per session is depicted for the same set of network parameters. From these four graphs we make the following observations:

- While for M1 P_b increases with network size, for M3 it decreases and in particular it does not vary if we increase the size from 20 to 50 nodes. The two metrics react differently when the node density changes; in particular if we increase the number of nodes and assume a fixed transmission range, then we increase the connectivity of the network (which implies reduced average distance between nodes and hence more short distance links). That being the case, M1 attempts to route the calls over multiple short hop links and blocks more resources; hence future calls experience higher P_b . M3 instead favors the direct links (and since $d_{max} = 50$ there are a lot of those) and hence future calls that cannot use the shortest paths (in terms of M3) still have good chance to get through along multi-hop paths.
- E_s decreases with network size because a denser network provides additional short hops. Note that in the case of M1 this decrease is more dramatic whereas for M3 it is not as significant.
- Finally note that M3 is less sensitive to network parameters: in fact it is less sensitive to network size, since the difference both in P_b and E_s is relatively small from 20 to 50 nodes whereas for M1 it is more significant.

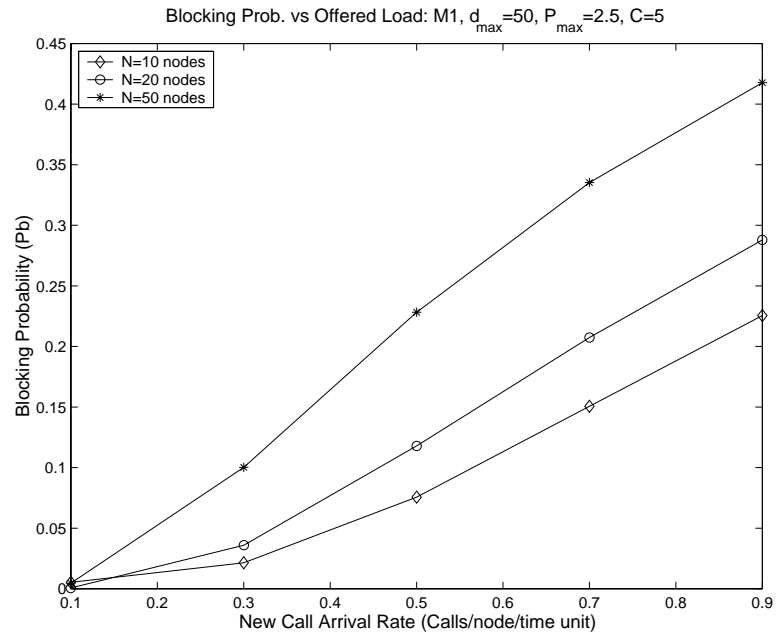


Figure 2.16: Blocking probability vs arrival rate for variable network sizes and M1

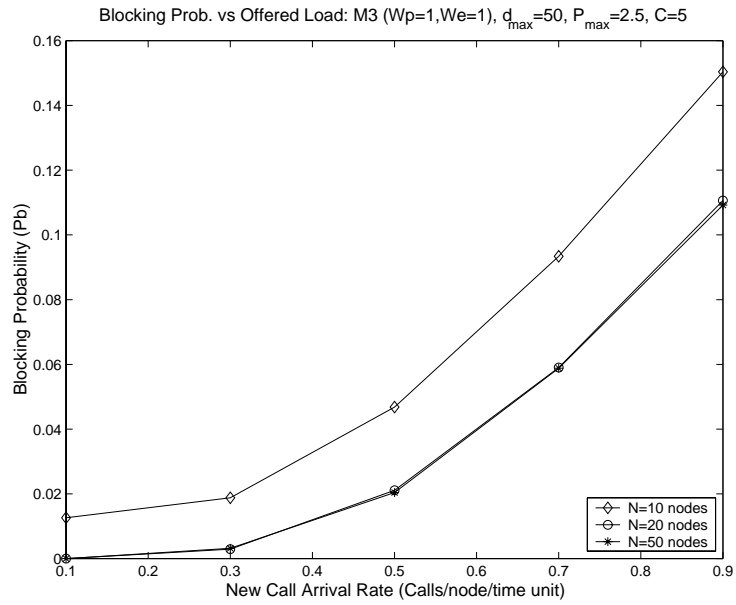


Figure 2.17: Blocking probability vs arrival rate for variable network sizes and M3

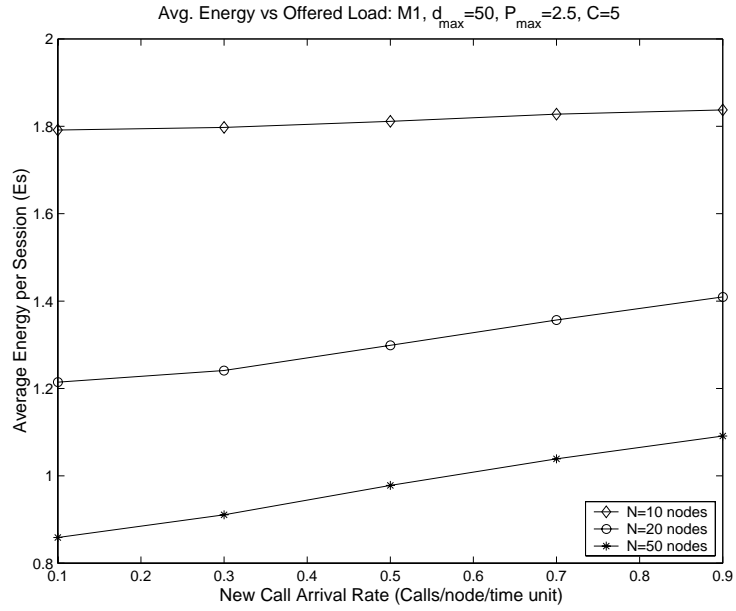


Figure 2.18: Energy per session vs arrival rate for variable network sizes and M1

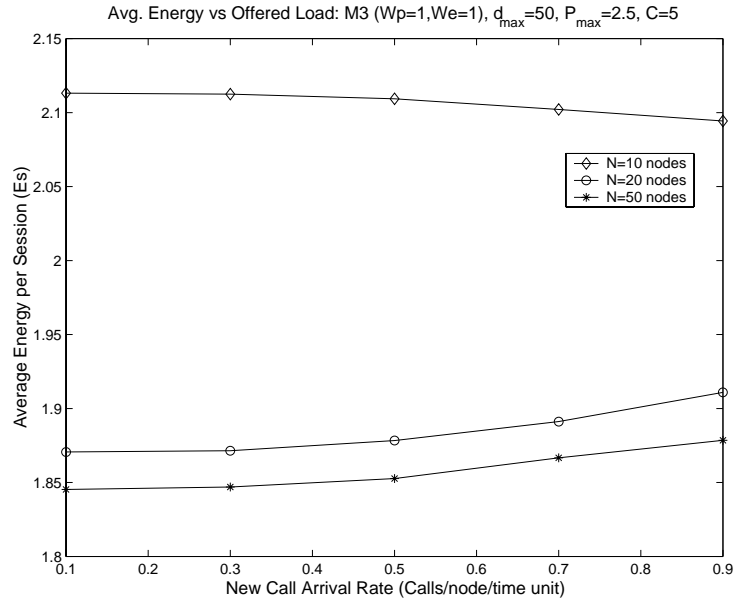


Figure 2.19: Energy per session vs arrival rate for variable network sizes and M3

2.5.4 Effect of average node degree on performance

In addition to network size and node density, performance was evaluated as a function of the average node degree as well. Due to the random selection of the studied topologies, we observed that the average node degree was not always the same given the number of nodes and the transmission range. For instance, for $N=20$ and $d_{max} = 50$ our 100 sample networks had average node degrees which ranged from 7 to even 14. Hence a valid guess is that an increase in the node degree translates into additional paths and hence reduced blocking. However, we often experience situations in which networks with nearly equal average node degrees exhibited quite different P_b 's. This was particularly common for the cases of M1 and M2. In figures 2.20 and 2.21 we plot the values of P_b and E_s respectively, versus the average node degree. We consider $N = 20$, $d_{max} = 50$ and $\lambda = 0.5$. We observe that:

- From figure 2.20, M3 is less sensitive to the average node degree compared to M1 and M2.
- From figure 2.21 all metrics result in a decrease in E_s as the node degree increases. All metrics exhibit a “linear” behavior.

Figures 2.22 and 2.23 show the values of P_b and E_s respectively, for all 100 sample networks and for all metrics. We observe that even though performance depends on the topology under consideration (in terms of node degree etc) this is true for all metrics and their relative performance does not change. Also note that again M3 shows very small dependence on the randomness of the topology which makes it less sensitive to the network parameters.

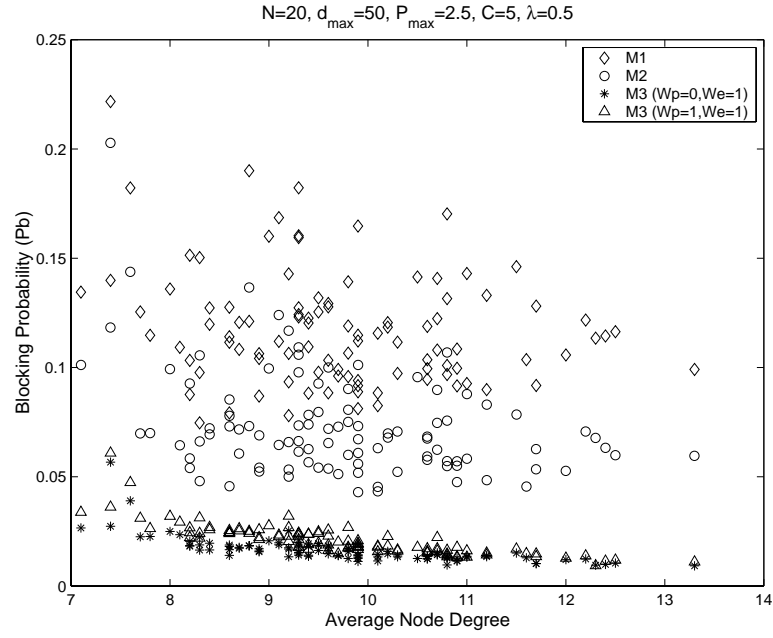


Figure 2.20: Blocking prob. vs average node degree, $N = 20, d_{\max} = 50, \lambda = 0.5$

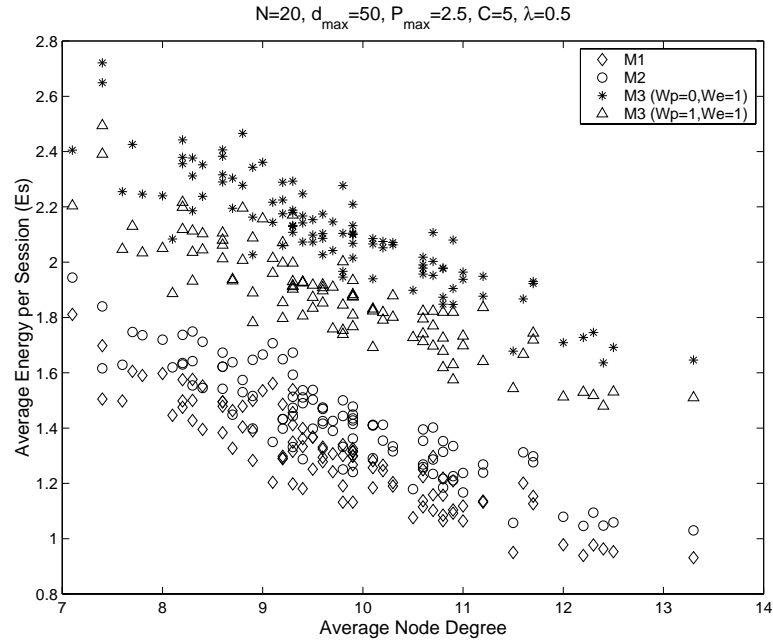


Figure 2.21: Energy per session vs average node degree, $N = 20, d_{\max} = 50, \lambda = 0.5$

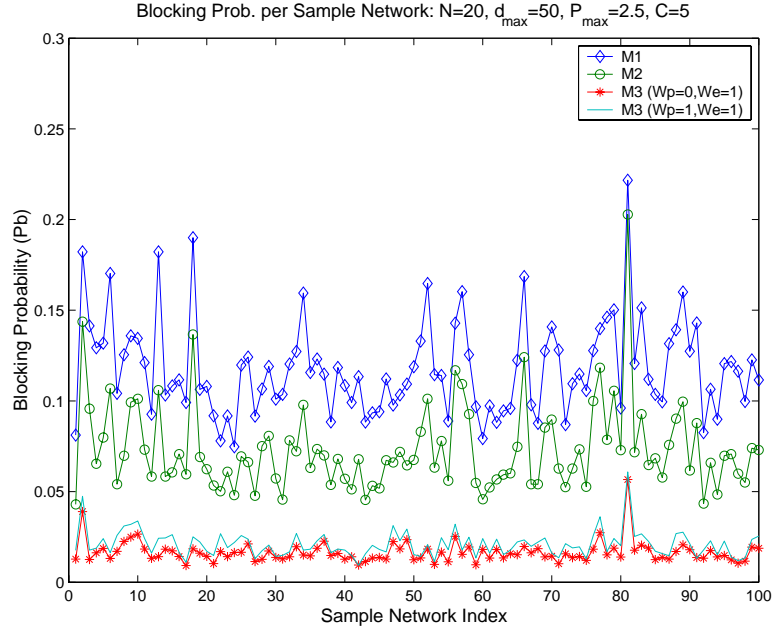


Figure 2.22: Blocking probability for all samples, $N = 20$, $d_{\max} = 50$, $\lambda = 0.5$

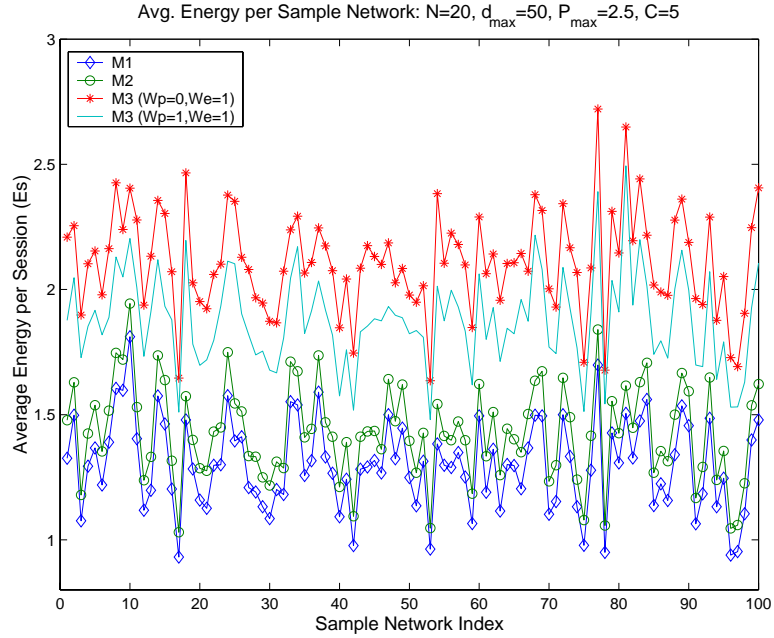


Figure 2.23: Energy per session for all samples, $N = 20$, $d_{\max} = 50$, $\lambda = 0.5$

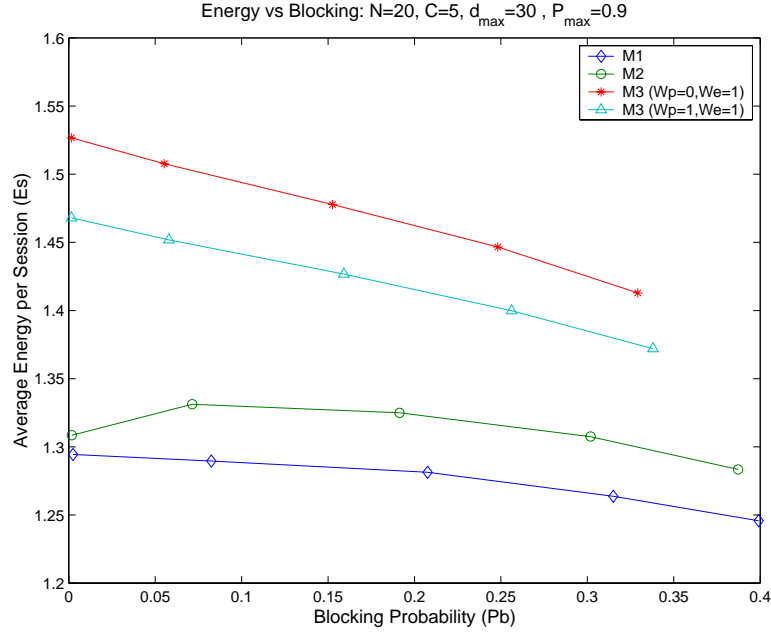


Figure 2.24: Energy-Blocking trade-off

2.5.5 Energy versus blocking trade-off and yardstick (Y) performance

It is rather clear from the results presented thus far that there is an inherent trade-off between P_b and E_s . In figure 2.5.5 we attempt to quantify this trade off by plotting the energy per session versus the average blocking probability. The data are from the set of sample networks with $N = 20$, and $d_{max} = 30$. Clearly we can achieve low E_s at the cost of high P_b and vice versa. Plots of this type can be useful in system implementation, where given an upper bound on one of the two performance measures we can estimate the performance of the other, depending on the link metric selected.

In equation 2.1 we defined a global reward yardstick Y in order to address the interdependencies between blocking probability and energy usage on network

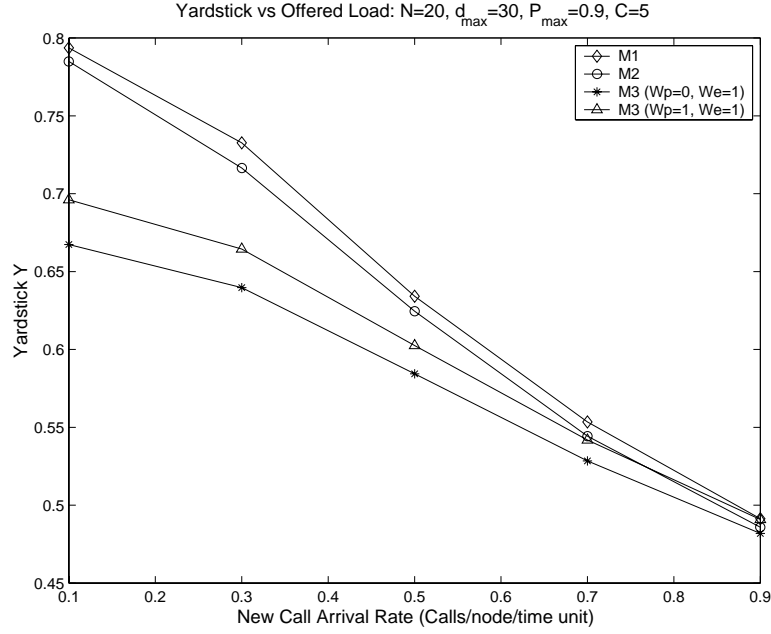


Figure 2.25: Yardstick Y vs. per node arrival rate for $N = 20$, $d_{max} = 30$.

performance. Figure 2.25 shows how Y varies with the arrival rate for $N = 20$ and $d_{max} = 30$. Note that even though M1 and M2 seem to achieve higher values of Y , if λ increases (higher blocking) then all metrics exhibit similar performance. Similar conclusions can be drawn also from figure 2.26 where we have increased the number of nodes to 50. Here M3(1,1) outperforms the rest of the metrics for high values of arrival rates.

2.5.6 Effect of receive and processing power on energy consumption

Throughout the results presented so far, we assumed node processing power to be negligible compared to transmission power. In actual systems however, wireless transceivers consume a significant amount of energy for signal processing and

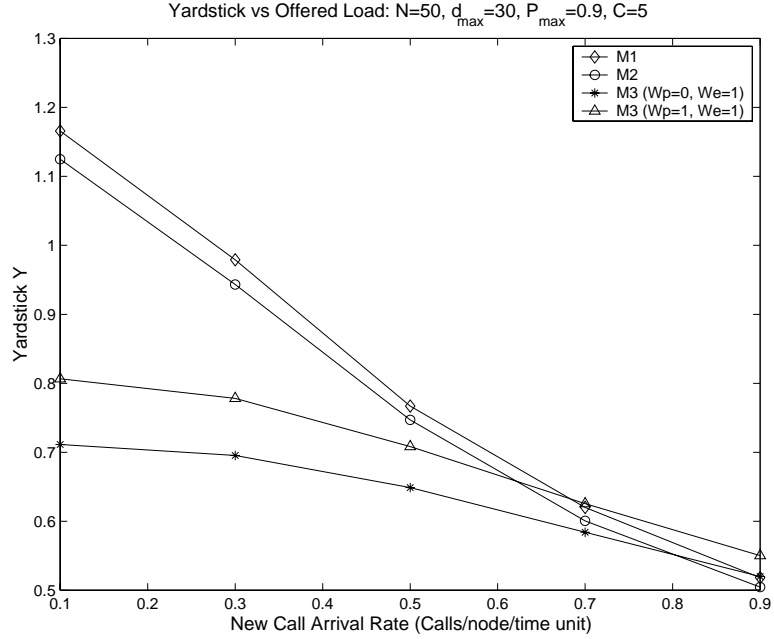


Figure 2.26: Yardstick Y vs. per node arrival rate for $N = 50, d_{max} = 30$.

other tasks that are critical for performing relaying of sessions. A key feature of our simulation model enables us to quantify the effects of non-negligible processing power. Although it is extremely hard to capture the actual energy depletion pattern, we have assumed that each wireless transceiver consumes a constant amount of power (for processing and receiving), denoted by P_{proc} , whenever it is being used to "serve" an active session. Such an assumption is not unreasonable as in fact receive and processing power do not depend on distance from the transmitter.

For simulation purposes we consider 100 random topologies with $N = 20$ nodes. We have pre-calculated the average transmission power for all sample networks in the case of $P_{max} = 2.5$. The average value of the transmitted power was equal to $\bar{P}_{tr} 1.1$. Given a fixed arrival rate ($\lambda = 0.5$) we ran simulations for all metrics for different values of processing power. In fact we chose P_{proc} to be 0, 1%, 10%, 30%

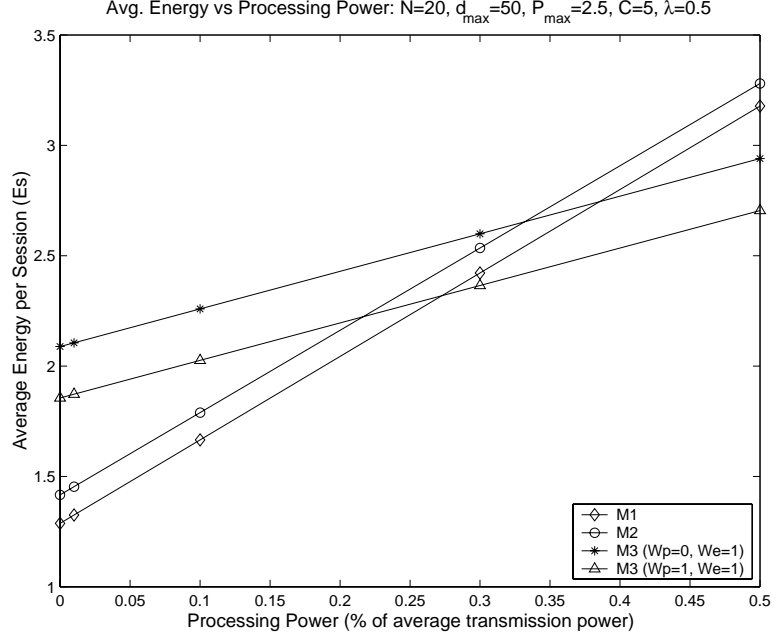


Figure 2.27: Effect of processing power on E_s

and 50% of the average transmission power and nodes consume energy at a rate of P_{proc} throughout the duration of the sessions they serve. The results are depicted in figure 2.5.6. We observe that E_s has a higher slope for M1 and M2 rather for M3. Even though for $P_{proc} \leq 0.2 \times \bar{P}_{tr}$ M1 and M2 perform better, after P_{proc} exceeds 25% of \bar{P}_{tr} M3 starts performing better. This is because M1 and M2 favor the use of multiple small hops which at the same time involve operation of more nodes. Clearly these results indicate that the contribution of processing power to the overall expenditures (and therefore to system performance) should not at all be neglected.

2.5.7 Network “lifetime”

In all previous experiments we assumed that nodes always have sufficient energy to continue operating until the completion of the simulation. In this paragraph, we study the performance of a network under the effect of node failures due to the exhaustion of their energy reserves. We show what kind of effect we get on the admitted traffic when some nodes run out of battery power and turn their transceiver “OFF”. We also compare the average - per node - energy consumption for different metrics in order to determine which case yields considerable fairness among the network nodes.

The results presented here are for a topology of 10 nodes. We consider three different values for the maximum transmission power, with corresponding maximum transmission ranges of $d_{max} = 30, 40$ and 50 units respectively. The resulting connectivities are depicted in figure 2.28.

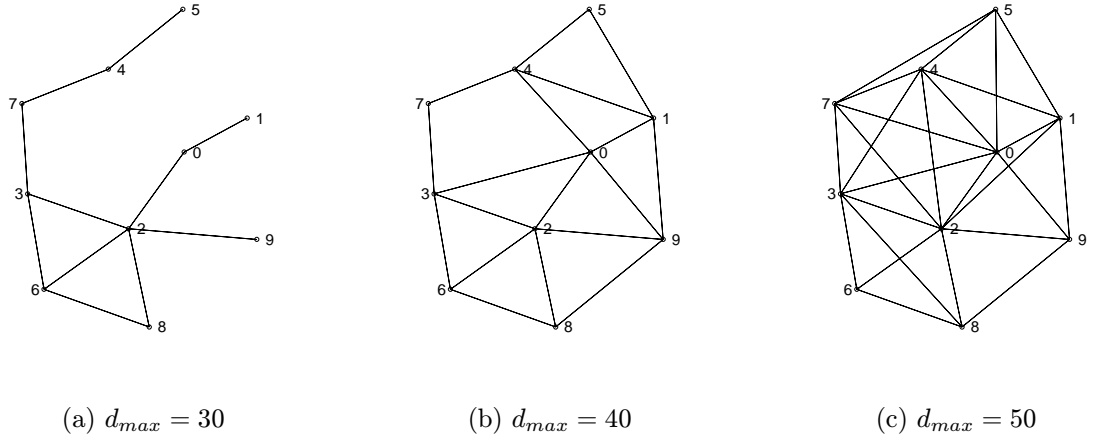


Figure 2.28: Sample network connectivities with $N=10$ for studying effects of energy exhaustion

In figures 2.29 and 2.30 we plot the cumulative number of accepted calls versus

the simulation time for the case of the network of figure 2.28(b) and for $\lambda = 0.3$ and 0.9 respectively. We compare performance of M1 versus M3 ($W_p = 1, W_e = 1$) and observe the following:

- As nodes begin to switch to OFF state, the rate of accepted calls starts decreasing. Therefore, in order to maintain acceptable performance, an algorithm should try to balance the energy consumption evenly among all nodes so that the time until the first node turns OFF is maximized. Metric M3 achieves that to some significant extent, since the interval from the beginning of the simulation until the first node turns its power OFF is longer.
- The results are not sensitive to the rate of offered traffic, as far as the relative performance of the metrics is concerned. Obviously, higher λ results in shorter network lifetime.

When we increase the maximum transmission range to $d_{max} = 50$ (see figure 2.28(c)), we observe that M3 results in more rapid network partitioning. In figures 2.31 and 2.32, we plot the cumulative number of accepted calls versus the simulation time for the case of the network of figure 2.28(c) ($d_{max} = 50$ and for $\lambda = 0.3$ and 0.9 respectively). Due to the nature of M1 to “favor” lower power paths, certain nodes get over-loaded and the time until the first node turns its power OFF is shorter as compared with M3. However, due to the increased transmission range, we observe from the connectivity map that there exist a lot of direct links between nodes which will be “favored” by M3. Even though M3 tries to maintain a balance among all nodes in terms of energy consumption, most of its nodes will turn OFF shortly after the first node does so, and the average time until the network gets partitioned is shorter compared to the case of M1.

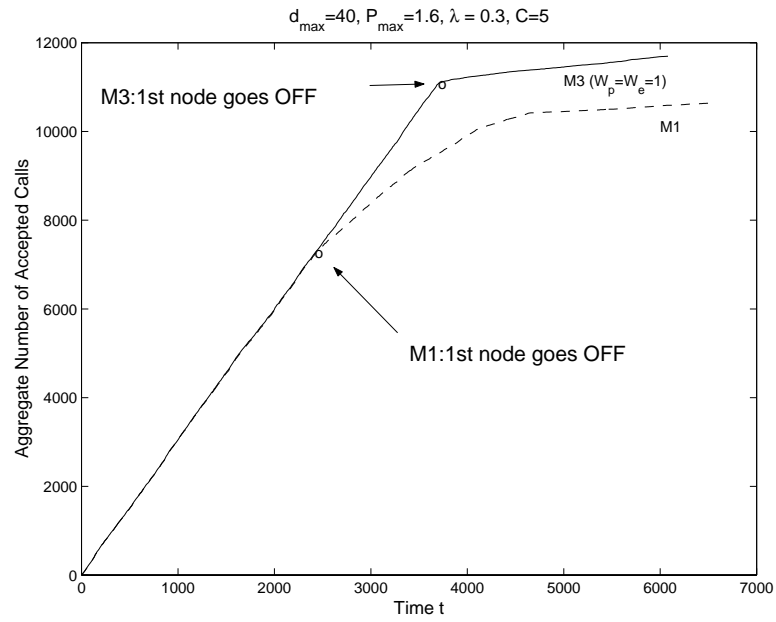


Figure 2.29: Number of accepted calls vs time; $N = 10$, $d_{max} = 40$ and $\lambda = 0.3$

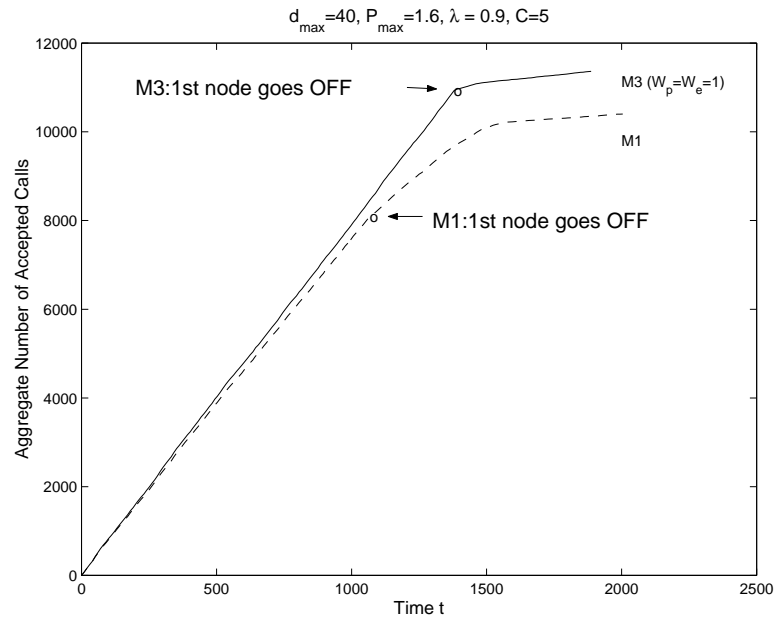


Figure 2.30: Number of accepted calls vs time; $N = 10$, $d_{max} = 40$ and $\lambda = 0.9$

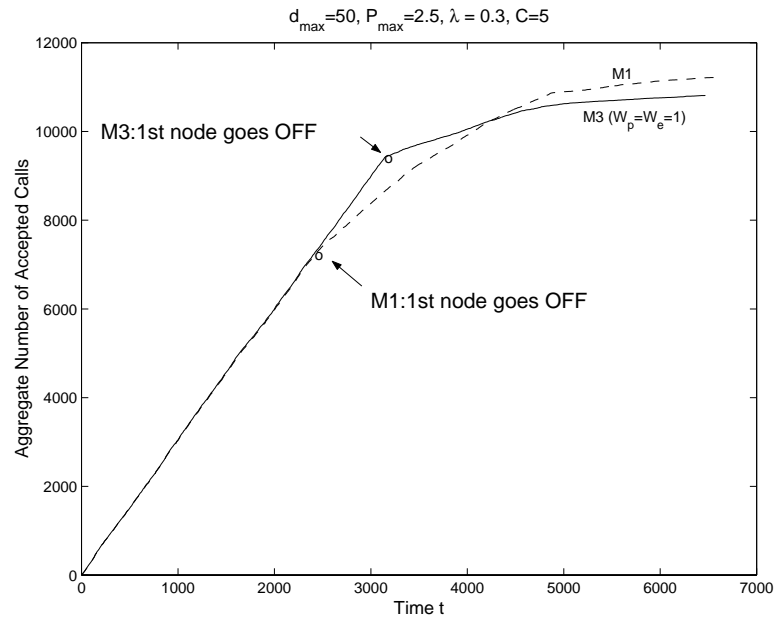


Figure 2.31: Number of accepted calls vs time; $N = 10$, $d_{max} = 50$ and $\lambda = 0.3$

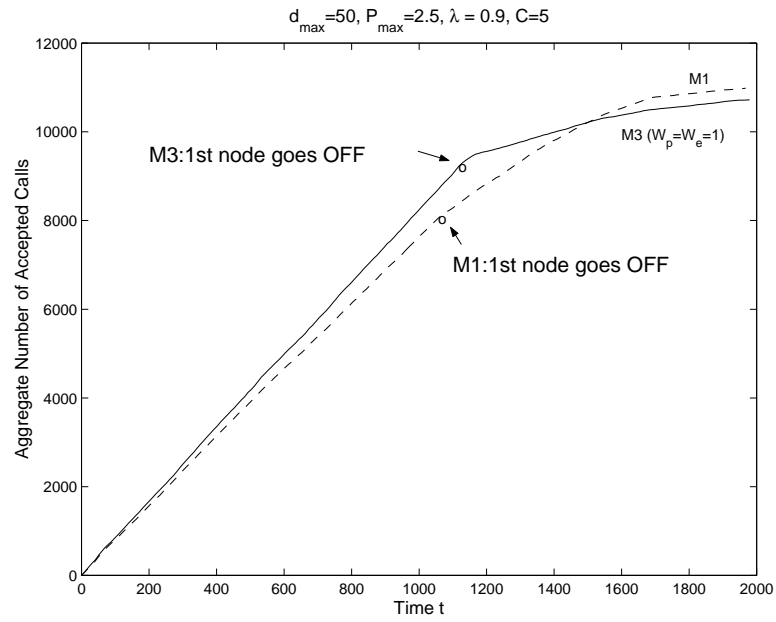


Figure 2.32: Number of accepted calls vs time; $N = 10$, $d_{max} = 50$ and $\lambda = 0.9$

To verify our intuition that M3 produces some amount of fairness among nodes, we ran some experiments for all three connectivity maps of figure 2.28 and examined the energy reserves of all nodes in each case. In particular, let $E = [E_0, E_1, \dots, E_{N-1}]$ represent a vector of energy expenditures, with E_i being the ratio of energy spent versus initial energy for node i . Our simulations terminate before any node runs out of energy and in tables 2.2 and 2.3 we summarize the statistics of our measurements. Each cell contains four quantities, the mean value (averaged over all N nodes) the standard deviation, the minimum and the maximum amounts of energy consumed by any node in the following format:

| |
|---|
| $Mean(E) \quad ; \quad StDev(E)$ $Min(E) \quad - \quad Max(E)$ |
|---|

We make the following observations:

- The average energy per node for the case of M1 does not vary by increasing the transmission range, whereas this is not the case for M3.
- For M3, E_s exhibits smaller standard deviation, which means that the energy levels are more balanced among all nodes.

2.6 Conclusions

We compared a set of link metrics that can be used for selecting routes in a wireless static ad-hoc network where the objective is to minimize blocking probability subject to energy constraints. We illustrated the trade-offs between blocking and energy consumption and compared these metrics under different values of the network parameters. Metric M3 combines local information of the transmission power

| $N = 10, \lambda = 0.3$ | | | |
|---------------------------|----------------------------------|----------------------------------|----------------------------------|
| Metric | $d_{max} = 30$ | $d_{max} = 40$ | $d_{max} = 50$ |
| M1 | 0.314 ; 0.256 (0.057 - 0.844) | 0.277 ; 0.165 (0.086 ; 0.536) | 0.277 ; 0.165 (0.089 ; 0.537) |
| M3 ($W_p = W_e = 1$) | 0.318 ; 0.231 (0.059 - 0.744) | 0.287 ; 0.079 (0.171 - 0.383) | 0.328 ; 0.100 (0.147 - 0.488) |

Table 2.2: Consumed energy per node for low traffic

| $N = 10, \lambda = 0.9$ | | | |
|---------------------------|----------------------------------|----------------------------------|----------------------------------|
| Metric | $d_{max} = 30$ | $d_{max} = 40$ | $d_{max} = 50$ |
| M1 | 0.210 ; 0.154 (0.037 - 0.515) | 0.253 ; 0.104 (0.140 - 0.409) | 0.254 ; 0.103 (0.144 - 0.405) |
| M3 ($W_p = W_e = 1$) | 0.212 ; 0.143 (0.039 - 0.473) | 0.258 ; 0.070 (0.155 - 0.331) | 0.303 ; 0.091 (0.137 - 0.454) |

Table 2.3: Consumed energy per node for high traffic

and the residual energy of the receiving node and achieves better performance in terms of blocking probability. We also saw that M3 is less “sensitive” to network parameters including size, node density and transmission power levels. Finally we presented some examples where M3 exploits its property of balancing energy consumption among all nodes in a fair way, so that network lifetime is increased. In situations where the average energy per session is the crucial parameter, we saw that M1 and M2 exhibit better performance, as long as the offered traffic load is kept low.

Chapter 3

Energy-Efficient Routing of Connection-Oriented Traffic, Part II: Limited Bandwidth Resources

3.1 Introduction

In the first part of our study on energy-efficient routing (chapter 2) we assumed infinite bandwidth resources so that any node could access the wireless channel on demand, without any need for contention and without causing any interference to other neighboring nodes. A call request would be admitted to the system provided a path existed with at least one transceiver available at every node. In a realistic wireless system however, spectrum is scarce and links are bandwidth constrained making the problem of efficient and interference-free sharing of common bandwidth resources very crucial for the overall network performance. Depending on the base technology used to isolate traffic from different stations, bandwidth resources may be modeled by either transmission time-slots or frequency channels or CDMA orthogonal codes. In this chapter, our focus is on the development of algorithms for routing connection-oriented traffic under energy and bandwidth limitations. Every node is assumed to have a sufficiently large number of transceivers so that calls are

never blocked due to unavailability of a transmitter or a receiver. We propose a reservation-based scheme that supports end-to-end sessions based on the efficient sharing of a set of distinct frequency channels and we investigate techniques of jointly addressing the problem of power-sensitive route discovery and conflict-free allocation of frequency channels to transmitting nodes.

Recall that wireless ad-hoc networks differ from other types of wireless architectures (e.g. cellular systems, wireless LANs, etc.) in that communication is not always possible via a direct-hop link from the origin to the destination; in fact it is very common to route traffic over multi-hop paths. A transmission by a node gets received by all its one-hop neighbors causing interference to non-intended recipients. By contrast, in wire-line networks where a link connecting two nodes is exclusively used by these nodes without interfering with neighboring transmissions. Hence, a channel access mechanism is required for the interference-free scheduling of transmissions. However, the lack of complete connectivity among all nodes allows more than one nodes to simultaneously use the channel without causing conflicts, provided they are spatially separated. Notice though, that the number of simultaneous transmissions that can take place interference-free is not known a priori and can only be determined by complete knowledge of the set of network parameters consisting of the topology map, transmission power, number of available frequency channels, transceivers per node and other information.

A fundamental design choice on the multiple access scheme to be used depends on the type of workload that is carried by the network. Multiple access techniques that have been extensively used in packet-based networks are generally classified into two broad categories: random access schemes and reservation-based mechanisms. Random access schemes (e.g. Aloha, CSMA, etc.) are more appropriate

for single hop access and are typically based on a simple or modified “free-for-all” approach, in which nodes send packets either immediately or after sensing the carrier and utilize sophisticated algorithms for retransmitting collided packets. On the other extreme, reservation-based schemes (TDMA, FDMA, CDMA, etc.) utilize a perfectly scheduled approach (it could be static or dynamic) in which according to some rules nodes may transmit or receive at specific intervals and on reserved frequencies. Random access schemes are more appropriate for networks carrying datagram traffic (in which for example it is more efficient to negotiate link access on a packet by packet basis). By contrast, in systems carrying connection-oriented traffic stations generate steady streams of information and it is preferable to allocate part of the link to the source for its exclusive use, thus avoiding the additional overhead of negotiating link access for every packet in the stream. At the same time, and in order to support connection-oriented traffic, nodes must be capable of receiving and transmitting simultaneously, necessitating therefore the use of sufficiently separated frequency channels.

Although the use of a frequency division multiple access scheme (FDMA) introduces the difficult problem of assigning non-interfering frequencies to transmitting nodes, it is the most appropriate for our problem. We could possibly eliminate this difficulty by considering a system based on code division multiple access (CDMA), in which quasi-orthogonal codes would be used. However, in direct-sequence CDMA systems nodes are not allowed to handle simultaneous transmission and reception in the same frequency band. It would also be of interest to study systems that use time-division multiple access (TDMA), rather than multiple transceivers, to support multiple sessions simultaneously. In fact such systems have been studied [13, 14] in the context of scheduling problems and for

datagram traffic scenarios. In TDMA-based systems, the need to assign specific time slots creates a much more difficult problem than that of simply assigning any (of perhaps several available) transceiver to a new session. Therefore the study of TDMA-based systems is a topic deferred for future research.

Throughout this chapter we focus on methods of allocating frequency channels to radio links in a way that we can minimize interference. By considering FDMA systems, we are able to assess the impact of limited bandwidth resources, and thereby to form the basis for future studies of specific systems, including those that use CDMA and TDMA. FDMA has also been proposed for use in energy efficient multicasting and broadcasting of sessions. In particular, *Wieselthier et.al.* have studied in [4] the effects of limited resources on the performance of a class of algorithms for constructing minimum energy trees for broadcasting and multicasting as those were proposed in [3]. We strictly consider unicast here and even though some objectives may be parallel, the actual algorithms, metrics and trade-offs are quite different.

The problem of efficient channel allocation is directly coupled to the problem of transmission power-level selection. A node that increases its transmission power to reach a remote receiver, will possibly interfere with a larger set of neighboring nodes. On the other hand, if a path consisting of multiple short hops is used, the total power required for transmission may be lower, but there is need for a larger set of non-conflicting frequency channels to be used by the consecutive links of the path. Therefore the routing decision must be based on both energy and bandwidth considerations and to these ends we concentrate on developing routing algorithms that jointly address the following two objectives:

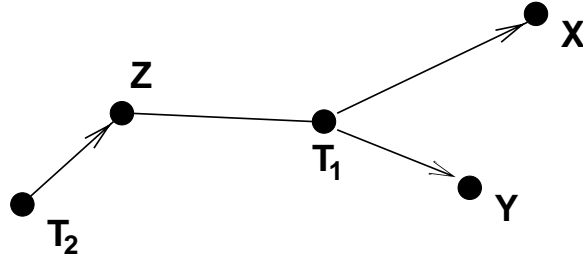


Figure 3.1: Example: Route selection involves power and frequency selection

- (a) efficient usage of the available energy
- (b) assignment of frequency channels in a conflict free fashion

Even in the simple scenario in which all nodes may only transmit at the same power level, the problem of assigning frequency channels to the links of a unicast path does not have a unique solution. In fact such a problem has not been studied yet for the case of connection-oriented traffic. It is a problem of combinatorial nature and if multiple feasible channel assignments exist, it is not clear why one solution would be preferable versus another. One way to quantify the effect of a candidate allocation scheme would be to select an assignment that utilizes the least number of channels; even in that case the problem is not really how many channels are being used but which are these channels.

To better illustrate these remarks, consider the example shown in figure 3.1. Node T_1 is ready to transmit and has to select between X and Y as its next hop neighbor. If all nodes transmit at the same power level, then in terms of energy it will cost the same to transmit to either X or Y . Regardless of the recipient, any transmission from T_1 will block node Z from receiving at the same frequency, thus node T_2 gets blocked from transmitting.

If we allow the transmitting node to adjust its power depending on the intended receiver, we can associate each candidate link with a cost metric that captures both the energy and the interference cost. Consider again the example of figure 3.1 but now with the possibility to transmit at multiple power levels depending on the distance from the intended recipient. Denote by $d(A, B)$ the distance between any two nodes A and B . If $d(T_1, Y) < d(T_1, X)$ the transmission power is lower if Y is selected as the receiver. Additionally, if $d(T_1, Y) < d(T_1, Z) < d(T_1, X)$ a transmission from T_1 to Y does not prohibit T_2 from transmitting at the same frequency, whereas this is not the case if T_1 transmits to X . Clearly, such situations occur frequently in the context of wireless ad-hoc topologies and our objective is to define a method for modeling interference which also takes into account the transmission power level.

The remaining of the chapter is organized as follows. In the next section we extend our wireless network model of chapter 2 to address interference effects. We define a set of rules regarding conflict avoidance situations and in the sequel we discuss the difficulties encountered in developing an optimized solution and we provide an overview of our approach. We continue with a detailed description of our proposed algorithms and study their properties and implementation requirements. In the final section we present a detailed performance analysis, based on our simulation model and wrap up the chapter with a summary of conclusions.

3.2 Interference model

The network topology is modeled by a directed graph $G = (V, E)$ where the elements of V represent the network nodes and each directed edge $(i, j) \in E$ denotes

a radio communication link between the communication nodes i and j . Similarly to our model defined in chapter 2 we denote by $\mathcal{R}(x)$ all one hop neighbors of node x , ie all nodes that are located within the transmission range of x defined as a circle centered in x with radius equal to d_{max} .

A total of m frequency channels are available for use, denoted by f_1, f_2, \dots, f_m . Each node i maintains a set of *channel status* vectors, one for each node $j \in \mathcal{R}(i)$. These vectors consist of 0's and 1's that indicate whether a channel is *free* or *blocked* respectively. Therefore the channel-status vector of node i for transmission to node j will be given by:

$$f^{(i,j)} = [f^{(i,j)}(1), \dots, f^{(i,j)}(m)] \quad (3.1)$$

where for all k we define:

$$f^{(i,j)}(k) = \begin{cases} 1 & \text{if } k^{th} \text{ channel is available} \\ 0 & \text{otherwise} \end{cases} \quad (3.2)$$

In order to admit a new session request, a path p must exist from the source to the destination, such that all nodes $i \in p$ have at least one frequency channel available for transmission; moreover a conflict free channel allocation must exist that satisfies the following requirements:

- A node cannot transmit and receive in the same frequency
- A node cannot simultaneously receive more than one signals in the same frequency
- A node cannot transmit simultaneously to more than one neighboring nodes (we strictly consider unicast here; in a broadcast scenario this would be an acceptable and in fact encouraged situation).

As a result of these conditions, a transmission over any link may prevent a subset of neighboring nodes from transmitting at the same frequency and at a certain power level. In order to determine conflict-free channel assignments, nodes must be aware of the frequencies they are allowed to use (along with the allowable power levels). We define a simplified interference model in which a receiver is assumed to ignore interference from simultaneous neighboring transmissions if the distance from the location of the interfering source exceeds d_{max} . In particular, we make a binary decision of whether we can allow or not a transmission, without detailed calculation of SIR at every node, since such a task would increase the complexity of an already difficult problem. Nonetheless, in principle, a more accurate model for interference can be incorporated in our model.

Under these considerations, a transmission over link (A, B) using frequency f_k results in the blocking of the following neighboring links:

– **Primary conflicts:**

P1: Any link (v, A) , $v \in \mathcal{R}(A)$, because A cannot receive and transmit at the same frequency.

P2: Any link (A, v) , $v \in \mathcal{R}(A)$, because A cannot transmit to more than one nodes simultaneously.

P3: Any link (v, B) , $v \in \mathcal{R}(B)$, because B cannot receive from more than one nodes simultaneously.

P4: Any link (B, v) , $v \in \mathcal{R}(B)$, because B cannot transmit and receive at the same frequency.

– **Secondary conflicts:**

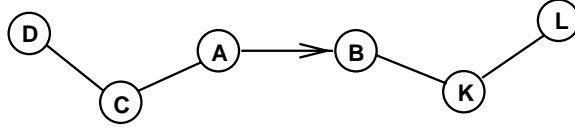


Figure 3.2: Example network to illustrate interference model

- S1:** Any link (v, u) with $u \in \mathcal{R}(A)$ and $v \in \mathcal{R}(u)$, if and only if $d(A, u) \geq d(A, B)$. Transmission over (v, u) is allowed only in the case that transmission over (A, B) is not received by u .
- S2:** Any link (u, v) with $u \in \mathcal{R}(B)$ and $v \in \mathcal{R}(u)$, if and only if $d(u, v) \geq d(u, B)$. Transmission over (u, v) is allowed only in the case that it is not received by B .

Consider for example the case shown in figure 3.2. Without loss of generality assume that an ongoing session from node A to node B is using link (A, B) at frequency f_k . The status of the neighboring links during this transmission is listed in table 3.1.

3.3 Algorithmic considerations

Our objective is to develop algorithms that determine an appropriate unicast path for each newly arriving session, so that a set of performance requirements are satisfied. Since bandwidth is limited, a session can be admitted only if a path exists with sufficient bandwidth along every link and with the property that all nodes may simultaneously transmit and receive, using a conflict-free frequency allocation scheme. Energy-efficiency is of paramount importance, hence the ideal algorithm should select among all available paths one with minimum aggregate

| Link | Status | Conflict type |
|----------|--------------------------------|---------------|
| (A, C) | Blocked | P2 |
| (C, A) | Blocked | P1 |
| (C, D) | Free | - |
| (D, C) | Free if $d(A, B) < d(A, C)$ | S1 |
| (B, K) | Blocked | P4 |
| (K, B) | Blocked | P3 |
| (K, L) | Free if $d(KL) < d(KB)$ | S2 |
| (L, K) | Free | - |

Table 3.1: Frequency blocking status for example of figure 3.2

transmission power which would result in minimum energy expenditures for the session under consideration. In the optimal case, the selected path should also have the least effect on the blocking of future calls. In this section we discuss the main issues encountered in the development of such an algorithm. Proposing a scheme that can meet all of these objectives turns out to be a very complicated task.

Of crucial importance in developing such an algorithm are the assumptions we will make on the available information about the network state. We assume that all nodes are aware of their neighbors (defined as the nodes located within transmission range) as well as the power required to successfully transmit to these neighbors. In addition to that, all nodes keep up to date information on which frequency channels are available or blocked from transmitting. An ideal situation occurs

when “complete” information on the network state is available. Such information includes the full connectivity map with detailed transmission power levels and the frequency channels being used or blocked by every node. At the establishment or termination of a call this information must be updated and be made available either to all nodes or to some central coordinator. Even if we neglect the cost of obtaining and maintaining complete information, the best possible solution would involve the use of a greedy algorithm that would maximize an expected reward function on a per call basis. In that case for example, the reward can be defined either as the total transmission power required, or as a linear combination of total power and number of blocked resources. Such a method requires the exhaustive search of a large state space which grows exponentially with the network size and therefore it is impractical except for trivially small networks.

Since it is extremely costly (in terms of overhead and time complexity) to maintain complete state information, an alternative approach would look for suboptimal solutions that rely on local information in order to determine the routes to be used. Local information can be acquired through the periodic exchange of control packets between neighboring nodes. Similarly to the mechanisms developed for the case of unlimited frequency channels (chapter 2), we examine heuristic algorithms that do not require a complete information map and restrict the search to a significantly smaller space. In particular, we can define link metrics that capture local parameters and use the Bellman-Ford algorithm to determine the minimum cost path. Nevertheless, there is no direct way of predicting what blocking impact a specific frequency channel might have on future calls. In fact the set of neighboring nodes that get blocked is the same regardless of the choice of transmission frequency. In the case of plentiful bandwidth resources, the existence of one transceiver along

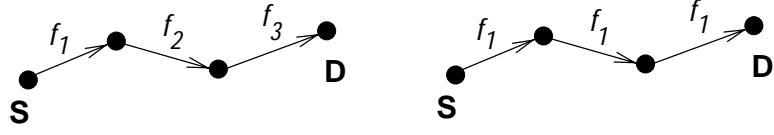


Figure 3.3: Two instances of the same path showing the available frequencies

every node in the path was sufficient to guarantee the availability of the path. By incorporating such information into the link metrics (link cost was set to infinite if one of the two edge nodes of the links had no transceivers available), the algorithm would always determine a feasible path. Apparently, any finite cost path was a candidate path for admitting the new session. If we were to follow a similar approach for the case of limited frequency bands, there would be no guarantee that a finite cost path would also be appropriate for establishing the session. The existence of at least one available frequency channel in each link of a path does not guarantee call admission; instead an interference-free allocation of channels must be determined. Such an allocation is not directly related to the number of channels available for each node but rather to which are these channels. We illustrate our point through a simple example shown in figure 3.3, where two instances of the same path are depicted as well as the available channels of each link. We define our link metric to be equal to the inverse of the number of available channels so that we favor links with multiple free bands. Both cases result in the same path cost; however, only for the path on the left can we have interference-free transmission.

Another limitation is that the nodes of a path cannot select which frequency to use (among the set of available channels) independently. For every channel assignment made over one link, neighboring nodes that experience interference must update their blocked-frequency table before they make their assignment.

Therefore a channel allocation algorithm must generate the frequency assignments on a hop-by-hop basis.

Based on the above discussion and remarks our approach continues as follows. We first present a class of heuristic algorithms that are easier to implement but their performance has to be evaluated. We then discuss complexity issues of exhaustive search methods and propose two schemes that can be used as a common comparison basis in relatively small network examples. A detailed performance evaluation section follows in which the algorithms are compared and their most significant features are discussed.

3.4 Heuristic algorithms

The heuristics we have proposed evolve in the following two stages:

- a minimum cost path (as measured by energy and blocked resources) is first determined (referred to as the *candidate path*)
- if an interference-free channel assignment can be determined along that path, the call request is admitted to the system.

3.4.1 Link metrics for determining minimum cost path

In this section, we propose the *minimum power metric* (MPM) and the *power and interference based metric* (PIM) for determining the cost of the links.

(a) Minimum power metric (MPM)

MPM accounts for energy requirements only and is a direct measure of the power needed to transmit over the specific link, provided that at least one frequency

channel is free for transmission. The cost of using link (i, j) as expressed through this metric is defined by:

$$D_{ij}^{(MPM)} = \begin{cases} P_{ij} & \text{if } \sum_{k=1}^m f^{(i,j)}(k) > 0 \\ \infty & \text{otherwise} \end{cases} \quad (3.3)$$

Clearly MPM is similar to M1 which was used for the case of unlimited frequency channels in the previous chapter (see equation 2.3) and is expected to produce the minimum transmission power path available.

(b) Power and interference based metric (PIM)

To address the blocking effects a transmission may cause to neighboring nodes we define PIM by incorporating into MPM interference effects. We first introduce the following notation:

- $B^{(i,j)}(k)$ denotes the set of transmissions (transmitter - receiver pairs) that are blocked whenever node i transmits to j over frequency f_k
- $|B^{(i,j)}(k)|$ is the cardinality of $B^{(i,j)}(k)$
- $|E|$ is the cardinality of the set of all transmitter-receiver pairs.

PIM is then defined as follows:

$$D_{ij}^{(PIM)} = \begin{cases} \frac{P_{ij}}{P_{max}} + \frac{|B^{(i,j)}(k)|}{|E|} & \text{if } \sum_{k=1}^m f^{(i,j)}(k) > 0 \\ \infty & \text{otherwise} \end{cases} \quad (3.4)$$

Note that PIM is the sum of two different quantities, namely the transmission power and the number of blocked resources, where we normalize each of these quantities respectively with the maximum transmission power and the maximum number of blocked transmissions (which equals the number of links) so that both terms take values in the $(0,1]$ interval.

3.4.2 Frequency allocation algorithms

Once a candidate minimum cost path has been identified, an interference-free channel allocation must be determined for those nodes that will be transmitting. In this section we discuss the details of two frequency allocation mechanisms:

- a heuristic that allocates channels to the links of the candidate path starting from the origin and proceeding link-by-link towards the destination. We will refer to it as the *link-by-link greedy (LLG)* frequency allocation algorithm
- a second heuristic that assumes complete knowledge of the candidate path and allocates channels to its links starting with the most congested. We will refer to it as the *most congested link first (MCLF)* frequency allocation algorithm.

(a) Link-by-link greedy frequency allocation (LLG)

The motivation for the link-by-link greedy allocation scheme comes from the use of similar greedy channel allocation schemes in linear cellular networks. Channel allocation is performed along the candidate path in a hop-by-hop manner, starting from the origin node and moving towards the destination, selecting an available channel for each link (and updating blocked frequencies after each allocation). Since the candidate path is a finite cost path, all its nodes have initially at least one frequency channel available for use. However, as the step by step reservation proceeds, a node may run out of frequencies due to blocking by neighboring transmissions and if a link is not allocated a frequency successfully the call is blocked.

We first illustrate how this scheme operates by providing a simple example. Consider an isolated path from the source node S to the destination D as shown

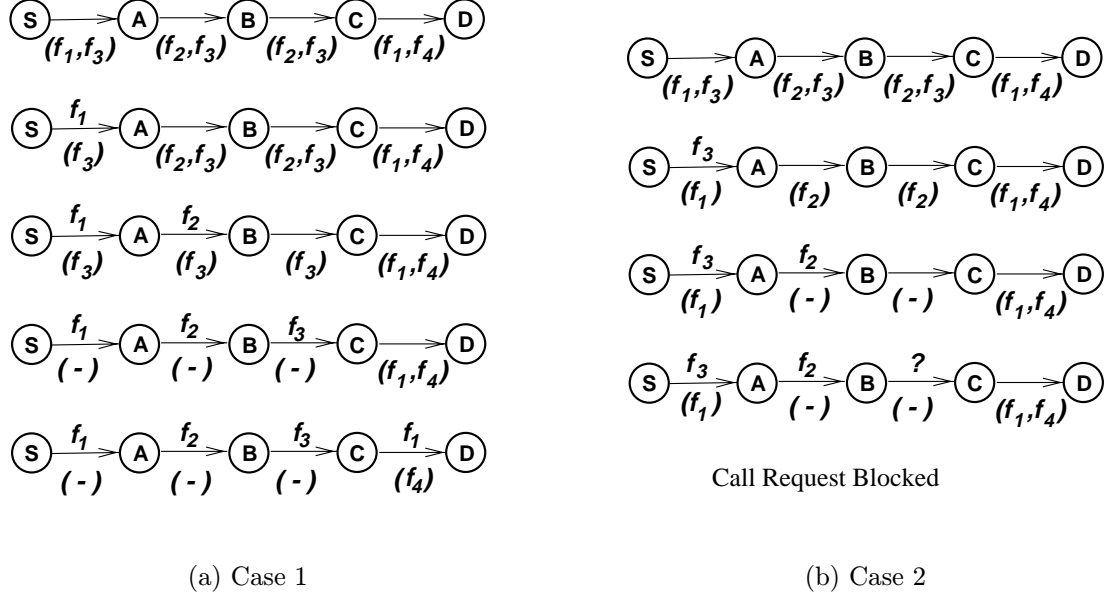


Figure 3.4: Example of purely greedy scheme operation

in figure 3.4(a). Node S needs to establish a session to node D via the path that consists of the nodes A, B and C . We list in parentheses right below each link the frequency channels that are available at every instant and above each link the frequency channel that gets reserved at every step. We show how frequency allocations are made link by link from node S towards D and which one and two-hop neighbors are blocked from transmitting according to our interference model. In this example we were very fortunate, in that all links had available channels when they were needed. Consider now the case depicted in 3.4(b). This time link (S, A) randomly chose frequency f_3 leaving links (A, B) and (B, C) with only one channel available. Link (A, B) has only one choice and this leaves link (B, C) with no available channels; thereby the call is blocked.

Next we describe the algorithm for the general case of a path p that consists of k nodes i_1, i_2, \dots, i_k . Each link (i_j, i_{j+1}) is associated with a “pool” of available

frequency channels denoted by $F(i_j, i_{j+1})$. Every node i_j is aware of its immediate next hop neighbor i_{j+1} in the path.

LLG algorithm:

1. $j = 1$
2. If $|F(i_j, i_{j+1})| = 0$ drop call; goto 7
3. i_j randomly selects a frequency channel $f_x \in F(i_j, i_{j+1})$ for transmission over link (i_j, i_{j+1})
4. Block neighboring links according to the interference model and update their $F(\cdot, \cdot)$
5. $j = j + 1$
6. If $j \neq i_k$ goto 2
7. Terminate.

In LLG there always exists a possibility that the path may run out of resources, even though all nodes may have had initially at least one channel available. Clearly, given a path and the available channels of each link we have a finite number of permutations, some of which result in feasible assignments, whereas others don't. Nevertheless, LLG can be implemented in a fully distributed manner without the complexity of an exhaustive search.

(b) Most congested link first (MCLF) frequency allocation

In order to increase the possibility of producing a feasible allocation, we propose a second heuristic in which we assume full knowledge of the path and the available

frequencies at each node along the path. Such information allows us to give priority to nodes with smaller numbers of available channels to make their reservations first (since those are the nodes more likely to run out of resources). We describe the algorithm for a path p ; let $E_p = \{\text{all } (i, j) \in p\}$ and assume that $\forall (i, j) \in E_p$, $F(i, j)$ and its cardinality $|F(., .)|$ are known. The algorithm proceeds as follows:

MCLF algorithm:

1. Sort elements of E_p in increasing order, starting with the one with minimum value of $|F(., .)|$.
2. Remove the first element (i, j) of E_p .
3. If $|F(i, j)| > 0$, randomly select $f_x \in F(i, j)$ for transmission over (i, j) ; else go to 6.
4. Block neighboring links according to the interference model and update their $F(\cdot, \cdot)$.
5. If $E_p \neq \emptyset$ go to 1.
6. Terminate.

Note that there still exists some randomness in the way the frequency channels are selected, as was the case with LLG, but we believe that the probability of success is higher, since we expect to avoid situations where nodes with many available channels would block neighboring nodes in the path with a single channel, just because of an unfortunate choice of transmission frequency.

3.5 Exhaustive search mechanisms

As was discussed in section 3.3, if complete network state information is considered an exhaustive search among all possible allocations can determine the path and assignment that maximizes a per-call reward function. A path from the source to the destination node is characterized as available if an interference-free frequency channel assignment exists. If the reward function is defined as the total transmission power for using the path, our mechanism should search among all available paths and return the minimum power path. Alternatively, we could consider a reward function as a combination of power and amount of blocked resources. In any case, such a technique is still greedy in that it optimizes the reward produced by a given call, based on the current network state. We describe next an implementation of an exhaustive search, referred to as ExSrch, that determines the available path with the maximum reward. We also consider a scheme that restricts the search to the candidate path. Note that both schemes are useful for performance evaluation purposes but their huge complexity prohibits their implementation in an actual system.

3.5.1 Complete exhaustive search implementation (ExSrch)

1. A call arrives at node $i \in V$ destined for node $j \in V$
2. Given the network state consider the subgraph $G' = (V, E')$ where $E' \subset E$ such that: $E' = \{(i, j) \in E \mid \sum_{k=1}^m f^{(i,j)}(k) > 0\}$.
3. Find all available paths $\in G'$ from i to j (with their corresponding frequency allocations).

4. If no path can be found drop the call and go to 7; otherwise assign the call to the path that maximizes the reward.
5. According to the interference model block the nodes that should not transmit at the same frequency.
6. Update network state.
7. Terminate.

The main advantage of the exhaustive search is that it always determines the minimum cost path among all available paths at the time the new session arrives to the system. However, performing an exhaustive search over a random (and possibly varying) network topology is an extremely complex task. It is rather impractical to think of it as a possible solution to our problem and will only be used as a basis for comparison. Even in that case it can only be applied to simple examples with few nodes, therefore it can not lead to significant conclusions. However, in order to illustrate how complex it may be to get to the optimal solution consider the following example:

Example:

Consider the topologies shown in figure 3.5. If these nodes are deployed in a 100×100 square grid and the transmission range is set to $d_{max} = 35$ units (figure 3.5.a), the total number of paths between all possible source-destination pairs is 642. Assume that a new call arrives at node 4 destined for node 6. There exist 9 possible paths connecting node 4 to node 6. Of these paths, 2 consist of 3 links, 4 of 4 links and 3 of 5 links. If the number of frequency channels in the network were 5, we could have a total number of $3^5 \times 2 + 4^5 \times 4 + 5^5 \times 3 = 13957$ frequency

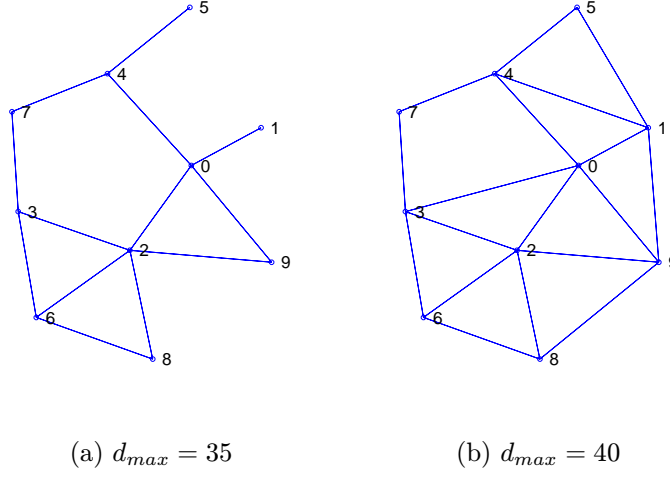


Figure 3.5: Network topologies of example 1

allocations along these paths. Due to interference constraints, some of these allocations are not permissible and of course a lot of them might not be feasible due to blocked frequencies or other on going transmissions, but we still have to search and evaluate a large number of possibilities. If the network connectivity is denser, the search space increases rapidly. For example the maximum transmission power is augmented to make the transmission range equal to $d_{max} = 40$ (figure 3.5.b), the total number of paths for all origin-destination pairs in the network becomes 6090. For the same source and destination (4,6) we now have 93 paths and nearly one million combinations.

3.5.2 Exhaustive search of minimum-cost path (ESMP)

Exhaustive search can also be limited in the minimum cost path in order to reduce the size of the solution space. We propose the Exhaustive Search of Minimum-cost Path (ESMP) scheme, which searches among all possible channel allocations of the

candidate path and selects an interference-free assignment to carry the session. Oftentimes there may exist multiple such allocations and ESMP will select the first one to be discovered, for no allocation is classified as better or worse than any other. Since the whole state space is searched, if no allocation can be found there doesn't exist one along the specific path, given the current network state; hence the session is not admitted to the system. In a sense, ESMP operates as an admission control algorithm which admits a new session only if it can route it along the minimum cost path. Moreover, since ESMP only examines the minimum cost path, it can form an important comparison metric for the evaluation of LLG and MCLF.

Compared to ExSrch, ESMP is less complex, even though it still has to perform a search among all possible frequency permutations. Given the number of nodes N in the network and the number of frequency channels m , the worst case scenario would occur for a path of maximum length ($N - 1$ links) if the search had to examine all possible allocations, ie a total of $(N - 1)^m$ possibilities. ESMP remains an impractical method for large topologies especially since the search space grows exponentially with the network size. Thereby, our comparison between ExSrch, ESMP, LLG and MCLF is limited to small-sized topologies.

3.6 Performance analysis

For the purposes of performance evaluation of the algorithms presented in this chapter, we have extended the simulation model developed for the algorithms in chapter 2 (described in appendix A) to support the case of limited frequency channels as well. We have incorporated the interference model and have implemented

all the algorithms presented in this current chapter.

The assumptions that were made in chapter 2 regarding the traffic models, the node topologies (randomly generated networks) and the performance measures continue to hold. The enhanced model differs from before in that there is no limit in the number of transceivers per node and as a consequence a call may be blocked only due to unavailability of frequency channels.

3.6.1 Comparison of frequency allocation heuristics versus exhaustive search mechanisms

We have evaluated the performance of the heuristics for frequency channel allocation and compared the results against those provided by an exhaustive search. Due to the enormous amount of computation that is required for the case of exhaustive search, we have limited our comparison to two sample topologies of 10 nodes. In each example we consider use of the MPM metric for link cost assignment and evaluate the heuristics for the cases of $m^f = 3$ and $m^f = 6$ frequency channels.

Example 1

In this example we consider the topology examined in section 3.5.1, shown in figure 3.5, which consists of 10 nodes. We evaluate two different instances of the same network that correspond to maximum transmission range of $d_{max} = 35$ (fig. 3.5(a)) and $d_{max} = 40$ (fig. 3.5(b)) units respectively. Performance results for this example are summarized in Tables 3.2 (blocking probability) and 3.3 (energy per session).

We do observe that in most of the situations the exhaustive search (ExSrch) provides better performance in terms of blocking probability, which would be ex-

| | $m^f = 3$ | | $m^f = 6$ | | |
|-----------|----------------|----------------|----------------|----------------|-----------|
| λ | $d_{max} = 35$ | $d_{max} = 40$ | $d_{max} = 35$ | $d_{max} = 40$ | Algorithm |
| 0.1 | 0.193 | 0.129 | 0.006 | 0.005 | ExSrch |
| | 0.220 | 0.190 | 0.013 | 0.009 | ESMP |
| | 0.224 | 0.187 | 0.013 | 0.010 | MCLF |
| | 0.226 | 0.197 | 0.015 | 0.013 | LLG |
| 0.3 | 0.442 | 0.373 | 0.110 | 0.075 | ExSrch |
| | 0.442 | 0.399 | 0.122 | 0.093 | ESMP |
| | 0.446 | 0.409 | 0.129 | 0.101 | MCLF |
| | 0.457 | 0.413 | 0.134 | 0.104 | LLG |
| 0.5 | 0.556 | 0.506 | 0.258 | 0.202 | ExSrch |
| | 0.555 | 0.519 | 0.250 | 0.208 | ESMP |
| | 0.559 | 0.521 | 0.253 | 0.218 | MCLF |
| | 0.565 | 0.528 | 0.262 | 0.209 | LLG |
| 0.7 | 0.634 | 0.593 | 0.357 | 0.297 | ExSrch |
| | 0.627 | 0.594 | 0.359 | 0.304 | ESMP |
| | 0.626 | 0.589 | 0.362 | 0.297 | MCLF |
| | 0.629 | 0.595 | 0.368 | 0.325 | LLG |

Table 3.2: Blocking probabilities for topology of Example 1

| | $m^f = 3$ | | $m^f = 6$ | | |
|-----------|----------------|----------------|----------------|----------------|-----------|
| λ | $d_{max} = 35$ | $d_{max} = 40$ | $d_{max} = 35$ | $d_{max} = 40$ | Algorithm |
| 0.1 | 1.409 | 1.472 | 1.416 | 1.393 | ExSrch |
| | 1.329 | 1.326 | 1.406 | 1.387 | ESMP |
| | 1.336 | 1.306 | 1.389 | 1.376 | MCLF |
| | 1.315 | 1.309 | 1.403 | 1.382 | LLG |
| 0.3 | 1.364 | 1.489 | 1.430 | 1.454 | ExSrch |
| | 1.252 | 1.287 | 1.379 | 1.371 | ESMP |
| | 1.276 | 1.278 | 1.396 | 1.374 | MCLF |
| | 1.236 | 1.237 | 1.346 | 1.380 | LLG |
| 0.5 | 1.290 | 1.454 | 1.466 | 1.596 | ExSrch |
| | 1.194 | 1.274 | 1.361 | 1.391 | ESMP |
| | 1.170 | 1.252 | 1.352 | 1.401 | MCLF |
| | 1.177 | 1.235 | 1.324 | 1.370 | LLG |
| 0.7 | 1.232 | 1.457 | 1.426 | 1.393 | ExSrch |
| | 1.148 | 1.250 | 1.355 | 1.396 | ESMP |
| | 1.143 | 1.236 | 1.344 | 1.381 | MCLF |
| | 1.108 | 1.189 | 1.342 | 1.377 | LLG |

Table 3.3: Energy per session for topology of Example 1

pected since for every incoming request this method explores all routing possibilities and blocks the call only if no path and frequency allocation exists. Of course this comes at the cost of higher E_s since the call admission is now restricted to the minimum cost path.

It is remarkable to point out that in some isolated situations we have observed that either the ESMP scheme or one of the heuristics (LLG or MCLF) resulted in better performance than the ExSrch. For example, in the case of $d_{max} = 35$, $\lambda = 0.5$ and $m = 6$, ESMP and MCLF provided lower blocking than ExSrch. Similarly, for $d_{max} = 35$, $\lambda = 0.7$ and $m = 3$, ExSrch had the worst performance among all methods. Even though such a behavior was not expected, it is a consequence of the fact that the ExSrch does not guarantee a global optimum since it works on a per call basis. In fact, a global optimum would be obtainable only if complete knowledge of the traffic pattern was available prior to the beginning of the simulation. Of course, for a certain call and given the current network state, no heuristic can provide a better solution than the ExSrch. Sometimes however, there may exist more than one valid frequency assignments along the minimum cost path; every valid assignment though, has the same effect on blocking of neighboring nodes (ie the number of blocked transmissions does not depend on the selected channel but it depends only on the power level and the receiving node) but may have different effect on future calls, depending on the future traffic characteristics. Hence, it is possible that by accepting a call via the exhaustive search (a call that would have been otherwise blocked via one of the heuristics) future calls may be adversely affected (ie in a way worse than that of the heuristic). Of course, all the heuristics work on a per call basis, so on the average scale such situations are not very likely to happen and as our results indicate they do happen only in few cases, which is

consistent with the above explanation.

Although our performance results have indicated so far that in terms of blocking probability ExSrch has on an average scale the best performance, it is interesting to analyze how well or how bad the heuristics perform compared to it. Note that on an average scale ESMP performs better than the two heuristics, with MCLF coming next and LLG exhibiting the highest values of P_b . The results of table 3.2 indicate that when the transmission range increases, ESMP and the two heuristics perform much worse than ExSrch. Such a behavior could be expected since even a small increase in the transmission range results in a large number of new paths and ExSrch is the only scheme that explores all possible paths between the origin and the destination.

It is also of interest to observe the difference between the worst and best performing algorithm for each set of arrival rates. For the case of $m = 3$, when the traffic load is light there is significant difference in the values of P_b between ExSrch and the rest, whereas for heavy traffic they are pretty close. On the other hand for $m = 6$ the difference seems to be greater for heavy traffic, which is more intuitive since it would be expected that the heuristics would perform less poorly when traffic is light. An explanation that can be applicable for the case of $m = 3$ is that because of the very small number of channels, it becomes less likely to determine a feasible assignment along the minimum power path, since typically this would rather be a multiple hop path; by contrast the ExSrch has the flexibility of using higher power paths, even the highest available (which could be a long direct transmission) as long as a channel assignment can be found. If we look at the values of E_s (table 3.3) our explanation is verified from the increased values of E_s that the ExSrch causes.

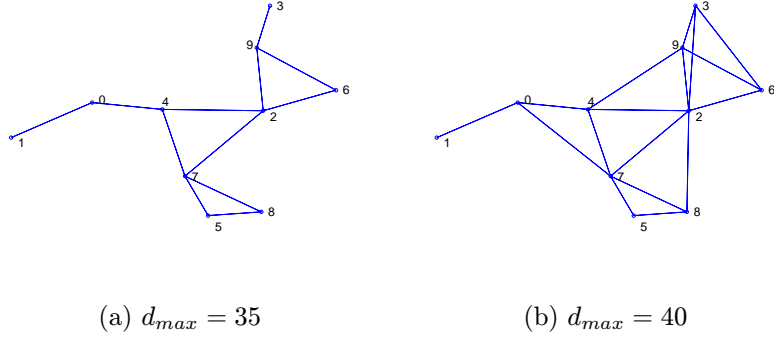


Figure 3.6: Network topology of Example 2

(b) Example 2

In order to verify the consistency of the results we have simulated some additional example topologies. In this example we present the same set of measurements obtained in another 10-node network, depicted in figure 3.6. Again we consider two values for the transmission range (namely $d_{max} = 35$ and $d_{max} = 40$). Tables 3.4 and 3.5 summarize the performance results for these two cases. The observations made in the case of example 1 continue to hold which verifies the accuracy of the simulations.

3.6.2 Performance comparison of LLG versus MCLF for random topologies

In this section we focus on the performance of the frequency allocation heuristics. We assume that the candidate path is selected via use of the MPM metric and we compare LLG and MCLF in terms of blocking probability, for the simulation parameters summarized in table 3.6. In each case we have simulated 100 randomly generated topologies and we have computed the average values of P_b .

| | $m^f = 3$ | | $m^f = 6$ | | |
|-----------|----------------|----------------|----------------|----------------|-----------|
| λ | $d_{max} = 35$ | $d_{max} = 40$ | $d_{max} = 35$ | $d_{max} = 40$ | Algorithm |
| 0.1 | 0.271 | 0.200 | 0.028 | 0.011 | ExSrch |
| | 0.277 | 0.231 | 0.029 | 0.015 | ESMP |
| | 0.275 | 0.229 | 0.028 | 0.018 | MCLF |
| | 0.296 | 0.244 | 0.034 | 0.024 | LLG |
| 0.3 | 0.499 | 0.436 | 0.177 | 0.127 | ExSrch |
| | 0.497 | 0.459 | 0.179 | 0.139 | ESMP |
| | 0.501 | 0.456 | 0.180 | 0.139 | MCLF |
| | 0.517 | 0.462 | 0.193 | 0.152 | LLG |
| 0.5 | 0.596 | 0.562 | 0.322 | 0.249 | ExSrch |
| | 0.599 | 0.569 | 0.324 | 0.268 | ESMP |
| | 0.602 | 0.570 | 0.320 | 0.271 | MCLF |
| | 0.598 | 0.570 | 0.339 | 0.279 | LLG |
| 0.7 | 0.652 | 0.633 | 0.416 | 0.364 | ExSrch |
| | 0.655 | 0.637 | 0.428 | 0.373 | ESMP |
| | 0.654 | 0.631 | 0.416 | 0.368 | MCLF |
| | 0.662 | 0.638 | 0.434 | 0.378 | LLG |

Table 3.4: Blocking probabilities for topology of Example 2

| | $m^f = 3$ | | $m^f = 6$ | | |
|-----------|----------------|----------------|----------------|----------------|-----------|
| λ | $d_{max} = 35$ | $d_{max} = 40$ | $d_{max} = 35$ | $d_{max} = 40$ | Algorithm |
| 0.1 | 1.301 | 1.363 | 1.343 | 1.332 | ExSrch |
| | 1.337 | 1.319 | 1.403 | 1.346 | ESMP |
| | 1.298 | 1.294 | 1.394 | 1.365 | MCLF |
| | 1.309 | 1.286 | 1.397 | 1.340 | LLG |
| 0.3 | 1.181 | 1.273 | 1.277 | 1.332 | ExSrch |
| | 1.168 | 1.205 | 1.336 | 1.326 | ESMP |
| | 1.164 | 1.178 | 1.356 | 1.340 | MCLF |
| | 1.152 | 1.161 | 1.331 | 1.326 | LLG |
| 0.5 | 1.106 | 1.239 | 1.266 | 1.298 | ExSrch |
| | 1.091 | 1.133 | 1.286 | 1.309 | ESMP |
| | 1.076 | 1.157 | 1.285 | 1.315 | MCLF |
| | 1.015 | 1.073 | 1.271 | 1.279 | LLG |
| 0.7 | 0.997 | 1.193 | 1.177 | 1.317 | ExSrch |
| | 0.985 | 1.082 | 1.250 | 1.276 | ESMP |
| | 0.992 | 1.062 | 1.229 | 1.256 | MCLF |
| | 0.975 | 1.043 | 1.218 | 1.221 | LLG |

Table 3.5: Energy per session for topology of Example 2

| | |
|-------------|------------------|
| N | 10 and 20 |
| P_{max} | 0.9 and 2.5 |
| d_{max} | 30 and 50 |
| λ | $\in [0.1, 0.9]$ |
| μ | 1 |
| m^f | 6 and 9 |
| Link Metric | MPM |

Table 3.6: Simulation parameters for comparing LLG with MCLF

Figures 3.7 and 3.8 graphically illustrate the relative performance of LLG and MCLF for $d_{max} = 30$ and 50 respectively. We show the curves for 10-node and 20-node networks. For all network sizes and transmission ranges, MCLF provides slightly better performance.

Figure 3.9 graphically illustrates the relative performance of LLG and MCLF for both cases of $m = 6$ and $m = 9$. MCLF provides consistently a slight improvement versus LLG, and by increasing the number of channels we get lower values of P_b with MCLF providing relatively better improvement. Of course the trade-off that needs to be accounted for is the need for centralized operation by MCLF versus the fully distributed nature of LLG.

3.6.3 Performance characteristics of link metrics for use with link-by-link greedy frequency allocation scheme

Thus far, we have discussed only the performance of the heuristics and the exhaustive search methods for allocating frequency channels to selected routes for

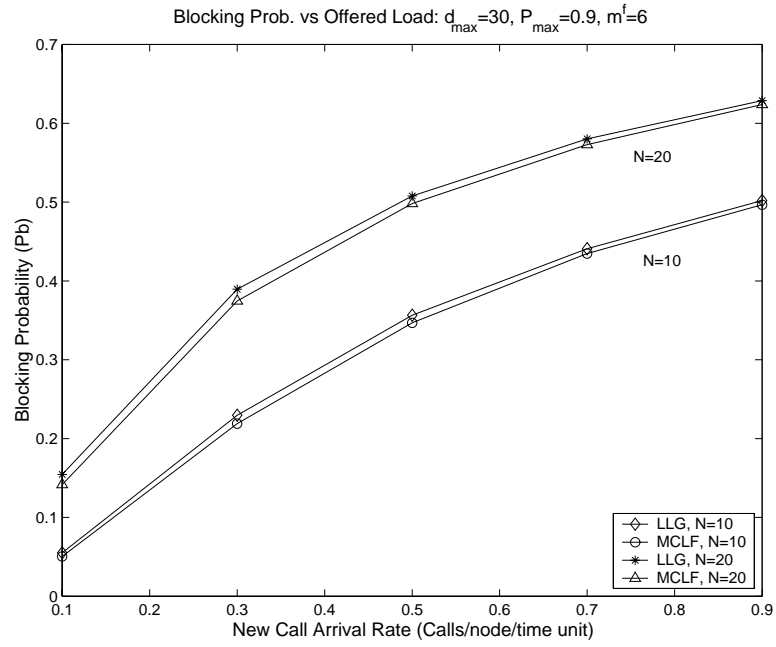


Figure 3.7: Comparison of LLG, MCLF through blocking probability, $d_{\max} = 30$

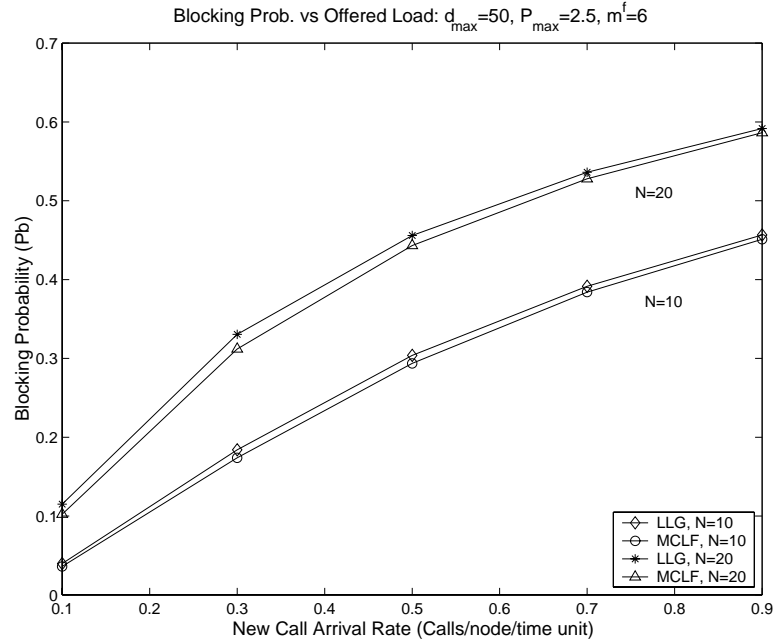


Figure 3.8: Comparison of LLG, MCLF through blocking probability, $d_{\max} = 50$

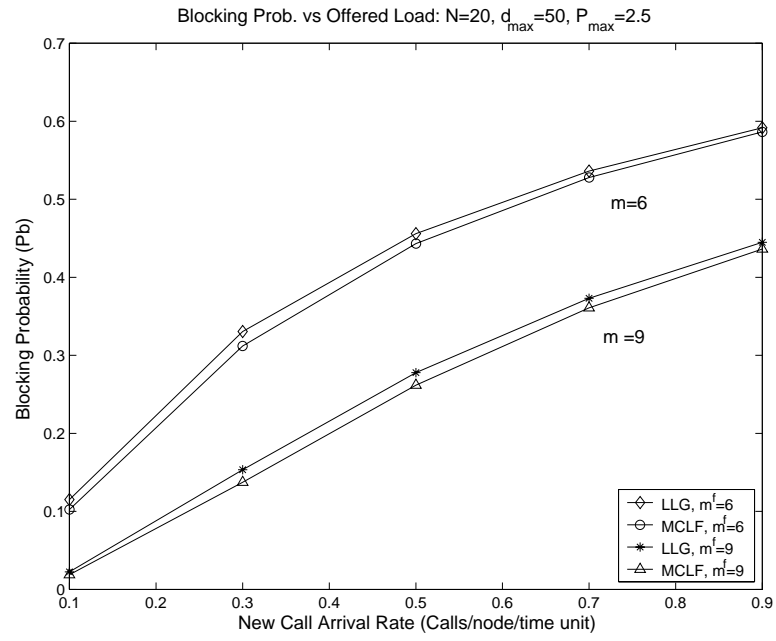


Figure 3.9: Comparison of LLG, MCLF through blocking probability and number of frequency channels, $N = 20$, $d_{\max} = 50$

admitting new calls. In all the experiments we considered the link metric to be given by MPM (equation 3.3). In this section we evaluate the relative performance of MPM and PIM metrics for joint use with LLG as a channel allocation algorithm. Figures 3.10 – 3.15 illustrate graphically the relative performance of MPM and PIM. For each set of values of λ , d_{max} and N , we have run simulations for 100 randomly generated topologies and we have computed the average values of our performance measures, namely P_b , E_s and Y . Table 3.7 summarizes the simulation parameters for the results presented in this section.

| | |
|-----------|------------------|
| N | 10 and 20 |
| P_{max} | 0.9 and 2.5 |
| d_{max} | 30 and 50 |
| λ | $\in [0.1, 0.9]$ |
| μ | 1 |
| m^f | 6 |

Table 3.7: Simulation parameters for comparing MPM with PIM

From the graphs shown in figures 3.10 and 3.11 we observe that use of PIM provides better performance in terms of blocking probability in all of the cases. Note that when the network becomes denser (larger N), P_b increases. It is also of interest to point out that PIM achieves better improvement in P_b relatively to MPM for larger d_{max} .

By contrast, MPM performs better when the performance metric is the average energy per session (figures 3.12 and 3.13). Clearly, this improved performance can be attributed to the fact that MPM's only criterion for selecting the candidate

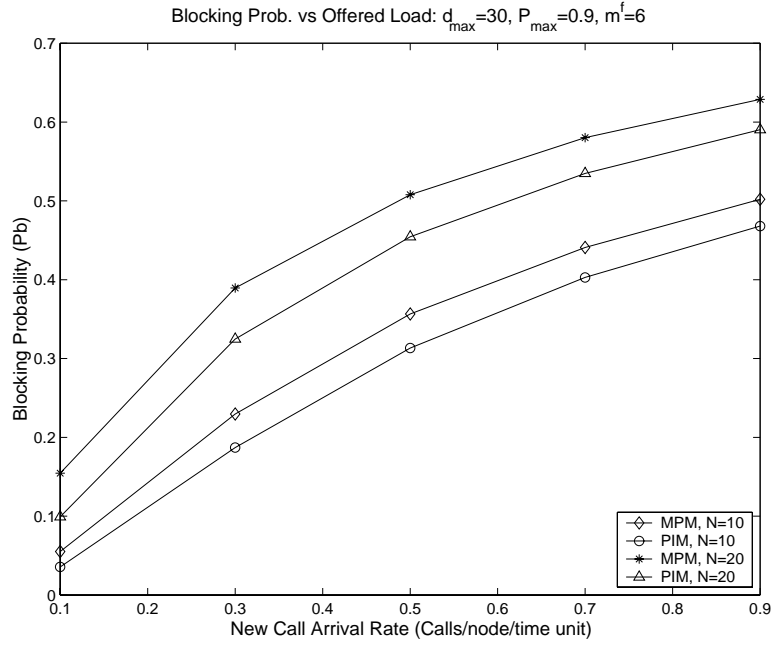


Figure 3.10: Comparison of MPM and PIM in terms of P_b ($d_{max} = 30$).

path is the minimum power consumption. Notice again that when the transmission range increases, for equal sized networks MPM provides much better improvement in the values of E_s .

Finally, figures 3.14 and 3.15 show the performance yardstick versus the call arrival rate. Except for the case of $N = 20, d_{max} = 30$, MPM seems to outperform PIM.

3.7 Conclusions

We developed a set of algorithms that jointly address the problem of routing and frequency allocation for connection oriented traffic under the case of limited bandwidth resources. We approached the problem in two stages, first with the selection

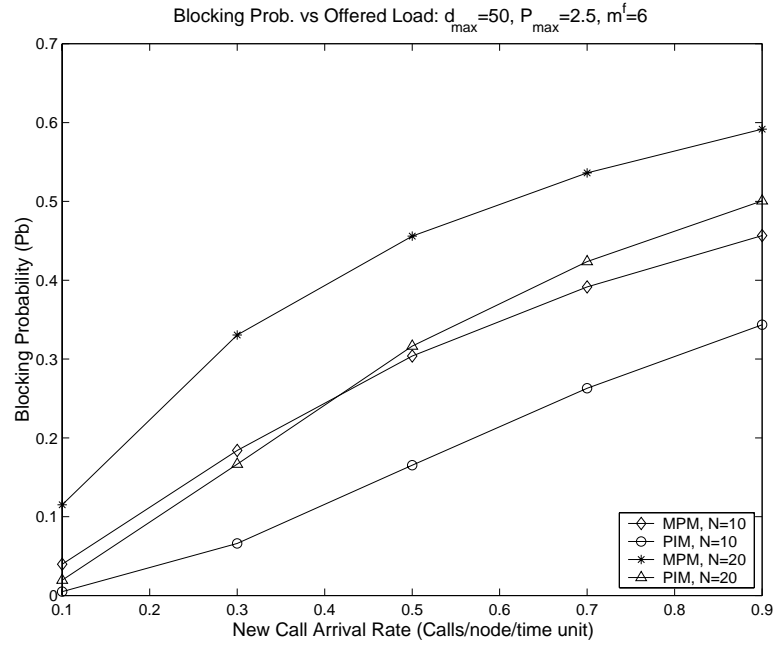


Figure 3.11: Comparison of MPM and PIM in terms of P_b ($d_{max} = 50$).

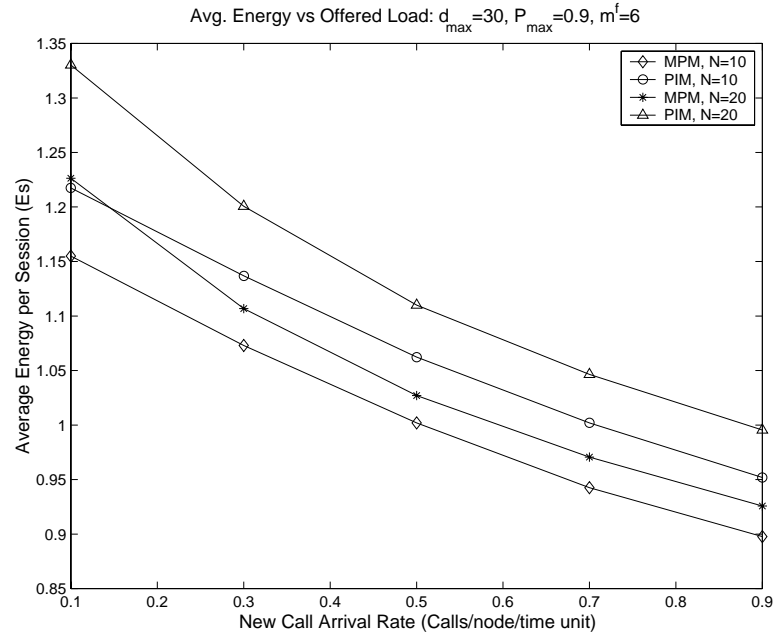


Figure 3.12: Comparison of MPM and PIM in terms of E_s ($d_{max} = 30$).

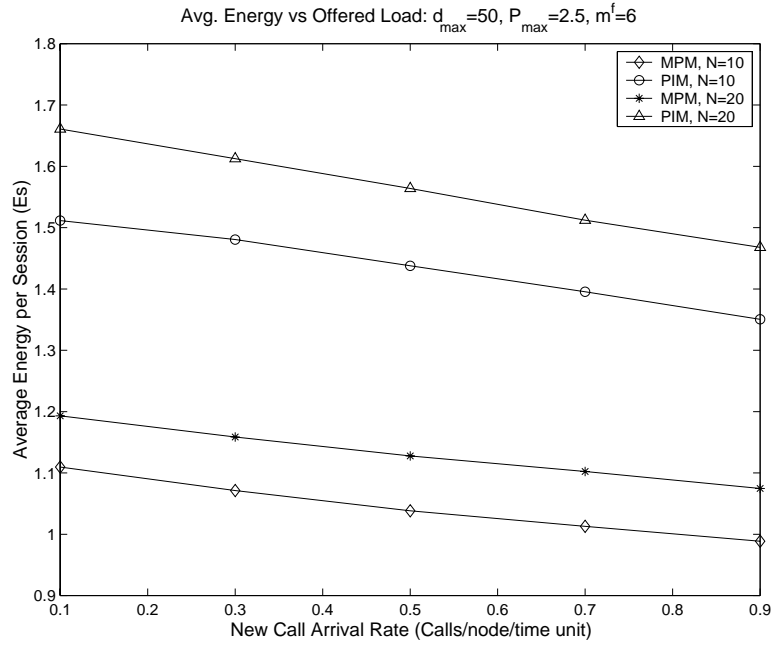


Figure 3.13: Comparison of MPM and PIM in terms of E_s ($d_{\max} = 50$).

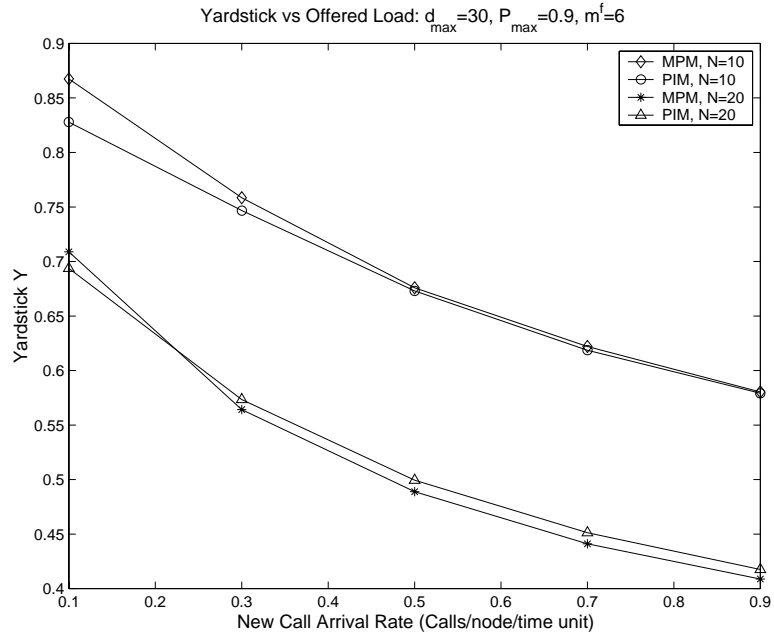


Figure 3.14: Comparison of MPM and PIM in terms of Y ($d_{\max} = 30$).

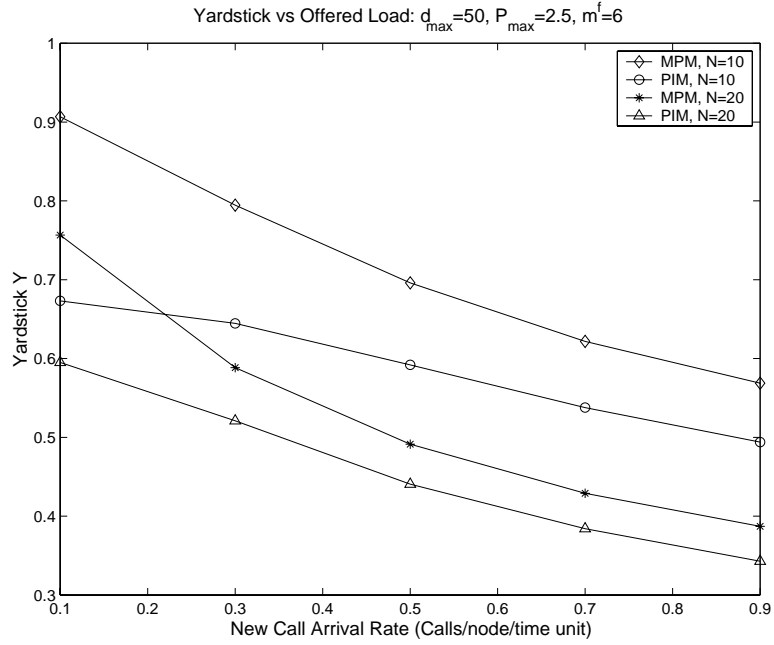


Figure 3.15: Comparison of MPM and PIM in terms of Y ($d_{max} = 50$).

of a candidate path (as the minimum cost path in terms of transmission energy and blocking effects) and then with a set of frequency allocation heuristics so that interference-free communication can be achieved. Our results indicate that improved performance can be obtained by jointly considering the transmission power and the bandwidth allocation selection. We also demonstrated that even with a greedy channel allocation scheme, performance is comparable to that of exhaustive search mechanisms, whereas implementation complexity is extremely lower.

Chapter 4

A “Blueprint” towards an Integrated Scheduling, Access Control and Routing Scheme in Wireless Ad-Hoc Networks

4.1 Motivation

While the Internet is evolving into a true integrated services network, wireless data networks are becoming an integral part of the new global communication infrastructure. In order to support a variety of applications with a wide range of Quality-of-Service (QoS) requirements (e.g., audio and video conferencing, multimedia information retrieval, ftp, telnet, WWW, etc.), efficient link management and scheduling algorithms are necessary. In this chapter, we review state-of-the-art work on fair resource allocation/packet scheduling for wireline and wireless networks and address the unique issues that arise when similar schemes must be applied to wireless ad-hoc environments.

In wireline networks, a popular model for providing fairness and bounded delay link access is the fluid fair queuing model ([15, 16]). A variety of fair queuing

algorithms have been proposed ([16, 17, 18]) that are based on the notion of approximating the fluid model, in which packet flows are modeled as fluids that traverse a shared pipe. Although algorithms that follow this model perform well in wireline networks, they do not carry over their properties to the wireless environment. In fact, most have been shown to lose their desirable properties such as fairness and tight delay bounds in varying capacity links. Moreover, the unique characteristics of the wireless channel such as location-dependent and bursty errors and location-dependent capacity often lead to situations of unfairness.

The adaptation of packet fair queuing algorithms to wireless networks has motivated a significant amount of research work [19, 20, 21, 22, 23]. Most of these proposed algorithms are designed for a wireless cellular environment (with the base station acting as a coordinator node) and are capable of achieving long-term fairness by arbitrating among flows with good and bad channel error attributes differently, and suggesting mechanisms for compensating "lagging" flows at the expense of "leading" flows. However, they rely on the existence of a base station which plays the role of the local arbitrator and thus are not appropriate for other types of network architectures such as ad-hoc networks.

Wireless ad-hoc networks present some key characteristics that necessitate a modified approach to the problem of fair scheduling. Channel access is not always controlled by a central arbitrator node but has to be achieved in a distributed fashion and in a way that collisions are avoided (to the degree this is feasible). At the same time, the possibility to re-use bandwidth gives rise to the trade-off between fair scheduling and maximum resource utilization. Most important, loading and congestion at each node is not dependent on the scheduling discipline only but also on routing decisions. If the routing algorithm and the metrics used to make

routing decisions do not adequately capture the effects of the radio link quality and the capacity assignment by the access control and scheduling mechanisms, inefficient route assignments may result that could lead to increased congestion and lost throughput. On the other hand, methods of assigning the bandwidth need to be based on the traffic requirements at each node (based on new traffic originating and flows being routed through the node) as well as the quality of the links from a given node. Last, but not least, channel errors which are location-dependent and bursty in nature may affect flows selectively. Therefore, mechanisms to compensate for nodes and flows that experience poor channel quality must be part of every scheduling discipline.

Based on these remarks, we argue upon the fact that the design of efficient protocols for wireless multi-hop networks must address the dependencies between routing, access control and scheduling, and radio link functions. We propose a preliminary unified scheme which performs node-level access control (also called node-level scheduling), flow-level scheduling and route assignment in a hierarchical framework with interactions among the three protocol solutions. Our approach can be regarded as a "blueprint" towards the future development of more detailed unified solutions. The variety and the complexity of issues that arise due to the numerous trade-offs involved in such a design will become apparent as we discuss our methodology in the following sections. However, even with a simplified preliminary performance evaluation, useful conclusions on the interdependencies of our protocols are drawn that reveal the potential and the possibilities that exist towards these directions.

The rest of the chapter is organized as follows. In the next section we review a class of scheduling disciplines, used for scheduling best-effort traffic in wire-line

networks. We discuss the techniques that have been proposed in adapting these algorithms in wireless cellular networks and in wireless LANs along with recent work that investigates the problems of MAC layer fairness jointly with contention resolution mechanisms in multi-hop networks. We continue with an overview of our methodology and our network model and then with a detailed description of our hierarchical scheduling and routing framework. Finally, we present a set of preliminary simulation results and discuss implementation aspects and proposed future enhancements of our model.

4.2 Background

In this section we review related work on wire-line and wireless scheduling and fair queuing. We describe a variety of algorithms that have been shown to exhibit good performance in wire-line networks and then discuss their adaptations to a wireless environment. We also discuss some recent work on fairness models for shared wireless channels such as wireless LANs or wireless multi-hop networks which, because of their unique characteristics, make the scheduling problem even more challenging.

4.2.1 Scheduling disciplines for wire-line networks

A wide range of scheduling algorithms for wire-line networks have been proposed in the literature. Such algorithms are capable of supporting several classes of multimedia traffic, oftentimes with different delay and throughput performance requirements. All scheduling algorithms are based on the notion of approximating the fluid model, in which packet flows are modeled as fluids that traverse a shared

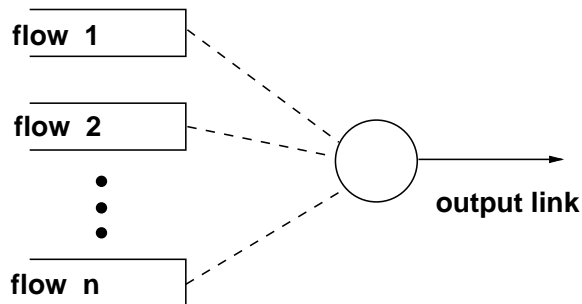


Figure 4.1: A node with several flows sharing a common channel

pipe. Consider for example the system shown in figure 4.1, where packets from several flows are stored in different queues of the same node before being transmitted to an output link. A fair scheduling algorithm is required for determining which flow to serve at every time so that a set of fairness criteria are satisfied. We describe the most fundamental of these schedulers and discuss their main principles of operation.

Generalized Processor Sharing (GPS)

The fair queuing algorithms proposed in the literature attempt to approximate the Generalized Processor Sharing discipline proposed in [15]. GPS is an ideal scheduling discipline that visits each nonempty queue in turn and serves an infinitesimally small amount of data, so that in any finite time interval, it can visit each logical queue at least once. Moreover, connections can be associated with service weights and receive service in proportion to their weights whenever they have data in their queue. However, GPS is not implementable because it is supposed to serve an infinitesimal amount from each nonempty queue. In actual systems, packets must be transmitted as a whole and this has motivated research in the area of packet fair queuing algorithms.

Round-Robin and Weighted Round-Robin (WRR)

The simplest emulation of GPS is a round-robin scheduler which serves one packet from each non-empty logical queue instead of an infinitesimal amount. If connections have different weights, a Weighted Round-Robin scheduler serves a connection in proportion to its weight. However, WRR approximates GPS reasonably well only if all packets have the same size. If packets have different sizes, the WRR scheduler divides each connection's weight by its mean packet size to normalize the weights. In some situations, a server may not know in advance the mean packet size of a connection (for example in the case of compressed video transmission) and then WRR cannot allocate bandwidth in a fair way. Another problem is that WRR is unfair over short time scales (some connections may get more service than others in one round-time) and if a connection has a small weight or if the number of connections is large, this may lead to long periods of unfairness.

Deficit Round-Robin (DRR)

Deficit Round-Robin [18] is a modification to WRR so that it can handle variable packet sizes without knowledge of the mean packet size of each connection in advance. In DRR implementation, each back-logged connection is associated with a deficit counter which is initially set to zero. The scheduler visits each back-logged connection in turn and tries to serve one quantum worth of bits from it. The only difference from the traditional round-robin is that if a queue is not able to send a packet in a previous round because its packet size was too large, the remainder from the previous quantum is added to the quantum for the next round. Thereby, queues that were short-changed in a round are compensated in the next round.

Weighted Fair Queuing (WFQ)

In Weighted Fair Queuing [16] (also referred to as Packet-by-Packet GPS [15])

packets are served in order of their *service* tags which are computed by simulating a hypothetical GPS on the side. Since packets must be served as a whole (and not a bit at a time), WFQ computes the *start tag* and then the *finish tag* of every new packet, the latter being the time the packet would have completed service if a GPS server was being used. Packets are then served in order of their finish tags. The finish tag computation depends on a variable called the *round number*, which increases at a rate inversely proportional to the number of active connections. In particular, if p_f^j and l_f^j denote the j th packet of flow f and its length, respectively, and if $A(p_f^j)$ denotes the arrival time of packet p_f^j at node i , then the start tag $S(p_f^j)$ and finish tag $F(p_f^j)$ of packet p_f^j are defined as:

$$S(p_f^j) = \max\{v[A(p_f^j)], F(p_f^{j-1})\}, \quad j \geq 1 \quad (4.1)$$

$$F(p_f^j) = S(p_f^j) + \frac{l_f^j}{\phi_j} \quad (4.2)$$

where $F(p_f^0) = 0$ and $v(t)$ is defined as:

$$\frac{dv(t)}{dt} = \frac{C}{\sum_{j \in B(t)} \phi_j} \quad (4.3)$$

where C is the capacity of the server, $B(t)$ is the set of back-logged flows at time t in the bit-by-bit round-robin server and ϕ_j is the weight associated with flow j . WFQ then schedules packets in the increasing order of their finish tags.

Although WFQ achieves fairness comparable to GPS, it is complex (in terms of implementation) because it needs to maintain per connection scheduler state which may be expensive for schedulers that serve large numbers of connections. Moreover, as it is demonstrated in [24], the computation of $v(t)$ requires simulation of a bit-by-bit round-robin server in real time which may in turn require processing

of $O(Q)$ events per packet transmission, where Q is the number of active queues. With the current definition of virtual time though, it has been shown in [17] that WFQ becomes unfair over variable rate servers and hence is not a reliable option.

Start-Time Fair Queuing (SFQ)

The Start-time Fair Queuing algorithm proposed in [17] overcomes some of the deficiencies of WFQ. It differs from WFQ in that packets are scheduled in order of their start-tags (computed by equation 4.1) instead of the finish-tags. Furthermore, $v(t)$ is defined as the start tag of the packet in service at time t . As is evident from this definition, the computation of $v(t)$ is inexpensive (in fact complexity is $O(\log Q)$ per packet where Q is the number of flows at the server). In addition to that, SFQ has been shown to retain fairness even when the capacity of the link is variable. However, the delay properties of SFQ for high throughput applications are not as good as those for the WFQ algorithm; it outperforms WFQ though for low throughput applications.

4.2.2 Scheduling disciplines for cellular wireless networks

Scheduling algorithms that work well in wire-line networks do not always carry over to the wireless environment and in most situations they have been known to lose their desirable properties, such as fairness and tight delay bounds. Part of this behavior is attributed to the following three characteristics of the wireless channel:

- capacity is severely limited and time varying
- channel errors are location-dependent and bursty in nature
- need for channel access control mechanisms in shared medium configurations.

Although the problem of varying capacity channels is partially addressed by use of SFQ schedulers, the problem of location- dependent and bursty channel errors may lead to undesirable situations. For example, sessions that experience errors may receive significantly less service than what they would be entitled to, whereas sessions that have access to error-free channels take advantage. In order to account for channel errors, wireless scheduling algorithms usually adapt a wire-line scheduling algorithm to the situation where flow specific errors are present. This means that wireless scheduling algorithms differentiate between flows experiencing channel errors from those with a clean channel. Each flow is labeled as being *leading*, *lagging* or *in sync* depending on whether its actual received service is ahead of, behind of, or in accordance to its *error-free* service which it would have received if a *clean-channel* was available all the time. Typically, flows that are scheduled and are experiencing channel errors are taken offline (and hence are considered as lagging) and the scheduler instead may choose to allocate the excess capacity to flows with clean wireless channels (resulting in their service leading the ideal service).

Different wireless algorithms choose to address the issue of lag and lead in different ways. In addition, almost all wireless algorithms require an estimate of the per flow channel characteristics (error, capacity). Since any estimate is prone to error, given the random nature of a wireless channel, wireless scheduling and admission control algorithms will under-perform the ideal wire-line scheduler when channel errors reduce per flow capacity. In order to compensate for the ambiguity and error in capacity estimates, wireless algorithms must have compensatory mechanisms such as the lag/lead compensation system or a method where buffer capacity is always reserved to help accommodate flows with poor channel quality.

A brief summary of the main wireless scheduling algorithms is given below:

- Channel State Dependent Packet Scheduling (CSDPS), in [21]: A weighted round-robin (WRR) scheduling discipline is used to schedule flows which are error free. There is no lag/lead measurement for flows and hence no compensation. Implementation complexity is low.
- Idealized Wireless Fair Queuing (IWFQ), in [19]: WFQ is used for error free service. The lag is upper bounded and the scheduler maintains lag and lead for each flow and favors lagging flows by allowing them to capture the channel as soon as they perceive error free channels. This algorithm has poor short term fairness properties and throughput bounds while long term fairness and bounds are provided.
- Wireless Packet Scheduling (WPS), in [19]: A modified version of WRR is used where the bandwidth allocation is as per the weights, but spread out rather than continuous. The algorithm maintain lag and lead measures and compensates for lags in two ways: changing weights of lagging flows in subsequent frames, or exchanging slots between error prone and error free flows in the same frame. The performance is similar to IWFQ.
- Channel Condition Independent Fair Queuing (CIF-Q), in [22]: STFQ is the error free service model. Lags and leads are computed and lagging flows are compensated only when leading flows relinquish slots. CIF-Q has the best short term and long term fairness and throughput properties though lagging flows may suffer poor short term fairness.
- Enhanced Class Based Queuing with Channel State Dependent Packet Scheduling, in [25]: This model combines the CSDPS scheduling with Class based

Queuing. Lag/lead compensation is similar to IWFQ.

- Wireless Fair Service (WFS), in [23]: An enhanced version of WFQ is used for error free service. Lead and lag are bounded for each flow. A leading flow with a lead l and a lead bound l_{max} relinquishes $\frac{1}{l_{max}}$ slots. WFS is shown to achieve the tightest short term fairness and throughput bounds among all algorithms. It also provides good long term performance. Lag compensation may be slow.

The idea of lag/lead compensation while temporarily subverting priorities and fairness provides ways of compensating for errors which are flow specific. Note that lag and lead bounds can be used to control the extent to which this mechanism actually redistributes bandwidth among lagging and leading flows.

4.2.3 Scheduling in wireless LANs

None of the scheduling algorithms listed above addresses explicitly the problem of channel access in a distributed topology. In all situations it is assumed that a central coordinator node exists (e.g. a base station) which performs the scheduling functions and allocates bandwidth to the contending uplink flows. Early work in medium access control (MAC) protocols for wireless LANs has focused on providing fully distributed schemes for channel access. Protocols such as MACA [26] and MACAW [27] were based on *Request-to-Send (RTS)*, *Clear-to-Send (CTS)* packet exchange and binary exponential back-off mechanisms to mitigate collision effects. They were limited though in that they attempted to provide equal share of bandwidth to different nodes, without differentiating among classes of service with different bandwidth requirements and without taking into account channel

errors. In a later work [28], *Vaidya et. al.* proposed a distributed *fair* scheduling algorithm motivated by the collision avoidance mechanisms of the IEEE 802.11 standard for wireless LANs. Their work suggests an emulation of start-time fair queuing in a distributed manner, by modifying the back-off interval mechanism, so that nodes ready to transmit packets with smaller tags have smaller back-off intervals. Even though in the performance evaluation location dependent channel errors were considered, there was no explicit mechanism on how to react or take into account poor quality link situations.

4.2.4 Scheduling in wireless multi-hop networks

Most of the features encountered in a wireless LAN environment are also present in wireless multi-hop networks. In fact, a single logical channel is again shared among many contending users and there is lack of global knowledge of the traffic flows in each node, since information is distributed. However, in multi-hop wireless networks, spatial reuse of the channel bandwidth is possible and thereby there is an inherent trade-off between achieving fairness among contending flows and at the same time maximizing channel utilization. In [29] a model is presented that addresses this trade-off. A centralized algorithm is first proposed that provides a minimum fair allocation of bandwidth for each packet flow and attempts to maximize spatial bandwidth reuse. A distributed implementation is then discussed based on a back-off channel contention scheme. Some relevant work is also presented in [30], where only the fairness problem is studied without taking into account channel utilization issues. This work focuses mostly on the MAC-layer aspects of the problem and on developing contention resolution algorithms that execute independently at each node and are translated into a sophisticated back-

off algorithm for achieving proportional fairness.

Although both [29] and [30] present some novel features on how to model fairness in a multi-hop network architecture, their focus remains on the implementation issues of contention resolution mechanisms in a distributed fashion. The effects of channel errors which, as was discussed earlier, constitute a significant hurdle in achieving fairness in wireless environments are not directly addressed. Moreover none of these studies, and no other study that we know of, considers the dependencies between scheduling algorithms and route assignments. Methods of assigning the bandwidth however, need to be based on the traffic requirements at each node as well as routing information and vice-versa. With this in mind, we propose in the next section a hierarchical scheduling scheme and a method of addressing the dependencies between capacity allocation and route assignments.

4.3 A unified approach to scheduling, access-control and routing in ad-hoc networks

4.3.1 Overview

We propose a hierarchical scheme that considers a wireless channel shared by multiple nodes. Capacity allocation is made at the node-level and the flow level based on link and flow-level error characteristics and the routing assignments. The routing algorithm is shortest-path based with the link-distance metrics calculated based on congestion information and the current node and flow-level schedules.

A two-tier scheduling mechanism is proposed, namely node-level and flow-level scheduling. Each node is associated with an adaptive metric/weight which is up-

dated periodically and is a function of the traffic requirements at the node (based on new traffic originating and flows being routed through the node) as well as the quality of the links from a given node (captured by number of lost packets due to channel errors). Once all the nodes have determined their bandwidth allocations, they schedule their flows individually using a similar mechanism with the difference that the metrics are now per-flow and depend on the traffic requirements and lost throughput of individual flows. With this multi-level approach we can handle errors that are flow-selective in nature and compensate flows that are lagging because they have been experiencing poor quality channels.

In order to address the dependencies between routing and scheduling, the routing assignments should be updated periodically. The concept of *least-resistance routing* (LRR), described in [31], can be used to determine link-distance metrics that depend on the link-quality. By updating the route assignments, flows that have been experiencing poor links due to location-dependent errors have the chance of re-negotiating their paths. Note that a flow is defined by its source-destination pair and therefore even if a link in the routing path suffers the whole flow will be affected. On the other hand, node-level and flow-level schedules always adapt to the most current routing vectors since they are determined as functions of the new traffic requirements.

4.3.2 Proposed model

We consider an ad-hoc network where nodes are organized into a number of overlapping clusters. Nodes that belong to the same cluster are connected with each other via direct links. For example, in the network of figure 4.2, nodes A, B and E belong to the same cluster; nodes B, C and D belong to a different cluster.

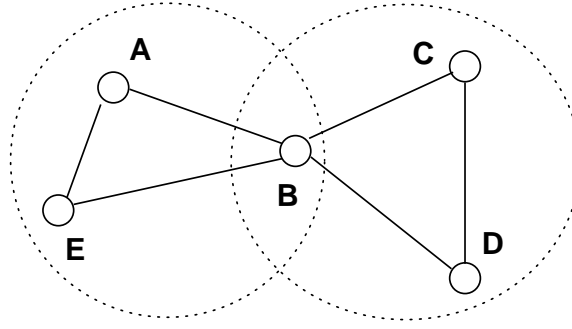


Figure 4.2: Example network topology organized into “clusters”

Notice that certain nodes may be members of more than one clusters at the same time (that is the case in our example for node *B*). In general, clustering provides a convenient framework for the operation of an efficient access control and bandwidth allocation scheme since capacity allocations are localized. In the literature [32, 33, 34] the problem of cluster formation and maintenance has been studied extensively, especially in the context of routing. Algorithms for cluster formation and organization have been proposed which are capable of reacting to connectivity changes and re-organizing their clusters. In most of these schemes however, it is assumed that all routing is performed through a local-coordinator node, called the “cluster-head”, limiting therefore the number of available paths and in some situations (especially in non-dynamically adjusting clusters) creating bottlenecks which degrade routing performance. Our approach differs in that the clustered architecture does not impose any restriction on routing and is only used for purposes of facilitating bandwidth allocation. As we will see in the sequel, any path can be used regardless of the clusters the nodes might belong to.

As of this work, we have assumed fixed topologies only and therefore the organization of the network into clusters is performed statically at the beginning

of network operation. Dynamic topologies necessitate the use of sophisticated clustering algorithms that react to topological changes by adjusting the cluster-memberships and dependencies and are beyond the scope and objectives of this study.

Nodes do not need to maintain global knowledge of the network parameters; instead, they rely on selected information that is exchanged periodically among members of a cluster to determine their weights and make the scheduling decisions in a distributed fashion. The operational environment consists of shared radio links with nodes operating in half duplex mode: they can either transmit or receive but not both simultaneously. Nodes belonging to more than one clusters can receive packets from only a single node in each cluster but not from multiple clusters simultaneously. For example, in the topology shown in figure 4.2, node B can receive packets from nodes A and C , but not from C and D in the same time slot. Multiple packet receptions from different clusters may be possible if nodes use directional/smart antennas, have multiple receiver elements and if the clusters are organized to isolate interference.

Time is slotted and slots are grouped into fixed length frames. We assume a single packet can be transmitted per slot. Allocations of slots to nodes and flows, and route selection of the flows can only be performed at the beginning of a frame. Since our focus is on the bandwidth sharing principles rather than on the implementation details of the MAC-layer protocol, we assume that every node's allocated slots get assigned to the appropriate portion of each time-frame by a mechanism that is not the purpose of this study. Nonetheless, the development of a MAC-layer protocol that implements our scheme can be performed at a future time.

Under these considerations, the approach to solving the node access, flow scheduling and routing problem jointly evolves as an iterative procedure between the following three steps:

Step 1. Node-level scheduling: Determine the capacity allocation to each node in the cluster based on a weighted round-robin scheme using fixed routing assignments for all flows in each node.

Step 2. Flow-level scheduling: Determine the capacity allocation to each flow in the node based on a weighted round-robin scheme using fixed routing assignments for all flows in that node.

Step 3. Route-updates: Determine the routes of the flows at each node: i.e., for all the flows in a particular node determine which of the nearest neighbors the flow must be directed to.

4.3.3 Link error adjusted rate (LEAR) measure

The node and flow-level scheduling is performed by a modified weighted round-robin algorithm in which the nodes and their serviced flows determine their weights in proportion to a measure called the *link error adjusted rate (LEAR)*.

Nodes are aware of the number of packets buffered for transmission at the beginning of every frame. Moreover, each node estimates the channel quality on each of its flows in terms of loss in throughput (ie. number of packets lost per frame). Assume for example that node C in figure 4.2 has packets to be transmitted to both B and D . Node C estimates loss in capacity due to channel errors for the flows directed to B and to D . A link error adjusted rate ($LEAR$) required by node

C is then computed by adding the average error free service rates required by all flows plus the lost throughput of all its links weighted in the proportion of flows directed to that destination. In particular, for this example, if $X_t(CD)$ represents the number of packets waiting to be transmitted from C to D at the beginning of frame t and $Y_{t-1}(CD)$ represents the lost packets for frame $(t-1)$ on link C to D and similarly $X_t(CB)$ are the packets to be transmitted from C to B and $Y_t(CB)$ are the lost packets on link C to B , the *LEAR* value is computed as follows:

$$LEAR_t(C) = X_t(CB) + X_t(CD) + Y_{t-1}(CD) \times \frac{X_t(CD)}{X_t(CD) + X_t(CB)} + Y_{t-1}(CB) \times \frac{X_t(CB)}{X_t(CB) + X_t(CD)} \quad (4.4)$$

The weights of the WRR scheduler are then determined in proportion to the *LEAR* values of each node rather than the average rate required. The two variables X and Y capture two different effects. While X models the congestion level at each node, Y estimates the link quality between a node and its neighbors. As congestion increases in a node, the values of the X variable increase and the node demands a higher share of the bandwidth. Also, the *LEAR* value increases as Y increases or the link quality decreases. The node thus tries to compensate for lost throughput by using higher bandwidth. This appears to be inefficient since nodes with poor quality links might hog bandwidth and throughput is lost. This is prevented though if the link metrics for the routing mechanisms are selected carefully to discourage use of links with poor quality and excessive delays. Also, as the queues in neighboring nodes increase, their X values increase and they obtain more bandwidth preventing starvation. This is a method for lag-lead compensation, as flows which are lagging have higher values of the *LEAR* measure and

obtain higher bandwidth.

4.3.4 Routing updates

In the determination of the node and flow capacity allocations, the route assignments are fixed, i.e. each node knows the immediate next-hop neighbor for each flow. At the beginning of each time frame, routes may be recomputed based on the current schedules, and used in the subsequent time frame. In order to determine the route for each flow, we associate each link with an adaptive distance-metric (cost of transmitting over that link) and use a distributed version of Bellman-Ford [12] algorithm for shortest-path computation. Link metrics should be selected in a way that preference is given to neighboring nodes with lower congestion (smaller aggregate queue size) and links with lower estimated service time. The metric we propose is proportional to an estimate of the average packet delay, which can be obtained if a packet is stamped when buffered at node so that upon departure its delay can be computed. More sophisticated metrics that may capture link congestion can be plugged in without having to modify the algorithm.

An appropriate update interval must be determined for periodically re-computing the link metrics and adjusting the route assignments. In practice, it cannot happen at the beginning of every frame, for the following reasons. First, the overhead of updating the link metrics, running the shortest-path algorithm and adjusting all the routing tables is too large. Second, if the routing tables are updated very frequently, oscillations may occur, affecting the great majority of packets that will have to travel along “loops” before reaching their intended destinations. The problem of determining a good update interval is re-visited in the performance analysis where we run experiments for a range of different intervals and examine

their effects on performance.

4.4 Description of algorithms

4.4.1 Notation

As was mentioned above, nodes are organized into clusters as in the example shown in figure 4.2 and each node may handle multiple traffic flows each of which has a specific source and destination. Note here that we define a flow from end-to-end unlike other schemes where a flow denotes a transmitter-receiver pair. We shall use the following notation:

- $X_t(i)$: total number of packets waiting for transmission at node i at the beginning of frame t .
- $X_t(i, j)$: total number of packets waiting to be transmitted from node i to node j at the beginning of frame t .
- $X_t^f(i, j)$: total number of packets from flow f waiting to be transmitted from node i to node j at the beginning of frame t .
- $Y_t(i, j)$: lost throughput (packets/frame) from node i to j during frame t , due to channel errors.
- $Y_t^f(i, j)$: lost throughput (packets/frame) of flow f from node i to j during frame t , due to channel errors.
- $N_t(i)$: set of neighbors of node i
- $R_t(i, f)$: neighbor receiving flow f from node i .

- C : number of slots per frame.

4.4.2 Node-level scheduling

Node-level scheduling refers to the access control mechanism of nodes sharing the radio link in the same cluster. At the beginning of every frame, and in order to determine their slot allocations, these nodes compute their *LEAR* measures based on the following equation:

$$LEAR_t(i) = \sum_{j \in N_t(i)} X_t(i, j) + \sum_{j \in N_t(i)} Y_{t-1}(i, j) \times \frac{X(i, j)}{\sum_{k \in N_t(i)} X(i, k)} \quad (4.5)$$

Each node then calculates its weight as the ratio of its *LEAR* to the sum of the *LEARs* of all the nodes belonging to the same cluster:

$$W(i) = \frac{LEAR_t(i)}{\sum_{j \in \text{cluster}} LEAR_t(j)} \quad (4.6)$$

The capacity allocation $C_t(i)$ of node i is then given by:

$$C_t(i) = \lfloor C \times W(i) \rfloor \quad (4.7)$$

Since the sum of the $C_t(i)$ may be less than the frame capacity C and in order not to waste slots, each node i maintains a *deficit* weight $W_d(i)$ equal to:

$$W_d(i) = C \times W(i) - C_t(i) \quad (4.8)$$

Clearly the number of unused slots will be less than the number of nodes in the cluster. If these excess slots are equal to m , then they will be allocated to the nodes with the m larger values of $W_d(i)$. The notion of the deficit weight is similar to the way the deficit round-robin works (described in section 4.2) and is utilized because packets must be transmitted as a whole, but no slots should remain unused.

Nodes that belong to multiple overlapping clusters need to perform an extra step. These nodes (for example node B in figure 4.2) will end up with more than one allocations from the above scheme, namely one for each cluster they are members of. To resolve this conflict, they choose as their final allocation that with the minimum number of slots. For example, if node i is a member of n different clusters, then it will come up with n different allocations, denoted by $C_{t,l}(i), l = 1, \dots, n$. According to our proposed "tie-breaker" rule, the final allocation will be given by:

$$C_t(i) = \min_{1 \leq l \leq n} C_{t,l}(i) \quad (4.9)$$

The tie-breaker rule in a sense guarantees that the aggregate number of slots allocated to the nodes of a single cluster never exceeds the size of a single frame. On the other hand, it may result in wasting some bandwidth in clusters where the "common" node was entitled to additional slots that it had to give up. This can be avoided by modifying the algorithm to proceed to a second round of scheduling where the unused slots are re-negotiated between the rest of the nodes in the cluster.

4.4.3 Flow-level scheduling

Once the node-level scheduling is complete, nodes must arbitrate among multiple flows they are serving. The task of the flow level scheduling mechanism is to divide the allocated bandwidth $C_t(i)$ of node i among its contending flows. We are using *LEAR*-based measures again, this time for determining the weights of the flows, similarly as we did in the previous section for the nodes. The *LEAR* measure of

flow f at node i is computed based on the following formula:

$$LEAR(i, f) = X_t^f(i, R(i, f)) + Y_{t-1}^f(i, R(i, f)) \times \frac{X_t^f(i, R(i, f))}{\sum_k X_t^k(i, R(i, k))} \quad (4.10)$$

The individual flow weights can be obtained by dividing each flow's $LEAR$ measure with the sum of the $LEAR$ s of one node's flows:

$$W(i, f) = \frac{LEAR_t(i, f)}{\sum_{k \in \text{flow in node } i} LEAR_t(i, k)} \quad (4.11)$$

The capacity allocation of flow f is then given by

$$C_t^f(i) = \lfloor C_t(i) \times W(i, f) \rfloor \quad (4.12)$$

Once again, as the sum of the $C_t^f(i)$ may be less than the node's allocated capacity C_t each flow f maintains a *deficit* weight $W_d(i, f)$ equal to:

$$W_d(i, f) = C_t(i) \times W(i, f) - C_t^f(i) \quad (4.13)$$

and the excess slots are again allocated to the flows with the larger values of deficit weights $W_d(i, f)$.

4.4.4 Routing

Routing is based on the periodic execution of the shortest-path computation algorithm; in particular a distributed version of Bellman-Ford [12] algorithm is employed. Each link is associated with an adaptive distance metric (the cost of using a particular link) which is updated periodically. The update interval (UI) is a parameter of the algorithm and indicates how often (in number of frames) the link metrics must be updated and the Bellman-Ford must be executed so that routing assignments are revised. The link distance-metrics are direct estimates of the average delay per packet transmitted over each link.

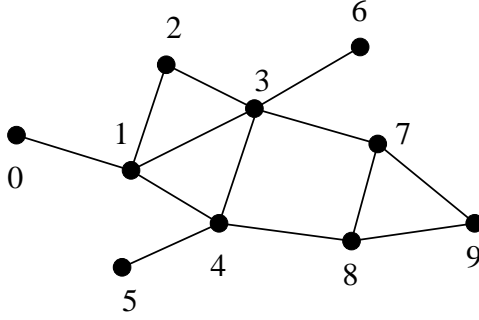


Figure 4.3: Sample network topology for simulation

4.5 Performance results

4.5.1 Network and traffic patterns

In this section we present a set of preliminary results in order to verify the inherent advantages of a unified scheduling and routing approach. We have simulated the proposed scheduling and routing algorithms for the topology shown in figure 4.3. We have used a discrete-event simulation model based on the simulation tool presented in Appendix A. Prior to the beginning of the simulation a simple clustering algorithm is executed to identify the network clusters.

We run simulations for 1000 time frames, each frame consisting of 48 time slots. Each node independently generates data packets from a Poisson distribution. In particular, we consider two types of packets (type I and type II) with different arrival rates $\lambda_1 = 0.1$ and $\lambda_2 = 2 \times \lambda_1 = 0.2$. Packet flows are distinguished by the source and destination IDs and whether they are of type I or type II. A random error channel model is assumed in which each time slot may experience channel error, independently from previous slots, with probability P_e .

4.5.2 Performance measures

Performance is measured in terms of average *throughput* (TP) and average *packet delay* D . Average throughput is computed as the percentage of generated packets delivered to their destinations during the simulation time. Average packet delay is the average time spent by all packets in the network. Note though, that for those packets delivered to the destination, the delay contribution is the complete end-to-end delay, whereas for packets not reaching the destination, the contribution is the amount of time from generation to the end of the simulation. Although this contribution may negatively bias the results as these packets never reach the destination, it is included since they contribute to the delay and the ratio of undelivered to delivered packets is not always negligible. For each packet received by the intended destination we calculate the packet delay and use it towards the computation of average packet delay. For each flow we calculate the number of delivered and undelivered packets and use them towards the calculation of the average throughput.

4.5.3 Simulation results

Tables 4.1 and 4.2 summarize performance results for the cases of “slot-error” rates of $P_e = 0.1$ and $P_e = 0.2$ respectively. The first column of each table lists the values of the update interval (UI) (the period, in number of frame, that we adjust the routing assignments). The last row F corresponds to the case of static routing, where the routing assignments did not change during the simulation. The average packet delays are normalized with respect to the minimum value obtained for each table.

| | Type I | | Type II | |
|------|--------|------|---------|------|
| U.I. | TP | D | TP | D |
| 1 | 0.59 | 2.56 | 0.61 | 2.29 |
| 5 | 0.75 | 1.25 | 0.75 | 1.24 |
| 10 | 0.76 | 1.22 | 0.75 | 1.25 |
| 20 | 0.78 | 1.10 | 0.78 | 1.10 |
| 40 | 0.79 | 1.07 | 0.80 | 1.02 |
| 100 | 0.81 | 1.01 | 0.80 | 1.00 |
| F | 0.79 | 1.03 | 0.79 | 1.06 |

Table 4.1: Performance results for average slot error rate $P_e = 0.1$

We observe in both cases and for both traffic types, that by adjusting the routes periodically we obtain lower values of D as compared to fixed routing. This does not happen however when $UI = 1$; clearly updating the routes at the beginning of every frame suffers from the disadvantages discussed earlier. Note also that for $P_e = 0.1$, the lowest values of average packet delay and the highest values of throughput are obtained for $UI = 100$, whereas when the slot-error rate doubles ($P_e = 0.2$), the optimum values are achieved when $UI = 40$. Therefore we conclude that the routing update period depends also on the average rate of channel errors.

4.6 Future directions

In this chapter, we discussed the problem of fair scheduling in wireless ad-hoc networks and proposed a hierarchical scheme to perform capacity allocation at the node-level and the flow level based on link and flow-level error characteristics

| | Type I | | Type II | |
|------|--------|------|---------|------|
| U.I. | TP | D | TP | D |
| 1 | 0.39 | 1.65 | 0.41 | 1.61 |
| 5 | 0.54 | 1.25 | 0.54 | 1.26 |
| 10 | 0.55 | 1.21 | 0.55 | 1.20 |
| 20 | 0.60 | 1.06 | 0.60 | 1.07 |
| 40 | 0.63 | 1.00 | 0.62 | 1.03 |
| 100 | 0.63 | 1.02 | 0.62 | 1.04 |
| F | 0.61 | 1.05 | 0.62 | 1.08 |

Table 4.2: Performance results for average slot error rate $P_e = 0.2$

and routing assignments. Routing is based on a shortest-path algorithm with the link-distance metrics calculated from an estimate of the average packet delays. We concluded that in order to address the dependencies that exist between routing and scheduling functionalities, routing must be adaptive and the algorithm must periodically adjust the link metrics and re-compute the shortest paths. A simple network model was simulated and the results illustrate that there is potential for improvement in performance, if such a hierarchical approach is followed. In particular, it was determined that the period of routing updates is a crucial parameter which depends on the traffic load and the slot error rate and must be carefully selected so that throughput is maximized, delays are minimized and routing oscillations that may cause excessive delays are avoided.

Even though the mechanics of the algorithms have been defined a lot of issues remain to be resolved so that a complete framework can be developed. The problem of cluster-formation for example was not addressed since we only dealt with static

topologies. In mobile, dynamic networks however, a clustering scheme, capable of reacting quickly to connectivity changes by reorganizing its clusters is necessary. Furthermore, it would be interesting to examine the performance for a variety of channel error models (bursty, location-dependent, etc.) and for different types of traffic (variable rates).

Chapter 5

Conclusions

We have studied a set of different problems that arise in the context of wireless ad-hoc networks. Our focus was on identifying issues related to several unique characteristics of multi-hop networks and on proposing solutions in the context of network control. In particular, we concentrated on problems related to the need for energy and bandwidth- efficient operation and a class of algorithms were proposed for achieving routing and bandwidth allocation of session-oriented traffic. The algorithms were evaluated through extensive simulations, using a simulation tool developed for the purposes of this study.

During the performance analysis, the existing trade-off between energy consumption and blocking probability became apparent. We were also able to convert session routing to link metric based, even though algorithms based on minimum distance paths are normally intended for packet-switched networks. Another key element was the monitoring of processing power and its effects to the overall energy consumptions. Other studies have been considering this quantity as negligible but our simulations indicated that its effects are quite important. Additional conclusions were drawn on the effects of node density and network size on performance

and on how to extend the network lifetime by carefully choosing link metrics that average energy expenditures over the whole set of network nodes.

The next step was a study of the problem of energy efficient routing under limited frequency resources, where we concluded that a two-step approach is most appropriate. A minimum-cost candidate path is first determined and an interference-free channel assignment is then searched. We proposed a set of heuristics for achieving channel allocation and our results showed that even a simple greedy heuristic, which has the advantage of ease of implementation and low complexity, can achieve performance which is not significantly worse than exhaustive search mechanisms. Another key point in this problem was the selection of an appropriate metric for determining the minimum cost path. We concluded that such a metric has to combine information on the power requirements as well as a term that indicates the number of blocked frequency channels by every transmission.

Last, we looked into the problem of fair scheduling and access control in wireless multi-hop networks carrying packet-switched traffic. Our focus was on addressing the dependencies between a two-level hierarchical approach to scheduling and route assignments. We proposed an adaptive scheme that iterates between scheduling and routing and adapts to traffic requirements, congestion and channel errors by periodically adjusting the capacity allocation at both the node and flow-level and the routing assignments (the latter at a different time scale). A preliminary performance evaluation indicated that there are a lot of possibilities for improving performance if a unified approach is followed.

Our studies were characterized by a tendency towards the vertical integration of protocol layer functions. We noticed for example that improved performance

can be obtained by jointly considering physical layer, MAC and network layer issues. This observation suggests that novel opportunities exist if we depart from the traditional protocol-layer approaches and jointly address the issues that arise in new types of network topologies with new requirements and innovative integrated services.

Further studies on energy-efficient network control could also examine in detail the problem of routing packet-switched traffic. In particular, a joint objective can be defined in the context of minimizing energy and delay. Moreover, significant amount of work has been exhibited in minimum energy wireless multicasting of sessions, which can also be extended to datagram traffic where the concept of minimizing delay adds a new dimension to the problem. And even though some of the objectives may be parallel, the actual algorithms, metrics and trade-offs are quite different.

Appendix A

Simulation model for energy-efficient routing algorithms

We have developed a discrete-event simulation model for evaluating the algorithms presented in chapters 2 and 3 of the dissertation. The programs are written in ANSI C code and many of the simulation components have been developed from scratch so that with minor modifications they can be reused in other simulations (for example part of the programs were useful in the simulations of chapter 4). In this section we provide an overview of our model, its main components and the routines which handle the algorithmic functions.

Event scheduler

An event scheduler has been implemented that keeps a linked list of events waiting to happen. Two types of events are considered; new call arrivals (**New Call**) and call terminations (**Term Call**). Every event is associated with a specific time instant t at which it is scheduled to occur and a pointer to the routines that will be executed. During one event the scheduler may be called to schedule future events. In particular when a **New Call** event occurs, the scheduler must schedule the next arriving call for the node under consideration and if the call is admitted

to the system it must also schedule its termination (**Term Call**).

Event scheduling is performed by keeping an ordered linked list (**Event List**) of future event notices. The first entry in the list represents the next earliest event and therefore removal from the list is straightforward. Inserting a new event in the list requires some search since the right place for the entry must be identified. Even though this approach may not be optimal (the worst case scenario requires a full search of the list), its implementation is simpler and for networks not exceeding a few tens of nodes we have to maintain a **New Call** event per node (the next arrival) and all the **Term Call** events (for the ongoing calls), hence the length of the list does not increase in an uncontrolled way.

Simulation clock and time advancing mechanism

A global variable is maintained representing the simulated time, referred to as the **global-time**. We follow an event-driven approach in which the scheduler increments the **global-time** automatically to the time of the next earliest occurring event. Thus there is no need for a unit-time approach in which the clock would be incremented in constant time intervals.

Session representation

Each session is represented by a unique triple that consists of the source node ID, the destination node ID and a counter that gets incremented by one for every newly arriving session between the same source destination pair. Hence the **sessionID** structure is represented as follows:

| | |
|-------------------------------|---|
| <code>sessionID.source</code> | <i>source node of session</i> |
| <code>sessionID.dest</code> | <i>destination node of session</i> |
| <code>sessionID.index</code> | <i>counter of sessions between each source-destination pair</i> |

Network model

The network is represented by a graph. Since the number of nodes for a simulation run remains constant (ie no nodes may be added or deleted from the topology) we declare a structure that represents a graph and consists of two entities: **nodes** and **arcs**. Each node is a structure that consists of the appropriate identification information (node id and location coordinates) as well as routing information that is discussed in the next paragraph. The field **arcs** is a two-dimensional array representing every possible ordered pair of nodes. The value of each array element will be either **True** or **False** depending on whether or not the two nodes are adjacent to each other.

Node model

In addition to ID and location information that was mentioned above, each node must maintain the following structures:

- an array of **transceiver status** which indicates whether a transceiver k is **free** or **in use**; if a transceiver is in use, the corresponding **sessionID** along with the incoming and outgoing links are stored in a one-dimensional array of size equal to the number of transceivers, referred to as the **connectivity table** and consisting of the following fields (each element of the array corresponds to a unique transceiver):

| | |
|--|---|
| connectivity-table[k].sessionID | <i>session in service</i> |
| connectivity-table[k].in-node | <i>node from which session is received</i> |
| connectivity-table[k].out-node | <i>node to which session is transmitted</i> |
| connectivity-table[k].transceiver-status | <i>status of transceiver</i> |

- an array of **frequency channel status** which indicates whether a frequency channel k is **free** or **blocked** from transmission for every potential next-hop receiver; if

a frequency channel is in use, information about the next-hop neighbor and the ongoing `sessionID` is stored in the **frequency-based routing table** as follows (each element of the array corresponds to a unique frequency channel):

`routing[k].sessionID`

`routing[k].next-node`

- information about the minimum cost path. In particular each node i maintains an array with the minimum cost to reach every possible destination (`node[i].min-distance[dest]`) and the immediate neighbor that leads to that destination (`node[i].next-hop[dest]`).

Routines

We summarize hereafter in pseudocode the routines that are used for establishing and terminating sessions over the selected routes, for both cases of limited number of transceivers (**Establish**, **Terminate**) and limited number of frequency channels (**EstablishF**, **TerminateF** and **ClearPathF**). Note that both **Establish** and **EstablishF** routines return the total power consumed by the nodes in the path if the call is admitted, whereas **Terminate**, **TerminateF** and **ClearPath** are called to "tear-down" admitted or partially admitted sessions and do not return any value.

`establish(sessionID)`

{

`power = 0;`

`tr-node = sessionID.source;`

`if (tr-node.min-distance[sessionID.dest] < ∞)`

`/* ie a feasible path exists */`

`while(tr-node \neq sessionID.dest)`

```

{
    rc-node = node.next-hop[sessionID.dest];
    reserve(tr-node,rc-node);
    /* reserve updates the connectivity table and */
    /* transceiver status */
    power += power for transmission from tr-node to
            rc-node;
    tr-node = rc-node;
}
return(power);
}

```

```

terminate(sessionID)
{
    tr-node = sessionID.source;
    while((tr-node  $\neq$  sessionID.dest) AND
        ( $\exists k$  s.t. tr-node.connectivity-table[k].session==sessionID))
    {
        rc-node = tr-node.connectivity-table[k].rc;
        clear(tr-node, rc-node);
        current-node = rc-node;
    }
}

```



```

establishF(sessionID)
{
  power = 0;
  tr-node = sessionID.source;
  if (tr-node.min-distance[sessionID.dest] <  $\infty$ )
    /* ie a feasible path may exist */
    while(tr-node  $\neq$  sessionID.dest)
    {
      rc-node = node.next-hop[sessionID.dest];
      if ( $\exists k$  s.t. frequency channel[k] == free)
      {
        reserve(tr-node,rc-node,k);
        /* reserve updates the frequency-based */
        /* routing table */
        blocking(tr-node,rc-node,k)
        /* block neighboring nodes in accordance to */
        /* interference model */
        power += power for transmission from tr-node
                to rc-node;
        tr-node = rc-node;
      }
    }
  else
  {
    clogged-node = tr-node;
    clearpathF(sessionID, clogged-node)
  }
}

```

```

                                power = 0;
                                break;
                                }
                        }
    return(power)
}

```

```

terminateF(sessionID)
{
    tr-node = sessionID.source;
    while((tr-node  $\neq$  sessionID.dest) AND
        ( $\exists k$  s.t. tr-node.routing[k].session==sessionID))
    {
        rc-node = tr-node.routing[k].rc;
        clear(tr-node, rc-node,k);
        unblocking(tr-node,rc-node,k);
        tr-node = rc-node;
    }
}

```

```

clearpathF(sessionID, clogged-node)
{
    tr-node = sessionID.source;

```

```

while((tr-node  $\neq$  clogged-node) AND
      ( $\exists k$  s.t. tr-node.routing[k].session==sessionID))
{
  rc-node = tr-node.routing[k].rc;
  clear(tr-node, rc-node,k);
  unblocking(tr-node,rc-node,k);
  tr-node = rc-node;
}

```

Input parameters

A set of input variables define one simulation iteration which may have to be repeated several times with different seeds. Therefore a single execution of our simulation consists of several iterations (associated with different input sets) and each iteration consists of several repetitions to ensure independence of the results from the seeds selected. Before every simulation run, the input variables must be determined which are read during the initialization from an input file. Table A.1 summarizes the input parameters. Besides the parameters of table A.1 which are read from the < input-file >, we must also declare the seed numbers for every repetition to initialize the random number generators which are used for generating the nodes' locations and the random distributions for traffic arrivals.

Initialization

Upon initialization, the following events take place:

- The input parameters are loaded from the input-file.

| | |
|--------------|---|
| λ | new call arrival rate per node per time unit |
| μ | average call service time |
| metric type | for minimum cost path computation |
| d_{max} | maximum transmission range |
| max-requests | cumulative number of simulated call arrivals |
| out-file | name of file to store performance measures |
| preset-net | set this to 0 for simulating a randomly generated network |
| W_p | coefficient for metric M3 |
| W_e | coefficient for metric M3 |

Table A.1: Input parameters for simulation iteration

- Network graph initialization; set location of nodes and determine set of network links based on given d_{max} .
- Each node schedules its first **New Call** event and places it in the event list.

Event reaction

As we mentioned above, we have two types of events, namely **New Call** and **Term Call**. Both types of events result in execution of some routines upon occurrence. Depending on the assumptions (limited transceivers or limited frequencies) replace **establish** and **terminate** with **establishF** and **terminateF** respectively.

```

if (event type == New Call)
{
    execute Bellman-Ford for sessionID.dest
    power = establish(sessionID);

```

```

if (power > 0)
{
    schedule Term Call;

    update link weights; /* based on link metrics */
    update measured parameters;
}

schedule next New Call;

advance global-time to next event;
}

else /* event type = Term Call */
    terminate(sessionID);

```

BIBLIOGRAPHY

- [1] M.S. Corson, J. Macker, and S.G. Batsell. Architectural considerations for mobile mesh networking. In *Proceedings IEEE MILCOM'96*, 1996.
- [2] J. E. Wieselthier, G. D. Nguyen, and A. Ephremides. Algorithms for energy-efficient multicasting in static ad hoc wireless networks. *To Appear in Mobile Networks and Applications (MONET)*, 2000.
- [3] J. E. Wieselthier, G. D. Nguyen, and A. Ephremides. Energy-efficient broadcast and multicast trees in wireless networks. *To Appear in Mobile Networks and Applications (MONET)*, 2000.
- [4] J. E. Wieselthier, G. D. Nguyen, and A. Ephremides. Algorithms for bandwidth-limited energy-efficient wireless broadcasting and multicasting. In *Proceedings Milcom 2000, Los Angeles*, October 2000.
- [5] C. Sankaran and A. Ephremides. Multicasting with multiuser detection in ad-hoc wireless networks. In *Proceedings of the 2000 International Zurich Seminar on Broadband Communications*, February 2000.
- [6] V. Rodoplu and T. Meng. Minimum energy wireless networks. *IEEE JSAC*, 17, August 1999.

- [7] J. H. Chang and L. Tassiulas. Routing for maximum system lifetime in wireless ad-hoc networks. In *Proceedings of the 37th Annual Allerton Conference on Communications, Control and Computing, Monticello, IL*, September 1999.
- [8] J. H. Chang and L. Tassiulas. Energy conserving routing in wireless ad-hoc networks. In *Proceedings Infocom 2000, Tel-Aviv, Israel*, March 2000.
- [9] R. Berry, S. Finn, R. Gallager, H. Kassab, and J. Mills. Minimum energy and delay routing in packet radio networks. In *Proceedings of the 3rd Annual FEDLAB Symposium*, February 1999.
- [10] A. Michail and A. Ephremides. A distributed routing algorithm for supporting connection-oriented service in wireless networks with time-varying connectivity. In *Proceedings 3rd IEEE Symposium on Computer and Communications (ISCC 98), Athens, Greece*, June 1998.
- [11] A. Michail, W. Chen, and A. Ephremides. Distributed routing and resource allocation for connection-oriented traffic in ad-hoc wireless networks. In *Proceedings of the Conference on Information Sciences and Systems, Princeton, New Jersey*, March 1998.
- [12] D. Bertsekas and R. Gallager. *Data Networks*. Prentice-Hall, 1992.
- [13] A. Ephremides and T. V. Truong. Scheduling broadcasts in multihop radio networks. *IEEE Transactions on Communications*, 38:456–460, 1990.
- [14] I. Cidon and M. Sidi. Distributed assignment algorithms for multihop packet radio networks. *IEEE Transactions on Computing*, 11:1110–1118, 1988.

- [15] A. Parekh and R. G. Gallager. A generalized processor sharing approach to flow control in integrated services networks. *IEEE/ACM Transactions on Networking*, 1:344–357, June 1993.
- [16] A. Demers, S. Keshav, and S. Shenker. Analysis and simulation of a fair queueing algorithm. In *Proceedings ACM SIGCOMM'89*, pages 1–12, September 1989.
- [17] P. Goyal, H. M. Vin, and H. Cheng. Start-time fair queueing: A scheduling algorithm for integrated services packet switching networks. *IEEE/ACM Transactions on Networking*, 5:690–703, 1997.
- [18] M. Shreedhar and Varghese G. Efficient fair queueing using deficit round robin. In *Proceedings ACM SIGCOMM'95*, pages 231–242, October 1995.
- [19] S. Lu, V. Bharghavan, and R. Srikant. Fair scheduling in wireless packet networks. In *Proceedings ACM SIGCOM'97*, August 1997.
- [20] T. Nandagopal, S. Lu, and V. Bharghavan. A unified architecture for the design and evaluation of wireless fair queueing algorithms. In *Proceedings of ACM Mobicom 99, Hungary*, 1999.
- [21] P. Bhagwat, P. Bhattacharya, A. Krishma, and S. Tripathi. Enhancing throughput over wireless lans using channel state dependent packet scheduling. In *Proceedings IEEE INFOCOM'97*, April 1997.
- [22] T.S. Ng, I. Stoica, and H. Zhang. Packet fair queueing algorithms for wireless networks with location dependent errors. In *Proceedings IEEE INFOCOM'98*, March 1998.

- [23] S. Lu, T. Nandagopal, and V. Bharghavan. Fair scheduling in wireless packet networks. In *Proceedings ACM MOBICOM'98*, October 1998.
- [24] S. J. Golestani. A self-clocked fair queueing scheme for high speed applications. In *Proceedings INFOCOM'94*, pages 636–646, April 1994.
- [25] M. Srivastava, C. Fragouli, and V. Sivaraman. Controlled multimedia wireless link sharing via enhanced class-based queueing with channel-state-dependent packet scheduling. In *Proceedings IEEE INFOCOM'98*, March 1998.
- [26] P. Karn. Maca - a new channel access method for packet radio. In *ARRL/CRRL Amateur Radio 9th Computer Networking Conference*, September 1990.
- [27] V. Bharghavan, A. Demers, S. Shenker, and L. Zhang. Macaw: A media access control protocol for wireless lans. In *Proceedings ACM SIGCOMM'94*, 1998.
- [28] N. H. Vaidya, P. Bahl, and S. Gupta. Distributed fair scheduling in a wireless lan. In *Proceedings of ACM Mobicom 2000, Boston MA*, August 2000.
- [29] H. Luo, S. Lu, and V. Bharghavan. A new model for packet scheduling in multihop wireless networks. In *Proceedings of ACM Mobicom 2000, Boston MA*, August 2000.
- [30] T. Nandagopal, T. Kim, X. Gao, and V. Bharghavan. Achieving mac layer fairness in wireless packet networks. In *Proceedings of ACM Mobicom 2000, Boston MA*, August 2000.

- [31] M. B. Pursley, H. B. Russel, and P.E. Staples. Routing multimedia packets in a frequency-hop packet radio network. In *Proceedings IEEE MILCOM 96*, November 1996.
- [32] D.J. Baker, A. Ephremides, and J.A. Flynn. The design and simulation of a mobile radio network with distributed control. *IEEE JSAC*, 2:226–237, January 1984.
- [33] P. Krishna, N. H. Vaidya, M. Chatterjee, and D. K. Pradhan. A cluster-based approach for routing in dynamic networks. In *Proceedings ACM SIGCOMM'97*, 1997.
- [34] M. Gerla, J. Tzu, and C. Tsai. Multicluster, mobile, multimedia radio network. *Wireless Networks*, 1:255–265, January 1995.